Fusarium infection and its effects on germination and deoxynivalenol content of oats and screening for resistance by VIS-NIR spectroscopic methods

Verknader av *Fusarium*-infeksjon på innhald av deoxynivalenol (DON) og spireevne i havre, og screening for resistens ved hjelp av VIS-NIR- spektroskopiske metodar

Philosophiae Doctor (PhD) Thesis

Selamawit Tekle Gobena

Department of Plant Sciences
Faculty of Veterinary Medicine and Biosciences
Norwegian University of Life Sciences

Ås, 2014

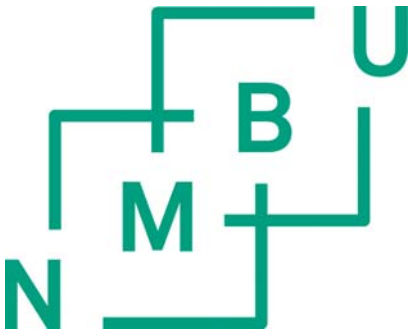

Thesis number 2014:78
ISSN 1894-6402
ISBN 978-82-575-1238-5

Supervisors

Professor Åsmund Bjørnstad
asmund.bjørnstad@nmbu.no
Department of Plant Sciences
Norwegian University of Life Sciences
P. O. Box 5003, 1432 Ås, Norway

Doctor Helge Skinnes
helge.skinnnes@nmbu.no
Department of Plant Sciences
Norwegian University of Life Sciences
P. O. Box 5003, 1432 Ås, Norway

Doctor Vegard H. Segtnan
vegard.segtnan@nofima.no
Nofima AS
Osloveien 1, 1430 Ås, Norway

Evaluation Committee

Doctor Catherine Howarth
cnh@aber.ac.uk
Institute of Biological, Environmental and Rural Sciences
Aberystwyth University
Penglais, Aberystwyth, Ceredigion, SY23 3DA, Wales

Doctor Ellen F. Mosleth
ellen.mosleth@nofima.no
Nofima AS
Osloveien 1, 1430 Ås, Norway

Professor Hilde-Gunn Opsahl Hoen-Sorteberg
hilde-gunn.hoen-sorteberg@nmbu.no
Department of Plant Sciences
Norwegian University of Life Sciences
P. O. Box 5003, 1432 Ås, Norway

Table of contents

Acknowledgements

This work is part of the projects 'Safe Grains: Mycotoxin prevention through resistant wheat and oats' and 'Mycotoxin contamination in Norwegian food and feed: Modeling reductive approaches and risk assessment with regards to the whole food chain' financed by the Norwegian Research Council and Graminor AS.

I am deeply indebted and grateful to my main supervisor Professor Åsmund Bjørnstad; learning from you has been a great privilege. I am very grateful for having Doctor Helge Skinnes and Doctor Vegard Segtnan as my co-supervisors for they have always been ready to help, explain, and comment. I thank you all very much for your kind words and encouragements.

I thank the co-authors in my papers, Professor Ruth Dill-Macky, Professor Anne Marte Tronsmo, Doctor Yanhong Dong, and Doctor Ingrid Måge and our project leader Doctor Guro Brodal for their invaluable work and assistance. Thank you very much.

Colleagues in our research group, Doctor Morten Lillemo, Yalew Tarkegne, and Anne Guri Marøy, also deserve heartfelt thanks for the discussions during our meetings and their assistance while running the experiments. I thank Bjørg Narum and Doctor Ulrike Böcker at Nofima AS for teaching me how to use the machines at the spectroscopy lab and answering my trivial questions.

My friends at Ås, Meseret Tessema, Mestawet Taye and Meley Mekonnen; getting together with you to complain about anything and everything was my favorite way of curbing my stress. I thank you.

My heartfelt gratitude goes to Ayana Gobena and his family in Stockholm for being there for me and encouraging me during all these years.

I thank my dear husband Alemayehu Kidane for always believing in me and encouraging me. I found a great companion and partner in you. And my sons Bereket and Haris, you are my joys. I love you all. Finally, I dedicate this work to my mother, Yewebdar Bekele who has sacrificed a lot to give my brother, Abiy, and me the best education and childhood. Thank you, Emaye.

Selamawit Tekle Gobena

Ås, August, 2014

List of papers

Paper I

Tekle, S.; Dill-Macky, R.; Skinnes, H.; Tronsmo, A. M.; Bjørnstad, Å., Infection process of *Fusarium graminearum* in oats (*Avena sativa* L.). *European Journal of Plant Pathology* **2012,** *132*, 431-442.

Paper II

Tekle, S.; Skinnes, H.; Bjørnstad, Å., The germination problem of oat seed lots affected by Fusarium head blight. *European Journal of Plant Pathology* **2013,** *135*, 147-158.

Paper III

Tekle, S.; Bjørnstad, Å.; Skinnes, H.; Dong, Y.; Segtnan, V. H., Estimating deoxynivalenol content of ground oats using VIS-NIR spectroscopy. *Cereal Chemistry* **2013,** *90*, 181–185.

Paper IV

Tekle, S. Måge, I., Segtnan V. H., Bjørnstad Å. Near infrared hyperspectral imaging of *Fusarium*-damaged oats (*Avena sativa* L.)**.** *Cereal Chemistry* **2014** *(Published online as 'First Look' paper).*

Abbreviations

AE	Anther extrusion
DON	Deoxynivalenol
FHB	Fusarium head blight
GC	Germination capacity
HSI	Hyperspectral imaging
NIR	Near infra-red
PLS-C	Partial least square components
PLS-R	Partial least squares regression
RPD	Residual predictive deviation
VIS	Visible

Summary

Fusarium head blight (FHB) causes a great concern in Norway, and in the world at large, due to the mycotoxins produced by the causative pathogens. Different cultural practices, including deployment of resistant cultivars, are used to manage FHB and reduce mycotoxin contamination in cereal grains in general. However, specific studies on FHB of oats are scarce as compared to the high numbers found in wheat or barley. Therefore in this PhD study, the infection process of *Fusarium* spp. and the different parameters of resistance in oats (Paper I and II) and the feasibility of spectroscopic methods as screening tools in *Fusarium*-inoculated oat nurseries (Paper III and IV) are investigated.

In the **first paper**, the infection pathways of *Fusarium* spp. into the oat floret and the optimal time of *F. graminearum* infection in oats were studied. Field-grown oats were spray inoculated with macroconidial suspension of *F. graminearum* at flowering, one week after flowering, and two weeks after flowering to study the optimal time of infection. The plants were most susceptible to infection at flowering with highest kernel infection and DON contamination, and the lowest germination capacity (GC). It was possible to infect the plants at later stages but DON level and the effect on GC were highly reduced. To study infection pathways, greenhouse-grown oats were spray-inoculated at flowering. Florets were collected for seven days following inoculation and examined under the microscope for patterns of infection and colonization. The fungus primarily entered through the floret mouth into the floret cavity to infect *via* the internal surfaces of the palea, lemma and the developing caryopsis. Both symptoms and fungal colonies appeared first at the apical portions of the florets. Retained anthers had profuse fungal growth during the first few days after inoculation suggesting the importance of anthers during the initial stages of infection.

The **second paper** deals with the effects of *Fusarium* infection on- and the relationship between GC and DON level as affected by the prevailing weather conditions and the inoculation methods used. Germination capacities and DON contents of several spray- and spawn-inoculated oat genotypes were determined from field experiments conducted from 2007-2010. High DON levels were accompanied by low GCs but low DON levels did not guarantee high GCs, showing factors other than DON play roles in determining GCs of *Fusarium*-affected oats. Strong correlations between DON level and GC were recorded in drier years and for spray inoculations compared to wet years and spawn inoculations. We hypothesized that this differential relationship between DON and GC was due to the

occurrence of late infections during wet seasons under spawn inoculation. Late infections neither kill the germ nor do not lead to significant accumulation of the toxin, but are able to lower germination by causing seedling blight and less vigor seedlings. To test this hypothesis, greenhouse-grown oats were spray inoculated at different developmental stages. Rapid reductions in DON level, but only steady increments in GC were observed for later inoculation. Number of *Fusarium*-infected kernels was consistently high for all inoculations. Further, vigor of oat seedlings was tested on water agar amended with different levels of DON (0, 2, 5, 10, 15, 20 ppm). The toxin did not inhibit initiation of germination, but retarded seedling growth and resulted in seedlings with abnormal morphology. These results showed that late infections can reduce GCs, even though they only lead to low DON contaminations and superficial kernel infections.

In the **third paper**, feasibility of visible and near infrared (VIS-NIR) reflectance spectroscopy to replace the costly chemical DON analysis was investigated. Second derivative spectra of 166 ground samples of more than 60 oat genotypes (DON level mean= 13.06 ppm range= 0.05-28.1 ppm) were modeled against the reference DON levels using partial least squares regression on a separate calibration (n= 111) and validation (n= 55) set samples. The best model developed used the whole spectral region (400-1,098 nm and 1,101-2,350 nm), had three partial least squares components, a root mean square error of prediction value of 3.16 and a residual predictive deviation value of 2.63. These values indicate that the model is good enough to use in *Fusarium*-inoculated nurseries; to discard the worst genotypes at early stages of a screening program. We were not able to attribute specific wavelength regions to DON and we had to rely on other effects of FHB on the grain. High-DON samples had lower water and fat content than low-DON samples. In addition, low-DON samples were lighter in color and finer in texture than high-DON samples. Including more genotypes from different growing seasons and sites to expand the DON range of the calibration set and update the model are recommended.

Hyperspectral imaging (HSI) combines spatial and spectral information and has higher sensitivity to minor constituents; attributes lacking in conventional NIR spectroscopy. The **fourth paper** was initiated to investigate the feasibility of this spectroscopic method to detect DON and *Fusarium* damage in single oat kernels. Kernels of *Fusarium*-damaged oat cv. Bessin were visually categorized as asymptomatic, mildly damaged, and severely damaged. Uninoculated kernels of the same cultivar were used as control. The calibration and validation

set samples consisted of 31 and 14 kernels of each category, respectively. Deoxynivalenol content of each kernel was determined after taking NIR hyperspectral images of the dorsal and ventral surfaces of each kernel. The average spectrum from each kernel was paired with the log-transformed reference DON value and a calibration model was fitted by partial least squares regression (PLSR). The prediction performance was validated by predicting DON (DON*= [log (DON)] ^3 values of the validation kernels. Linear discriminant analysis detected clear differences between the kernel categories and the first component of the prediction model separated the uninoculated/asymptomatic from the severely damaged kernels. Infected kernels showed higher intensities at 1920, 2070 and 2140, while non-infected kernels were dominated by signals at 1420, 1620 and 1850 nm. The correlation between predicted and measured DON* of the validation kernels was 0.82 showing that the prediction model is valid.

Key words: deoxynivalenol (DON), *Fusarium graminearum*, germination capacity, hyperspectral imaging, infection pathways, infection time, kernel infection, Oats (*Avena sativa* L.), screening for resistance**,** visible and near infrared spectroscopy.

Samandrag

Aksfusariose eller *Fusarium head blight* (FHB) skaper stor uro i norsk kornproduksjon, så vel som i verda elles. Dette kjem i stor grad av dei mykotoksina (soppgiftene) som dei ansvarlege soppartane lagar. Ulike dyrkingstiltak, mellom desse bruk av resistente sorter, blir nytta for å styre unna infeksjon og redusere nivåa av mykotoksin i korna. Uheldigvis er havre lite granska i så måte, jamført med det store talet på studiar i kveite og bygg. Difor tar denne PhD-avhandlinga for seg problema med mykotoksin i havre: korleis *Fusarium* spp. infiserer plantene og kva for mål (parametrar) for resistens som er best å bruke i havre (artikkel I og II). Vidare tar avhandlinga for seg om det er mogleg å erstatte kjemiske målingar av toksin i havre dyrka med høgt smittepress i forsøksfelt, med spektroskopiske metodar (artikkel III og IV).

Den **første artikkelen** tar for seg smittevegar av *Fusarium* spp. inn i ein havreblom og kva tidspunkt som er optimalt for *F. graminearum* å infisere. For å bestemme dette blei feltdyrka havreplanter inokulerte ved å dusje rislene med ei løysing med makrokonidiar av *F. graminearum* («spray»- metoden), ved blomstring, og ei og to veker etter. Plantene synte seg mest mottakelege ved blomstring. Då vart flest korn infiserte, innhaldet av DON høgast og spireevna (Germination capacity, GC) lågast. Det var mogleg å få til infeksjon seinare, men innhaldet av DON og verknaden på spireevna var då mindre. For å studere infeksjonsvegen, blei planter dyrka i veksthus inokulerte ved blomstring (også med spray). Blomar blei samla inn i sju dagar etter inokulering og undersøkte i mikroskop for å finne mønster i infeksjon og kolonisering. Soppen kom for det meste inn mellom spissen av agnene og inn i blomsterhola *via* innsidene av inneragna (palea), ytteragna (lemma) og det veksande frøet. Både symptom og soppkoloniar synte seg først nær spissen av blomen. Støvknappar fanga mellom eller innom agnene hadde frodig soppvekst dei første dagane av infeksjonen, noko som kan tyde på at støvknappvevet er viktig i tidlege fasar av infeksjonen.

Den **andre artikkelen** tar for seg verknader av *Fusarium*-infeksjon på, og forholdet mellom, GC og DON og korleis dette blir påverka av vêret og smittemetodane som blir nytta (spray eller alternativet, smitta korn strøydde på bakken, såkalla "spawn"). Spireevne og DON-innhald vart bestemt i havregenotypar i feltforsøk utførte frå 2007-2010 etter inokulering på begge måtar. Høge innhald av DON var fylgde av låg spireevne, men låge DON-innhald garanterte ikkje for spireevna, noko som tydde på at fleire faktorar enn DON virka inn på

spireevna i *Fusarium*- skadd havre. Sterke korrelasjonar mellom DON innhald og spireevne blei påviste i tørrare år og med spray-inokulering enn i våte år med smitte på bakken (spawn). Vi tolka det varierande sambandet dit at korrelasjonen i våte år vert påverka av seine infeksjonar, letta ved at kornsmitten – til skilnad frå spray - var til stades heile tida. Slike seine infeksjonar vil då ikkje drepe kimen eller medføre meir toksin, men svekke spireevna gjennom spiringsfusariose (sopphemming under spiringa). For å prøve denne hypotesen blei veksthusdyrka havre smitta på ulike vekststadium frå blomstring til gulmogning. Innhaldet av DON fall raskt etter blomstring, men spireevna tok seg først opp nærare gulmogning. Talet på *Fusarium*-infiserte korn heldt seg høgt uansett smittetidspunkt. Vidare vart spiringa (både evne og fart) undersøkt i friske korn dyrka på vatn-agar tilsett ulike nivå av DON (0, 2, 5, 10, 15, 20 ppm). Toksininnhaldet hadde ingen verknad på spireevna, men derimot sterkt på spirefarten og resulterte ofte i abnorme kimplanter. Med andre ord viser våre resultat at seine infeksjonar kan svekke spireevna, sjølv om dei ikkje fører til auka innhald av DON og med overflatiske infeksjonar.

Den **tredje artikkelen** tar for seg om screening med synleg og nær-infraraudt (VIS-NIR) reflektans spektroskopi kan erstatte dei kostbare kjemiske analysane av DON. Andre-deriverte sprektrum av 166 malne prøver frå 60 havregenotypar (gjennomsnittleg DON-innhald 13.06 ppm, spreiing frå 0.05- 28.1 ppm) blei modellerte mot referanseverdiar av DON-innhald ved hjelp av PLSR (Partial Least Squares Regression). Prøvene vart delte i eit kalibreringssett (n= 111) og eit valideringssett (n= 55). Den beste modellen bygde på heile spekteret av bylgjelengder (400–1,098 nm og 1,101–2,350 nm), hadde tre PLS-komponentar, ein middel prediksjonsfeil (root mean square error of prediction value) på 3.16 og eit prediktivt avviksresidual (residual predictive deviation value) på 2.63. Desse verdiane viser at modellen er god nok til å bli brukt til å screene for *Fusarium*-resistens i smittefelt og vil effektivt kunne ta ut mottakelege genotypar. Vi kan ikkje knyte bestemte bygjelengder til innhaldet av DON i og for seg fordi konsentrasjonen er for låg, kalibreringa bygger på andre verknader på reflektansen som infeksjonen medfører. Prøver med mykje DON har mindre innhald av vatn og feitt enn prøver med lite. Dessutan var prøver med lite DON lysare på farge og finare (meir normale) i tekstur. Modellen bør bli bygd ut ved å ta inn kalibreringsprøver frå fleire vekstsesongar og ei større spreiing i innhald av DON.

Hyperspectral imaging (HSI) er ein ny spektroskopisk metode som kombinerer *romleg* og *spektral* informasjon og er meir kjensleg for låge innhald av ulike stoff; begge desse

eigenskapane manglar i konvensjonell NIR spektroskopi. Den **fjerde artikkelen** tar for seg om det er mogleg med denne metoden å oppdage DON og *Fusarium* skade i einskildkorn av havre (til skilnad frå artikkel III, der malne prøver blei brukte). *Fusarium*-smitta korn av sorten Bessin blei først klassifisert visuelt som symptomfrie og mildt eller sterkt skadde. Usmitta korn av den same sorten vart nytta som kontroll. Prøvene vart delte i eit kalibrerings- og eit valideringssett (31 og 14 korn i kvar kategori). Etter å ha tatt hyperspektrale bilete i NIR av rygg- og buksida på kvart korn blei så innhaldet av DON i kornet bestemt kjemisk. Det gjennomsnittlege spekteret av kvart korn blei så analysert i høve til den log-transformerte referanseverdien for DON og ein kalibreringsmodell tilpassa med PLSR. Prediksjonsevna blei så validert ved å bestemme venta innhald av DON (DON*= [log(DON)]^3) i valideringssettet. Ein lineær diskriminant analyse påviste klare skilnader mellom dei ulike kategoriane av korn, der den første komponenten i prediksjonsmodellen skilde dei usmitta/symptomfrie korna frå dei sterkt skadde. Infiserte korn synte høgare intensitetar ved 1920, 2070 og 2140 nm, medan ikkje-infiserte skilde seg ut med sterke signal ved 1420, 1620 og 1850 nm. Korrelasjonen mellom predikert og målt DON* i valideringskorna var 0.82, noko som synte at prediksjonsmodellen var gyldig.

Nøkkelord: deoxynivalenol (DON), *Fusarium graminearum*, havre, *Avena sativa* L., spireevne, hyperspektral biletanalyse, infeksjonsvegar, infeksjonstidpunkt, korninfeksjon, screening for resistens**,** synleg og nær-infraraud spektroskopi.

1 Introduction

1.1 The oat crop

Oats (*Avena sativa* L.) is an important crop in northern Europe and North America; in Canada, Russia, Scandinavia, Germany and the United Kingdom (*1*). Russia and Canada together produce about 35% of the total world oats production, while 1% is produced by Norway (*2*). Oats production accounts for about 2% of the world grain production and is ranked sixth after maize, wheat, barley, sorghum, and millet (*2*). Global production of oats has been declining steadily due to decrease in feed demand to draft horses following the mechanization of agriculture and transport (*2, 3*). In recent years, however, production has stabilized due to the integration of oats in crop rotations and the increase in demand of oats as human food (*2*).

Unlike wheat and barley, most of the oats produce is directed towards animal feed (*2*). Fodder oats are also cultivated in many parts of the world where the growing season is short, or during the off-season in warmer areas (*1*). The high nutritive value of oats and the introduction of new oats-based food products such as pasta, bread, biscuits, in addition to the traditional hot breakfast cereal, are increasing the demand of this grain as human food (*1, 2*).

Oats contain one-third more protein, four times more fat, and less starch than wheat (*2*). It is recognized as 'health food' due to its exceptionally high nutritional quality and health promoting compounds. It is rich in the soluble dietary fiber β glucan and the avenanthramides which are known to have antioxidant activity (*1, 3, 4*). These components promote health, by lowering plasma cholesterol level and reducing the risk of cardiovascular diseases, diabetes, and cancers (*3, 5*). Increasing levels of *Fusarium* mycotoxins encountered in Norwegian oats (*6, 7*), however, is a matter of great concern.

Cultivated oats is a self-pollinated allohexaploid species with the genomes A, C, and D (*8*). Oats prefer cool and moist climates and are adapted to variable soil types than other small-grained cereals (*2*). Landraces and inter-fertile hexaploid relatives (*Avena sterilis* L.) provide a wide range of genetic diversity and opportunity to breed oats for improved yield, quality and resistance to biotic and abiotic stresses (*8*). In the Nordic countries, breeding efforts in the 20th century improved agronomic traits by developing cultivars adapted to short summers with short straw and high harvest index (*9*). These efforts, however, resulted in the loss of genetic diversity during the transition from landraces to modern cultivars (*9, 10*). Therefore,

collecting and conserving older materials and landraces, and introduction of modern cultivars to the Nordic gene pool are crucial to keep the genetic diversity for future breeding programs (*9, 10*).

1.2 Fusarium head blight

1.2.1 Importance and occurrence of Fusarium head blight in Nordic countries

Fusarium head blight (FHB), sometimes known as scab or panicle blight, is an important disease of small grained cereals worldwide (*11, 12*). It affects the heads or panicles during flowering and early to late kernel fill stages. It causes yield and quality reduction and contamination of grains with mycotoxins. Reduced germination capacity (GC) of affected seed lots is a major concern for the seed industry.

A nationwide survey during 1994-1996 found *F. avenaceum*, *F. poae*, *F. tricinctum* and *F. culmorum* to be most prevalent in Norway (*13*). Even though, *F. avenaceum* remains the most prevalent *Fusarium* species in Norway, recent records show increase in *F. graminearum* prevalence making this pathogen the major deoxynivalenol (DON) producer in the Norwegian grain (*6, 7*). Recent increases in prevalence of *F. graminearum* are also reported from Denmark (*14*). In Sweden, *F. graminearum* was isolated from more than 70% of wheat and oats samples collected in 2010 and 2011 (*15, 16*).

The expected climate change in Nordic countries to more warm and humid conditions will favor heavier FHB epidemics and mycotoxin contamination in the future (*17, 18*). Severe *Fusarium* epidemics have already occurred in Norway during 2008-2012 (*7*). These heavy epidemics were due to the above normal precipitation encountered during flowering and kernel fill stages during those years (*7*). Another proposed reason for the increased epidemics of FHB in Norway is the development of specialized cereal production regions which used to integrate grass/ herbage, potato and vegetable production in the past. These epidemics have led to increased levels of mycotoxins in small grained cereals, especially in oats (*7*).

1.2.2 The pathogens and disease epidemiology

Up to 17 pathogen species are associated with FHB (*11*). The most important and frequently isolated species in Europe and North America are *F. graminearum*, *F. culmorum*, *F. avenaceum*, *F. poae*, and *Microdochium nivale*. These pathogens also cause other inter-related diseases such as snow mould, seedling blight, foot and root rot, and leaf spot in cereals

and grasses (11). In addition to cereals and grasses, these pathogens are able to infect a wide range of host species such as *Arabidopsis,* tomato, tobacco, and soybeans (*19-21*).

Fusarium spp. can be identified based on cell culture, microscopic or molecular techniques. Choice of method depends on the purpose and the depth of information required. Colony morphology such as the color of the culture media, presence/absence of sporodochia, and extent of hyphal growth are used for fast identification. Further investigation of morphology of spores and fruiting bodies under the microscope gives more robust and accurate information. Molecular techniques like qPCR that detect and quantify target DNA sequence offer precise species identification.

Figure 1: Signs and symptoms of Fusarium head blight in oats and wheat: premature senescence and pink macroconidia on oats spikelet (A), early infection resulting in empty oats spikelet and dead pedicel (B), white fuzzy mycelia and pink macroconidia of *F. graminearum* on wheat head (C), and premature senescence of wheat head.

There is a wide variation for pathogenicity and aggressiveness within and between *Fusarium* spp. (*22, 23*). *Fusarium graminearum* and *F. culmorum* are the most pathogenic and produce higher levels of mycotoxins (*24*). *Fusarium graminearum* reproduces both sexually and

asexually and hence displays a wide range of aggressiveness, ability to colonize hosts, and produce mycotoxins (*22, 25*).

Fusarium head blight of wheat and barley is favored by warm and wet weather during flowering and early kernel fill stages (*11, 26*). Infection can occur up until yellow maturity if conditions are favorable (*27*). Symptoms include premature senescence of heads and appearance of pinkish-orange mycelia on infected spikelets. Heavy infection results in light-weighted and shriveled kernels. Chalky white appearance of wheat kernels and brownish discoloration of the hulls in oats and barley are common characteristics of *Fusarium*-damaged kernels (Figure 1, (*27*)).

The pathogens survive on soil surface and plant debris as saprophytic mycelia or as thick walled resting spores (*26*). The disease cycle begins with infection of heads by splash-dispersed conidiospores and/ or wind-blown ascospores. Successful head infection leads to FHB whereas leaf infection leads to *Fusarium* leaf spot. Contaminated seed or propagules surviving crop debris provide primary inoculum for seedling blight and foot rot (Figure 2, (*11*)).

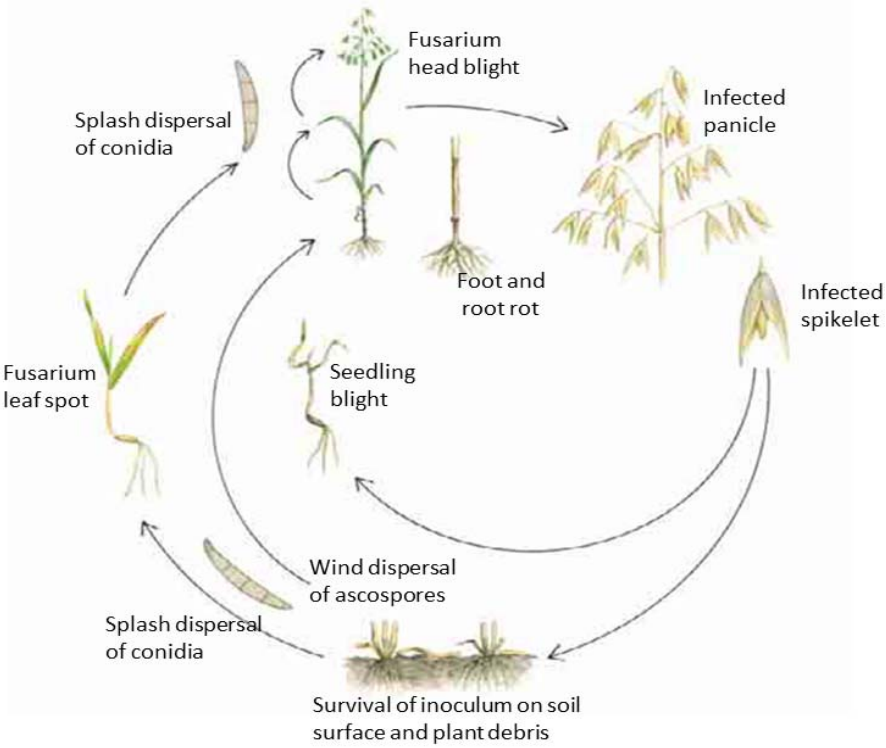

Figure 2: Disease cycle of *Fusarium* diseases. Drawing by Hermod Karlsen from Bioforsk Fokus (*28*).

Agronomic practices affect the incidence and severity of the disease and hence the level of mycotoxin contamination in cereals *(24, 29, 30).* Continuous planting of host species increases the risk of FHB epidemics and mycotoxin contamination of the grain *(24)*. The importance of the previous crop depends on the species, possibly associated with the rate of residue decomposition and amount of crop debris left on the soil surface after harvesting *(31, 32)*. For example, incidence and severity of FHB in wheat were greatest when the previous crop was maize and least when it was soybeans; in a study comparing maize, wheat and soybeans as previous crops *(31)*. Tillage practices also affect FHB through the extent of destruction and burial of crop residue which in turn affect the inoculum load on the current stand (*24, 31, 32*). One of the major reasons for the re-emergence of FHB in the USA is the widespread practice of 'no-tillage' to conserve soil and water (*33*).

Therefore, practices that favor pathogen survival and dispersal should carefully be evaluated. Good agricultural practices including choice of resistant cultivars, crop rotation with non-host species, appropriate residue management, proper application of fungicides and fertilizers, and weed and insect control are recommended to reduce the risk of FHB epidemics and contamination of grain with mycotoxins (*24, 30*).

1.2.3 Infection process of *Fusarium* spp. in small grained cereals

The oat spikelet comprises one to several florets covered by two outer leaves known as the glumes. The developing caryopsis in each floret is covered by the palea and the lemma. The palea covers the ventral surface (the surface with the crease) while the lemma covers the dorsal surface of the caryopsis. In naked oat varieties, the hulls (the palea and the lemma) are lost during threshing whereas in covered oats the hulls are removed during the commercial processing of the grain.

The thick-walled epidermal and hypodermal cells of the external surfaces of wheat and barley florets make direct penetration and infection of these surfaces by *Fusarium* spp. difficult (*34-37*). Since hyphae of *F. graminearum* are susceptible to desiccation (*38*), spores germinating on the external surfaces of florets must access the easily penetrable internal surfaces of the floret cavity to infect successfully (*34-37*). In wheat, spores germinating on the external surfaces of the lemma and the glumes grew over their edges to reach their inner surfaces where penetration of host tissues occurred (*36, 37*). Successful infection and penetration also occurred on the inner surfaces of the palea and the upper part of the ovary (*36, 37*). In barley, the floret mouth and the crevices between the overlapping palea and lemma were found to be

the principal entry pathways of *F. graminearum* into the floret cavity (*34*). A study on the infection process of *F. langsethiae* in oats showed that infection started on the apical part of the florets or between the overlapping palea wings and the lemma progressing into the floret cavity and the caryopsis (*39*).

Anthers play an important role at the initial stages of *Fusarium* infection. Wheat genotypes with high anther extrusion (AE) tended to develop less FHB and DON compared to genotypes with low AE (*40*). Earlier observations showed that initial symptoms of FHB and prolific mycelial growth of *F. graminearum* appeared on the anthers of wheat (*41-44*). Later, betaine and choline were isolated from anthers and characterized as the fungal growth stimulants (*45*). These chemicals were found in greater concentrations in anthers than in other floret parts (*46*). In barley, chasmogamous genotypes (with open flowering) were most susceptible to *Fusarium* infection at anthesis while cleistogamous genotypes (with closed flowering) were most susceptible 7-10 days after anthesis when spent anthers were pushed out by the developing caryopsis (*47*). Another study showed hyphal growth of *F. langsethiae* on the surfaces of the palea, lemma, and glumes of oats florets was facilitated by the presence of pollen (*39*). All these studies suggest that anthers are the foci for *Fusarium* infection.

However, there are studies that reported the role of anthers in floret colonization to be insignificant (*34, 36, 48*) Inoculated wheat heads were invaded by *F. culmorum* at other easily penetrable parts of the floret regardless of the presence or absence of anthers; even though retained anthers were densely colonized (*36*). Another study reported, the invasion of anthers by *F. graminearum* had only a minor role in the invasion of barley florets (*34*). In an *in vitro* experiment, spore germination and hyphal growth of *F. graminearum* was not affected by choline, betaine or by their combinations (*48*). These differences among reports on the role of anthers might be dependent on the genetic resistance of the crops, the crop and the pathogen species and the inoculation method used. Further studies are required to clarify these issues.

Time of infection affects severity of FHB (*47, 49-54*). This effect can be evaluated by comparing level of mycotoxin contamination, kernel infection and thousand seed weight of samples from heads infected at different developmental stages. Cereals are most susceptible around anthesis with decreasing susceptibility at later stages (*51-53*). Wheat was found to be susceptible to *F. graminearum* infection from flowering to the hard dough stage with highest incidence of scabby kernels and DON at flowering (*50*). Others reported highest disease incidence and DON at mid-anthesis with decreasing effects at later stages (*49*). Under

favourable conditions, however, significant kernel infection and mycotoxin accumulation can also occur at later stages (*27, 50*).

1.2.4 Effects of Fusarium head blight on germination and grain quality

Seed lots from FHB-affected areas often have reduced GC (*55-57*). Loss of germinability, reduced emergence, and post-emergence blight of seedlings are the various forms of reduced GC (*57, 58*). *Fusarium*-infected kernels may have viable germ (*59*). Kernels with viable germ, however, are contaminated by *Fusarium* toxins and pathogen propagules. Therefore, such kernels may produce less vigor seedlings due to the toxins and infections during germination. Reducing contamination, for example by surface sterilization, can increase GC of the seed (*60*). Other studies showed that seed dressing, cleaning, dehulling and size sorting improve GC by reducing pathogen propagules and removing *Fusarium*-damaged kernels from the lot (*56, 57, 60, 61*).

Fusarium spp. display different levels of aggressiveness in causing seedling blight; *F. graminearum* is the most aggressive and *F. poae* and *F. langsethiae* are the least (*62, 63*). The trichothecenes are one factors of aggressiveness (*64*). Seedling emergence and survival of barley, triticale, common and durum wheat were significantly lower when infected by trichothecene producing strain of *F. graminearum* compared to the non-trichothecene-producing strain (*64*). In addition, a significant correlation between disease index and DON content of blighted seedlings was found in barley infected with *F. culmorum (65)*. The toxin also proved to inhibit the growth of wheat seedlings in an *in vitro* experiment (*66*). This effect depends on the type and relative concentration of the trichothecenes (*67, 68*).

Fusarium head blight may seriously reduce grain quality. *Fusarium graminearum* infection in barley resulted in significant reduction in kernel plumpness (*56*). In wheat, infection resulted in poor baking performance and flour color, reduced loaf volume, and weak dough properties (*69-71*). Infection destroyed starch granules, storage proteins, and cell walls (*59, 71*). Wheat kernels infected with *F. culmorum* also displayed damaged starch granules, complete or partial lack of the protein matrix, and under severe infection, complete disappearance of the starchy endosperm (*72*). Significant degradation of the endosperm protein and lower content of storage proteins in *F. avenaceum*- and *F. graminearum*-infected wheat were also reported (*70*). Another study, however, suggested that high *Fusarium* infection and DON contamination are not necessarily associated with poor baking quality and good baking performance can still be attained even under heavy contamination (*73*).

1.2.5 Evaluation and types of resistance to Fusarium head blight

Resistance to FHB is partial or incomplete and has oligo- or polygenic inheritance (*74*). It is a complex quantitative trait and is non-specific to causative species or isolates within species (*75, 76*). Therefore, resistance to a given *Fusarium* species provides protection against other *Fusarium* species. Resistance is evaluated by artificially inoculating test genotypes in the field or in the greenhouse. Inoculum can be in the form of macroconidia, ascospores, chlamydospores or hyphal fragments depending on the chosen *Fusarium* species and the inoculation technique (*77*). In spray inoculation, macroconidial suspension of *Fusarium* spp. is sprayed on flowering heads. In point inoculation, the suspension is injected directly into the floret, giving the spores easy access into the floret cavity. In spawn inoculation, kernels colonized by *F. graminearum* are spread on the ground to produce perithecia and release ascospores into the air. Inoculation is followed either by regular periods of mist irrigation for 1-2 weeks, or covering of inoculated heads with plastic bags for 2-3 days to facilitate spore germination and infection (*77*).

Resistance mechanisms to this disease can be classified as active and passive. Active resistance mechanisms are physiological responses that are actively incited in the presence of infection. Five types of active resistance mechanisms have been defined in wheat (*27, 52*). Type I and type II are resistance to initial infection and resistance to spread of infection, respectively (*52*). Type III and type IV are resistance to kernel infection and tolerance, respectively (*27, 74*). Tolerant genotypes have minimal yield loss compared to less tolerant genotypes under the same disease pressure (*74*). Type V is resistance to toxins (*78*), which can be expressed as higher rate of toxin decomposition, insensitivity to toxins or lower toxin accumulation in the head tissue (*27, 74, 78*). These resistance types are independent but are often genetically linked (*27*); and hence have moderate correlation. These resistance types were defined in wheat; but they are also found and can be scored in other small grained cereals.

Passive resistance mechanisms are morphological traits that affect inoculum deposition and/ or establishment of infection on heads in one way or another. These mechanisms do not depend on the presence or absence of infection. Plant height and length of (the upper) internodes affect deposition of inoculum from the ground to the head, hence taller genotypes escape infection (*27, 74*). Spike morphology, such as presence or absence of awns, spike density, flower opening, and AE affect resistance by affecting the microclimate and

accessibility of the spike to infection (*27, 74, 79*). Genotypes with awn-less spikes, intermediate spike density, closed flowering and/ or high AE display higher level of resistance than genotypes with the opposite attributes, given the same level of active resistance (*27, 40*).

The different morphological traits linked to FHB resistance are found to be associated with the active resistance mechanisms. For example, QTLs for plant height and AE are associated with type I resistance in wheat (*80*). In oats, QTLs for lower DON and FHB were coincided with QTLs for days to heading, days to maturity, and plant height (*81*).

Figure 3: Resistant (A) and susceptible (B) oats genotypes in the field inoculated with *F. graminearum.* Plots were planted and inoculated on the same day.

1.2.6 *Fusarium* mycotoxins

Mycotoxins are secondary metabolites produced by field and storage fungi. Field fungi usually require higher moisture of about 22-25 % while storage fungi can contaminate produce at a lesser moisture level of 13-18 % (*82*). *Fusarium* spp. are among the field fungi that infect and contaminate grains during kernel development.

Fusarium spp. differ in their mycotoxin production profiles (*83*). *Fusarium graminearum* and *F. culmorum* produce DON and its acetylated derivatives (3ADON and 15ADON), nivalenol (NIV), zearalenon (ZON) and fusarenon X (FUS-X) (*83*). *Fusarium langsethiae* and *F. sporotrichioides* produce T-2, HT-2 and neosolaniol and diacetoxyscripenol (*83*).

Deoxynivalenol is phytotoxic and acts as a virulence factor (*84*). *Fusarium graminearum* strains capable of producing DON are more aggressive than the non-producing strains (*85*).

The trichothecenes are a major group among the *Fusarium* toxins. Based on their chemical structure, these toxins are broadly divided into two groups, as type A and type B. T-2 and HT-2 toxins, the most toxic among the trichothecenes (*86*), belong to type A trichothecenes. Deoxynivalenol, 3ADON, 15ADON, NIV, and FUS-X belong to type B trichothecenes.

Mycotoxins have significant impact on the health and performance of humans and animals. The trichothecenes are gastrointestinal toxins, dermatotoxins, immunotoxins, haematotoxins and gene toxins (*87*). These toxins cause acute and chronic illnesses both in humans and animals. These include skin inflammation, diarrhea, oedema, skin necrosis, hemorrhages in the stomach and large intestine, tumors of the thyroid and bile duct, feed refusal and vomiting (*87-89*). For example, pigs fed with DON-contaminated diet show poor performance and reduced weight gain and feed utilization efficiency (*90, 91*).

Regulations for maximum permissible levels of *Fusarium* mycotoxins in raw and finished food items are therefore in place to ensure consumer safety (*92*). The European Commission limits for DON and ZON in unprocessed wheat and oats are at 1750 and 100 ppb, whereas the limits in finished cereal-based food items are at 500 and 50 ppb, respectively (*93*).

Physical methods during grain processing, such as dehulling and size sorting and removal of discolored grains, are shown to substantially reduce mycotoxin contamination (*93-97*). These procedures remove the hulls and the highly contaminated, shriveled and scabby kernels. For example, substantial reduction of DON, ZON, HT-2 and T-2 toxins by up to 90-95 % was achieved during processing of raw oats to oat flakes (*93*), with the major reduction occurring during the dehulling process (*93, 96*). Heat-treating or kilning and removal of discolored groats were also proven to reduce mycotoxin contamination (*93, 97*). One should keep in mind, however, healthy looking sound kernels may still be contaminated with substantial level of mycotoxins (*98*).

1.3 Conventional and rapid methods for detection of mycotoxins and *Fusarium* damage

There are several conventional and rapid methods for detecting mycotoxins and *Fusarium* damage in grains and other food products. Methods for mycotoxin detection can be broadly categorized as chromatographic, immunochemical, and spectroscopic. Chromatographic and immunochemical methods are considered invasive because they involve sample destruction and some level of wet chemistry (*99*). On the other hand, spectroscopic methods are non-invasive and samples can be (re-) used for other purposes after recording spectral information (*99*).

Chromatographic methods include gas chromatography, liquid chromatography, high performance liquid chromatography, thin layer chromatography and others (*100, 101*). These methods are highly sensitive, selective and accurate (*100, 101*). They require extensive extraction and sample clean up procedures carried out by expert personnel (*101, 102*). These methods serve as standard reference methods but are not recommended for screening purposes where lower accuracy and precision suffice and quick results are required.

Immunochemical methods are rapid and inexpensive antibody-based methods (*103*). Enzyme linked immunosorbent assay (ELISA) and lateral flow devices (LFDs) are commonly used to detect DON in cereal matrices. ELISA do not involve sample clean up procedures and toxin detection can be carried out right after sample extraction. In LFDs, the sample flows by capillary forces along an analytical membrane that contains immobilized immunoreagents to give a 'yes' or 'no' result (*101*). Cross reactivity of antibodies with closely related toxins makes both ELISA and LFDs less accurate and less precise compared to chromatographic methods (*101, 103*). In addition, differences in the accuracy and precision within rapid test kits (ELISA and LFDs) in detecting *Fusarium* mycotoxins in naturally contaminated Norwegian oats and wheat (DON, 3ADON, T-2 and HT-2) was observed (*104, 105*).

Spectroscopic methods are very rapid methods that require no/ minimal sample preparation. They are environmentally friendly analytical tools as they do not involve the use of chemicals that end up in the environment (*106-108*). Three emerging spectroscopic methods; visible-near infrared (VIS-NIR) spectroscopy, hyperspectral imaging (HSI), and electronic nose are used for detecting *Fusarium* damage and mycotoxin contamination (*99*). In this thesis, VIS-NIR spectroscopy and HSI were used to detect DON-contamination and *Fusarium* damage in

oats. Therefore, the current status of VIS-NIR spectroscopy and HSI in detecting *Fusarium* damage and toxins are discussed in the following sections.

1.3.1 Visible and near infrared spectroscopy

The VIS region spans the wavelength range of 380-780 nm and the NIR region covers the 780-2500 nm region. A wide array of samples (samples containing C-H, N-H, S-H or O-H bonds) can be probed and analyzed by NIR spectroscopy (*109*). Near infrared spectroscopy is a type of vibrational spectroscopy and information is gathered from the interaction of matter with electromagnetic waves. When NIR beam passes through a sample, energy is absorbed at specific wavelength regions by molecules comprising the sample (*109*). Radiation interacting with samples may be absorbed, reflected or transmitted. Depending on the measurement mode of the spectrophotometer, one can have NIR transmittance, reflectance, transflectance, diffuse transmittance, or diffuse reflectance spectroscopy (*106, 107*).

Near infrared spectra are composed of absorptions due to overtones of fundamental vibrations, combinations of fundamental vibrations, and electronic absorptions occurring in the infrared region (*110*). The resulting spectra provide absorption characteristics of the sample giving quantitative and/ or qualitative information (*109*). Near infrared spectra provides multiconstituent measurements and is affected by the physical attributes of the sample (*106-108*).

There are a few limitations to NIR spectroscopy as an analytical tool. It is not a highly sensitive method and is generally applied to determine concentration of major constituents. The spectra is hardly selective and is influenced by a number of physical, chemical, and structural variables (*111*). In addition, utilization of NIR spectra relies on multivariate approach for calibration. The resulting model may be complex and difficult to interpret chemically (*109*). Calibration samples should comprise large number of samples that encompass the variations in physical and chemical properties of the population (*111, 112*). NIR spectroscopy is a secondary tool as it is always dependent on the standard reference method during calibration (*109*).

Several studies have utilized NIR spectroscopy to predict DON level in ground or whole kernels (*113-117*). Visible and NIR spectroscopy detect discoloration and changes in the main grain components like carbohydrates, proteins and lipids that result from *Fusarium* infection (*59, 72, 118*). These signals can be utilized while constructing a model to quantify a specific

Fusarium toxin (*119*). However, the correlation between degree of *Fusarium*-damage and toxin content can vary significantly (*98*). Therefore, accuracy of NIR spectroscopy is highly dependent on the relationship between degree of *Fusarium* damage and the actual toxin level (*119*). It is important to keep in mind that sound looking kernels can have a substantial DON level while scabby kernels are not necessarily contaminated with high levels of DON (*98*).

Most VIS-NIR spectroscopy studies for detection of mycotoxins and *Fusarium* damage in grains aim at detecting and removing *Fusarium*-damaged kernels from seed lots to reduce level of toxin contamination (*113, 120*). Others classify *Fusarium*-damaged from sound kernels based on the distinct physical and structural attributes of *Fusarium*-damaged kernels (*114, 115, 121*). This is of high significance in the grain industry that needs to meet mycotoxin legislations for maximum tolerable limits in food and feed items.

Near infrared spectroscopy successfully classified single wheat kernels as sound and scabby (*113, 114, 121*). Classification accuracy increased by including kernel mass in the NIR model (*113*). The wavelengths that were important to predict scab damage and DON contamination were found throughout the 500-1700 nm region (*114*). The effect of scab on starch and protein of the developing kernels (*59, 72*) was assumed to be the cause of the specific absorptions in the region (*114*). Sound kernels had higher spectral absorption due to their higher optical density resulting from their higher kernel weight and moisture content while scab-damaged kernels displayed the least absorption (*121*). A regression model that used near infrared transmittance spectra of a series of dilutions of *F. culmorum*-infected wheat flour had 11 PLS factors, R^2 value of 0.97 and SECV of 381 ppb (*116*). A model with R^2 value of 0.93 and SEP of 3.1 ppm was developed using NIR spectra of 188 barley samples (DON mean= 13.57 ppm) of four varieties from two experimental years (*117*).

1.3.2 Hyperspectral imaging

Hyperspectral imaging combines conventional imaging and spectroscopy to attain both spatial and spectral information from a sample (*108*). It has higher sensitivity to minor constituents than conventional NIR spectroscopy. Each pixel in a hyperspectral image contains the spectrum of that specific position. This information can be used to construct a chemical map of the parameter of interest in the sample (*122, 123*). It can also be used as a finger print from which multiconstituent information is extracted (*108*).

Hyperspectral imaging provides a three-way data matrix known as a hypercube with two spatial (x, y) and one wavelength (λ) dimensions (Figure 4). It is made of hundreds of single channel, grayscale images each representing a single band of spectral wavelength (*108*). The large magnitude of information in hyperspectral images requires extensive data processing and analysis to extract meaningful information (*122*).

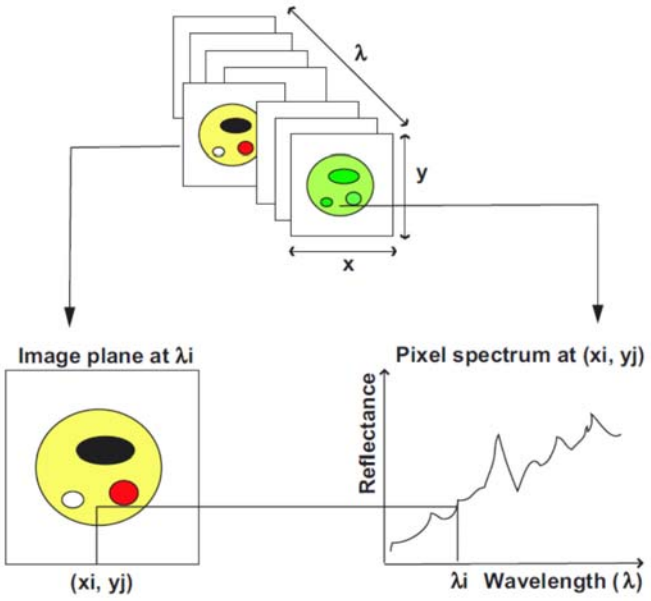

Figure 4: Relationship between spectral and spatial dimensions in a hyperspectral imaging hypercube. The hypercube can be considered as a three dimensional stack of images made of two spatial dimensions (x_i, y_j) and a wavelength dimension (λ_i) (*108*).

Four general steps; image correction, data pre-processing, classification, and image processing, are followed in analysis of hyperspectral images. Image correction is carried out to account for the background spectral response and 'dark' camera response. Data preprocessing is used to remove noise and non chemical biases from the spectra. Classification is used to identify regions of similar spectral characteristics using multivariate methods such as principal component analysis, partial least squares or linear discriminant analysis. Finally, image processing is conducted to map the differences developed during classification to show component distribution (*108, 122*).

Spectral information from pixels in a hyperspectral image can be used to classify kernels and kernel regions based on fungal damage and/ or DON contamination (*108, 123, 124*). For example, HSI successfully identified maize kernels and regions within each kernel infected

by *F. verticillioides* (*123*). It has also been used to detect *Fusarium* damage in wheat (*125-127*) and to differentiate between various species of toxigenic fungi (*128*). Visible-NIR (450-950 nm) hyperspectral imaging system was able to classify wheat kernels into sound and *Fusarium*-damaged with accuracy of 92% (*129*). It was possible to further classify the *Fusarium*-damaged kernels as severely and mildly damaged with an accuracy of 86 %. In another study, extended VIS-NIR (400-1000/ 1000-1700) hyperspectral imaging system was shown to discriminate between *Fusarium*-damaged and sound wheat kernels with an average accuracy of 95% (*125*). In this study, the spectral absorption near 1200 nm, which was tentatively attributed to ergosterol was found to be useful for classification (*125*).

1.3.3 Multivariate model construction

Spectroscopic methods rely on multivariate techniques to extract useful information from large collinear spectral data sets. Multivariate model construction follows a few general steps. It starts with assembling a calibration set of samples that encompass the chemical and physical variations of the population. Physical and multiconstituent information of the calibration set is then recorded by taking spectral data. The parameter of interest should then be determined by the standard reference method to be paired up with the spectral data for model construction. Noise and unwanted information from the spectral data must be removed by subjecting the spectral data to various data pre-treatments prior to model construction. These pre-treatments include normalization, derivatives, multiplicative scatter correction, standard normal variate, or their combinations. Principal component analysis or partial least squares are then used to reduce dimensionality and colinearity from the spectra. Multivariate methods such as multiple linear regression, principal component regression, or partial least squares regression (PLS-R) are used to establish the relationship between the spectra and the parameter of interest to make the calibration model. The developed model is then validated by predicting the parameter of interest in validation set samples that were not included in the calibration set. This will test the performance of the model in predicting the parameter of interest in future samples. Finally , the developed model will be applied to predict the value of the parameter of interest in unknown samples (*106, 112, 130*).

2 The thesis

2.1 Background

Fusarium head blight is a major concern of food and feed growers, processors and consumers. It is a concern for growers because of the significant yield reduction in the field (*12, 131*) and the monetary penalty associated with mycotoxin contamination and poor grain quality upon delivery. It is a concern to processors as it poses a challenge to meet current quality and food safety standards (*98*). It is a concern to consumers because of the various ailments that are associated with *Fusarium* mycotoxins (*132*). Plant breeding plays an important role in addressing these issues by producing resistant cultivars with good yield, less mycotoxin contamination and grain damage in spite of the presence of the causative pathogens and a favorable environment for disease development. It is the most economically feasible and environmentally friendly way of managing FHB.

Breeding for FHB resistance starts with collecting and testing diverse germplasm under natural infection or artificial inoculation in the field or in the greenhouse. Plants are evaluated in the field for type I and type II resistance. Post-harvest tests for kernel infection, GC and toxin contamination evaluate the other types of resistance. Field experiments and evaluations should be standardized to get repeatable results and reliable data. Understanding the infection process, in terms of the infection pathways and the optimal time of infection, is important to standardize inoculation experiments and increase precision in phenotyping. Knowledge about the relationships among the post-harvest parameters is important to properly interpret data and evaluate resistance. In addition, the cost of chemical DON analyses is a major hurdle during screening genotypes. Rapid tools, such as VIS-NIR spectroscopy and hyperspectral imaging, are attractive options to replace the costly conventional chemical analyses.

This PhD study has two major themes. The first focuses on *Fusarium* infection and its subsequent effects in oats. In this part of the study, the optimal time of infection, the infection pathways, and effect of infection on- and the relationship among GC, DON, and kernel infection were investigated (***Paper I*** *(133)* and ***II*** *(134)*). The second theme focuses on testing the feasibility of spectroscopic methods as rapid screening tools. The potential of conventional VIS-NIR spectroscopy and NIR hyperspectral imaging to discriminate *Fusarium*-infected oats based on the level of DON contamination and *Fusarium* damage were evaluated (***Paper III*** *(135)* and ***IV***).

2.2 Main results and discussions

2.2.1 The infection process of *Fusarium* spp. and effects on germination and DON level of oats (Papers I and II)

In the **first paper** (*133*) studies on the infection pathways of *F. graminearum* into oats florets and effect of time of inoculation on kernel infection, GC and DON contamination were reported. To determine the most susceptible stage of oats to *Fusarium* infection, field-grown oats were inoculated with macroconidia of *F. graminearum* at anthesis, and one and two weeks after anthesis. Uninoculated plants were used as control. Kernel infection, GC, and DON content were determined on harvested kernels. All the three parameters; kernel infection, GC, and DON content were significantly affected by time of inoculation. The most susceptible stage of oats to *F. graminearum* infection was found to be anthesis, as indicated by highest levels of kernel infection and DON content and lowest GC. Even though not as severe as the inoculation at anthesis, later inoculations also led to kernel infection, DON accumulation, and lowered the GC of the seeds.

To study infection pathways, greenhouse-grown plants were spray-inoculated with macroconidia of *F. graminearum* at anthesis; as anthesis was determined to be the most susceptible stage to *Fusarium* infection. Plants were placed in a moisture chamber for three days following inoculation and placed back in the greenhouse for the following days. Sixty florets were sampled every day, for one week following inoculation. These florets were fixed and stained in lacto phenol blue solution for microscopic study. To study the role of anthers during the initial stages of the infection process, anthers were collected two, three, four and seven days after inoculation and were studied under the microscope. In a separate study, five oats genotypes with different levels of AE were inoculated at flowering. Percentage of infected florets of the genotypes was compared to see if AE has role in the level of passive resistance.

Results showed that *F. graminearum* primarily entered *via* the floret mouth into the floret cavity to the easily penetrable internal surfaces of the palea, lemma, and the developing caryopsis. Both disease symptoms and fungal infections started at the apical portions of the florets. The basal portions were rarely found diseased, only after the whole floret has been colonized by the fungus. More profuse fungal growth was observed on the anthers than any other floret part during the first few days after inoculation. This explained the abundant apical

symptoms and infections compared to the rare basal symptoms and infections. Genotypes with higher AE displayed a much less infection level compared to genotypes with low AE.

In the **second paper** (*134*) studies on the relationship among GC, DON and kernel infection in *F. graminearum*-inoculated oats were reported. Growth chamber, greenhouse and field experiments were employed. The growth chamber study was designed to study the effect of different levels of DON on germination and seedling vigor of the oats cv. Hurdal. Kernels were placed on water agar amended with 0, 2, 5, 10, 15, and 20 ppm DON. Data on coleoptile and radicle length and GC were recorded at the end of a 14-day long incubation period. The GC of the control kernels (0 ppm) was 100%. All the kernels in the DON-amended WA (except for two kernels in the 15 ppm WA) started to germinate. However, the growth of these seedlings was retarded; the higher the DON the shorter the radicle and coleoptile lengths. Most of the seedlings exposed to more than 2 ppm DON would not be considered as 'germinated' according to the standard germination tests due to their poor vigor and abnormal morphology.

The greenhouse experiment was conducted to see the effect of late infection on DON level, kernel infection and GC of oats. Plants were spray inoculated with *F. graminearum* at 2 days before anthesis, 5, 12, 19 days after anthesis and at yellow maturity. Time of inoculation had significant effect on all measured parameters. Deoxynivalenol level was highest and GC was lowest for the inoculation done at 5 days after anthesis. Deoxynivalenol level decreased rapidly for later inoculations. However, the expected increase in GC was not as rapid. Kernel infection was high for all inoculation (61-91%). Therefore, we deduced that in addition to DON, level of kernel infection plays an important role in determining GC of *Fusarium*-affected seed lots. Another interesting observation from this experiment was that inoculation prior to anthesis resulted in lower DON contamination and higher GC than inoculating slightly after anthesis (5 days after anthesis in this case). This is in line with our observation that anthers are important factors in the infection process of *Fusarium* spp. in oats.

In the field experiments, several oats genotypes (n= 32-99) were spawn and spray inoculated during 2007-2010 experimental years. Germination capacity and DON level of the genotypes were determined at harvest. Correlation analyses were conducted and results were interpreted based on the inoculation method used and the weather conditions in July and August of the experimental years. Germination capacities were lower than the percentage of viable seeds (determined by the tetrazolium test) indicating further reduction of GC due to seedling blight

during germination. It was possible to eradicate seedling blight and raise GC to the percentage of viable seeds by combining dehulling and seed dressing. Neither dehulling nor seed dressing were effective enough when employed alone.

Negative and statistically significant correlations between DON and GC were found in all experiments. The strongest and the weakest correlations were found for spray and spawn inoculation of 2009, respectively. Since the genotypes were growing in the same weather conditions of that year, the difference in the relationship of DON and GC were attributed to differences in level of kernel infection. Spray inoculum is applied once at flowering while spawn inoculum is spread in the experimental fields to produce and release ascospores over an extended period of time. Therefore, infections can occur in spawn inoculated nurseries as long as the weather conditions are conducive for ascospore release and disease development. 2009 was a wet year and hence was conducive for late infections. Early infections are capable of killing the germ and significantly lower the GC. In addition, such infections can cause high DON accumulation in the kernels. On the other hand, late infections that can be facilitated by wet conditions late in the season do not kill the germ but can lead to low GC, most likely as a result of superficial infections causing seedling blight during germination and emergence.

2.2.2 Feasibility of VIS-NIR spectroscopy in screening *Fusarium*-inoculated oats genotypes (Papers III and IV)

The **third paper** (*135*) investigated the potential of conventional VIS-NIR spectroscopy as a rapid resistance screening tool. DON-contaminated samples of more than 60 genotypes from four experimental years were used for calibration (n= 111) and validation (n= 55). Kernels were ground before taking spectra to reduce heterogeneity arising from differences in level of kernel infection and DON contamination. Gas chromatography coupled with mass spectrometry was used as the standard reference method for DON determination. The spectra were pre-treated by the second derivatives and second polynomial order option of the Savitzky-Golay derivatives. Levels of absorption in both the original and 2nd derivative spectra segregated the samples as low- , medium- , and high-DON samples. In the original spectra, low-DON samples tended to have lower absorption level at the VIS region and higher absorption at the NIR region than high-DON samples. This effect was most likely due to differences in physical attributes such as color and texture of the samples. It was possible to tell by visual examination that low-DON samples were lighter in color and finer in texture while high-DON samples were darker in color and coarser in texture. The 2nd derivative

spectra resolved peaks that classified the samples in to two-three classes, indicating compositional differences among the different DON classes. For example, low-DON samples had more water (≈ 1432 and ≈ 1924 nm) and fat (≈1701 and ≈1725 nm) content than high-DON samples. The accuracy of VIS-NIR spectroscopy in predicting DON is highly dependent on the relationship between *Fusarium* damage on major seed constituents and DON level, as it is difficult to directly detect minor seed components such as DON using VIS-NIR spectroscopy.

Partial least squares regression (PLS-R) was used to develop a model predicting the level of DON by using the reference DON level as y-variable and the 2nd derivative spectra as x-variables. It was difficult to attribute specific wavelength region to DON *per se*; but it was possible to use the effect of *Fusarium* infection on the physical and chemical attributes of the kernels to develop regression models. In that way, we developed stable models that can satisfactorily predict DON level of the tested oats samples. The best model was developed by using the whole wavelength region (400-2350 nm). The model had only three PLS components and RPD value of 2.63. The RPD value is not excellent but is acceptable for rough screening of resistance at the early stages of breeding programs. Other models that were developed using only the VIS or the NIR region were poorer as displayed by their lower RPD values (2.19 and 2.36, respectively). Much higher RPD values than what we have found in our models are required for routine screening of samples at the milling industry or at later stages of a breeding program.

The **fourth paper** investigated the feasibility of NIR HSI in detecting *Fusarium* damage and DON contamination in whole oats kernels. Hyperspectral imaging has higher sensitivity to minor seed constituents than conventional VIS-NIR spectroscopy. In the third paper we have used ground samples to homogenize the variation in *Fusarium* damage and DON level among kernels of a sample. Therefore, we hypothesized that combining the higher sensitivity of NIR HSI and the DON variation of whole kernels would result in a better NIR calibration model to evaluate resistance of oats genotypes to FHB.

Kernels of the susceptible oats cv. Bessin from a *F. graminearum*-inoculated nursery were visually categorized as severely damaged, mildly damaged and asymptomatic. Uninoculated kernels of the same cultivar were included as control. Hyperspectral images of 31 calibration kernels and 14 validation kernels of each kernel category were taken. Deoxynivalenol content and weight of the kernels were determined following imaging. Surfaces of hulled and dehulled

kernels as well as cross sections from each kernel category were investigated under the scanning electron microscope.

The uninoculated and the asymptomatic kernels were plump and free of any fungal mycelia while the severely damaged kernels were shriveled and heavily colonized with *F. graminearum*. Dense mycelia were observed on the crease of the severely damaged kernels. The cross sections of uninoculated kernels revealed a well-formed aleurone layer and intact endosperm structure, while the severely damaged kernels showed a collapsed and highly colonized aleurone layer with partially digested endosperm structure. Damage to the seed coat and the aleurone layer were also observed in the mildly damaged kernels but the inner endosperm structure was intact.

The asymptomatic kernels had the highest mean kernel weight and the lowest mean DON content while the severely damaged kernels had the lowest mean kernel weight and the highest DON content. However, there were a few kernels with very low DON in the severely damaged kernels category and a few kernels with substantial DON in the asymptomatic kernels category indicating visual symptoms do not necessarily match the DON content of kernels.

A calibration model was developed using PLSR by pairing the average spectrum of each kernel with DON*= [log (DON)] ^3. The model was optimized by cross-validation, and the prediction performance was validated by predicting DON* values of the validation kernels. Linear discriminant analysis was used to classify kernels. The model predicted clear differences between kernel categories and the first component separated the uninoculated/ asymptomatic kernels from the severely damaged kernels. Infected kernels showed higher intensities at 1920, 2070 and 2140, while non-infected kernels were dominated by signals at 1420, 1620 and 1850 nm. The DON* value for the validation kernels were estimated using the average spectrum, and the correlation between predicted and measured DON* was 0.82 showing that the prediction model was valid.

2.3 Conclusions and future work

2.3.1 Conclusions

Oats are most susceptible to *Fusarium* infection at flowering. This was shown by the lowest GC and highest DON content and kernel infection for inoculations done at flowering compared to later inoculations. Anthers play an important role at this stage and AE may be a form of passive resistance in oats. Infections do occur at later growth stages and can lead to germination problems. Such infections cause less toxin contamination compared to earlier infections. However, this may still pose a concern for feed and food processors that need to meet mycotoxin regulations. Therefore, conditions that facilitate *Fusarium* infection should be monitored and addressed not only around flowering but also at later growth stages.

Heavy and/ or early *Fusarium* infections result in floret sterility, which can be more than 50% in very susceptible genotypes (unpublished data). Such infections also result in very light-weighted kernels which are blown away during harvesting. Relying only on laboratory tests (germination, seed infection, and DON analyses) on harvested kernels can therefore, underestimate the real effect of FHB. Therefore, integrating yield loss (or tolerance as described by Mesterhazy (*74*)) as a screening parameter in field trials should be considered.

The evaluations on the feasibility of conventional NIR spectroscopy and NIR HSI showed that spectroscopy could be used as a screening tool at the early stages of a breeding program where rough grading of genotypes is sufficient. In addition, the results from HSI study suggest that the method can be applied on whole kernels to detect and remove *Fusarium*-damaged kernels, thereby reducing toxin contamination and increasing industrial quality of oats seed lots.

2.3.2 Future work

I. Studies on the infection process of *F. graminearum* in oats indicate that anthers are a major avenue of infection. Therefore, a comprehensive study in a diverse collection of oats genotypes to investigate AE as a passive resistance mechanism in oats is recommended.
II. Clear understanding of the flowering biology of oats (in terms flower opening, AE) would be a good background for interpreting the FHB resistance parameters.
III. Results from the NIR work showed that conventional NIR spectroscopy can be used as a rough screening method in *Fusarium*-inoculated oats nurseries. The model should

be kept updated with new samples from different experimental environments and years. In addition, investigating VIS-NIR spectroscopy in *Fusarium*-inoculated wheat and barley nurseries will be of great significance to breeders.

IV. Hyperspectral imaging of *Fusarium*-damaged kernels showed that NIR spectroscopy can identify individual kernels with DON and *Fusarium* damage with better accuracy than visual inspection. Investigating the application of these findings in whole kernels (as bulk sample or single kernel NIR spectroscopy) is recommended

3 References

1. Marshall, A.; Cowan, S.; Edwards, S.; Griffiths, I.; Howarth, C.; Langdon, T.; White, E., Crops that feed the world 9. Oats- a cereal crop for human and livestock feed with industrial applications. *Food Security* **2013,** *5*, 13-33.

2. Strychar, R., World oat production, trade and usage. In *Oats chemistry and technology*, 2nd ed.; Webster, F. H.; Wood, P. J., Eds. AACC International: Saint Paul, 2011; pp 1-10.

3. Welch, R. W., Nutrient composition and nutritional quality of oats and comparisons with other cereals. In *Oats chemistry and technology*, 2nd ed.; Webster, F. H.; Wood, P. J., Eds. AACC International: Saint Paul, 2011; pp 95-107.

4. Peterson, D. M., Oat antioxidants. *Journal of Cereal Science* **2001,** *33*, 115-129.

5. Behall, K. M.; Hallfrisch, J., Oats as a functional food for health. In *Oats chemistry and technology*, 2nd ed.; Webster, F. H.; Wood, P. J., Eds. AACC International: Saint Paul, 2011; pp 255-273.

6. Hofgaard, I. S.; Aamot, H. U.; Klemsdal, S. S.; Elen, O.; Jestoy, M.; Brodal, G. In *Occurrence of Fusarium spp. and mycotoxins in Norwegian wheat and oats*, Nordic-Baltic Fusarium seminar, Ski, 2010; Hofgaard, I. S.; Fløistad, E., Eds. Bioforsk: Ski, 2010; p 37.

7. Sundheim, L.; Brodal, G.; Hofgaard, I. S.; Rafoss, T., Temporal variation of mycotoxin producing fungi in norwegian cereals. *Microorganisms* **2013,** *1*, 188-198.

8. Valentine, J.; Cowan, A. S. A.; Marshall, A. H., Oat breeding. In *Oats chemistry and technology*, 2nd ed.; Webster, F. H.; Wood, P. J., Eds. AACC International: Saint Paul, 2011; pp 11-30.

9. Nersting, L. G.; Andersen, S. B.; Bothmer, R. v.; Gullord, M.; Jørgensen, R. B., Morphological and molecular diversity of Nordic oat through one hundred years of breeding. *Euphytica* **2006,** *150*, 327-337.

10. He, X.; Bjørnstad, Å., Diversity of north European oat analyzed by SSR, AFLP, and DArT markers. *Theoretical and Applied Genetics* **2012,** *125*, 57-70.

11. Parry, D. W.; Jenkinson, P.; McLeod, L., Fusarium ear blight (scab) in small grain cereals—a review. *Plant Pathology* **1995,** *44*, 207-238.

12. Goswami, R. S.; Kistler, H. C., Heading for disaster: *Fusarium graminearum* on cereal crops. *Molecular Plant Pathology* **2004,** *5*, 515-525.

13. Kosiak, B.; Torp, M.; Skjerve, E.; Thrane, U., The Prevalence and distribution of *Fusarium* species in Norwegian cereals: a Survey. *Acta Agriculturae Scandinavica* **2003** *53*, 168-176.

14. Nielsen, L. K.; Jensen, J. D.; Nielsen, G. C.; Jensen, J. E.; Spliid, N. H.; Thomsen, I. K.; Justesen, A. F.; Collinge, D. B.; Jørgensen, L. N., Fusarium head blight of cereals in Denmark: species complex and related mycotoxins. *Phytopathology* **2011** *101*.

15. Fredlund, E.; Gidlund, A.; Sulyok, M.; Börjesson, T.; Krska, R.; Olsen, M.; Lindblad, M., Deoxynivalenol and other selected *Fusarium* toxins in Swedish oats - Occurrence and correlation to specific *Fusarium* species. *International Journal of Food Microbiology* **2013,** *167*, 276-283.

16. Lindblad, M.; Gidlund, A.; Sulyok, M.; Börjesson, T.; Krska, R.; Olsen, M.; Fredlund, E., Deoxynivalenol and other selected *Fusarium* toxins in Swedish wheat - Occurrence and correlation to specific *Fusarium* species. *International Journal of Food Microbiology* **2013,** *167*, 284-291.

17. Parikka, P.; Hakala, K.; Tiilikkala, K., Expected shifts in *Fusarium* species' composition on cereal grain in Northern Europe due to climatic change. *Food Additives and Contaminants* **2012** *29*, 1543-1555.

18. Uhlig, S.; Eriksen, G. S.; Hofgaard, I. S.; Krska, R.; Beltrán, E.; Sulyok, M., Faces of a changing climate: semi-quantitative multi-mycotoxin analysis of grain grown in exceptional climatic conditions in Norway. *Toxins* **2013,** *5*, 1682-1697.

19. Urban, M.; Danielsy, S.; Mottz, E.; Hammond-Kosack, K., *Arabidopsis* is susceptible to the cereal ear blight fungal pathogens *Fusarium graminearum* and *Fusarium culmorum*. *The Plant Journal* **2002,** *32*, 961-973.

20. Pioli, R. N.; Mozzoni, L.; Morandi, E. N., First report of pathogenic association between *Fusarium graminearum* and soybean. *Plant Disease* **2004,** *88*, 220-220.

21. Ali, S.; Rivera, V. V.; Secor, G. A., First report of *Fusarium graminearum* causing dry rot of potato in North Dakota. *Plant Disease* **2005,** *89*, 105-105.

22. Talas, F.; Kalih, R.; Miedaner, T., Within field variation of *Fusarium graminearum* isolates for aggressiveness and deoxynivalenol production in wheat head blight. *Phytopathology* **2012,** *102*, 128-134.

23. Stack, R. W.; McMullen, M. P., Head blighting potential of *Fusarium* species associated with spring wheat heads. *Canadian Journal of Plant Pathology* **1985,** *7*, 79-82.

24. Edwards, S. G., Influence of agricutural practices on *Fusarium* infection of cereals and subsequent contaminatin of grain by trichothecene mycotoxins. *Toxicology Letters* **2004,** *153*, 29-35.

25. Talas, F.; Parzies, H.; Miedaner, T., Diversity in genetic structure and chemotype composition of *Fusarium graminearum sensu stricto* populations causing head blight in individual fields in Germany. *European Journal of Plant pathology* **2011,** *131*, 39-48.

26. Sutton, J. C., Epidemiology of wheat head blight and maize ear rot caused by *Fusarium graminearum*. *Canadian Journal of Plant Pathology* **1982,** *4*, 195-209.

27. Mesterhazy, A., Breeding wheat for Fusarium head blight resistance in Europe. In *Fusarium head blight of wheat and barley*, Leonard, K. J.; Bushnell, W. R., Eds. The American Phytopathological Society: Saint Paul, 2003; pp 211-240.

28. Brodal, G.; Henriksen, B.; Sundheim, L., Sjukdommer i korn, oljevekster og kjernebelgvekster. In *Plantevern og plantehelse i økologisk landbruk*, Brandsæter, L. O.; Mangerud, K.; Birkenes, S. M.; Brodal, G.; Andersen, A., Eds. Bioforsk Fokus: Norway, 2009; Vol. 4.

29. Bai, G.; Shaner, G., Management and reistance in wheat and barley to Fusarium head blight. *Annual Reviews of Phytopathology* **2004,** *42*, 135-161.

30. Pirgozliev, S. R.; Edwards, S. G.; Hare, M. C.; Jenkinson, P., Strategies for the control of Fusarium head blight in cereals. *European Journal of Plant Pathology* **2003,** *109*, 731-742.

31. Dill-Macky, R.; Jones, R. K., The effect of previous crop residues and tillage on Fusarium head blight of wheat. *Plant Disease* **2000,** *84*, 71-76.

32. Obst, A.; Gleissenthall, J. L.-v.; Beck, R., On the etiology of Fusarium head blight of wheat in South Germany-preceding crops, weather conditions for inoculum production and head infection, proneness of the crop to infection and mycotoxin production. *Cereal Research Communications* **1997,** *25* 699-704.

33. McMullen, M.; Jones, R.; Gallenberg, D., Scab of wheat and barley: a re-emerging diseasae of devastating impact. *Plant Disease* **1997,** *81*, 1340-1348.

34. Lewandowski, S. M.; Bushnell, W. R.; Evans, C. K., Distribution of mycelial colonies and lesions in fieldgrown barley inoculated with *Fusarium graminearum*. *Phytopathology* **2006,** *96*, 567-581.

35. Bushnell, W. R.; Hazen, B. E.; Pritsch, C., Histology and physiology of Fusarium head blight. In *Fusarium head blight of wheat and barley*, Leonard, K. J.; Bushnell, W. R., Eds. The American Phytopathological Society: Saint Paul, 2003; pp 44-83.

36. Kang, Z. S.; Buchenauer, H., Cytology and ultrastructure of the infection of wheat spikes by *Fusarium culmorum*. *Mycological Research* **2000,** *104*, 1083-1093.

37. Kang, Z. S.; Buchenauer, H., Studies on the infection process of *Fusarium culmorum* in wheat spikes: degradation of host cell wall components and localization of trichothecene toxins in infected tissue *European Journal of Plant Pathology* **2002,** *108*, 653-660.

38. Skadsen, R. W.; Hohn, T. A., Use of *Fusarium graminearum* transformed with *gfp* to follow infection patterns in barley and *Arabidopsis*. *Physiological and Molecular Plant Pathology* **2004,** *64*, 45-53.

39. Divon, H. H.; Bøe, L.; Tveit, M. M. N.; Klemsdal, S. S. In *Histological studies of F. langsethiae infection on oats and wheat*, Nordic Baltic Fusarium Seminar, Uppsala, Sweden, 2012; Persson, P.; Kolseth, A.-K.; Borjesson, T., Eds. Nordic Association of Agricultural Scientists: Uppsala, Sweden, 2012; p 31.

40. Skinnes, H.; Semagn, K.; Tarkegne, Y.; Marøy, A. G.; Bjørnstad, Å., The inheritance of anther extrusion in hexaploid wheat and its relationship to Fusarium head blight resistance and deoxynivalenol content. *Plant Breeding* **2010,** *129*, 149-155.

41. Pugh, G. W.; Johann, H.; Dickson, J. G., Factors affecting infection of wheat heads by *Gibberella saubinetti*. *Journal of Agriculatural Research* **1933,** *46*, 771-797.

42. Strange, R. N.; Smith, H., A fungal growth stimulant in anthers which predisposes wheat to attack by *Fusarium graminearum*. *Physiological Plant Pathology* **1971,** *1*, 141-150.

43. Miller, S. S.; Chabot, D. M. P.; Ouellet, T.; Harris, L. J.; Fedak, G., Use of a *Fusarium graminearum* strain transformed with green fluorescent protein to study infection in wheat (*Triticum aestivum*). *Canadian Journal of Plant Pathology* **2004,** *26*, 453-463.

44. Ribichich, K. F., Histopathological spikelet changes produced by *Fusarium graminearum* in susceptible and resistant wheat cultivars. *Plant Disease* **2000,** *84*, 794-802.

45. Strange, R. N.; Majer, J. R.; Smith, H., The isolation and identification of choline and betaine as the two major components in anthers and wheat germ that stimulate *Fusarium graminearum in vitro*. *Physiological Plant Pathology* **1974,** *4*, 277-290.

46. Pearce, R. B.; Strange, R. N.; Smith, H., Glycinebetaine and choline in wheat: distribution and relation to infection by *Fusarium graminearum*. *Phytochemistry* **1976,** *15*, 953-954.

47. Yoshida, M.; Kawada, N.; Nakajima, T., Effect of infection timing on Fusarium head blight and mycotoxin accumulation in open- and closed-flowering barley. *Phytopathology* **2007,** *97*, 1054-1062.

48. Engle, J. S.; Lipps, P. E.; Graham, T. L.; Boehm, M. J., Effects of choline, betaine, and wheat floral extracts on growth of *Fusarium graminearum*. *Plant Disease* **2004,** *88*, 175-180.

49. Lacey, J.; Bateman, G. L.; Mirocha, C. J., Effects of infection time and moisture on development of ear blight and deoxynivalenol production by *Fusarium* spp. in wheat. *Annals of Applied Biology* **1999,** *134*, 277-283.

50. Del Ponte, E. M.; Fernandes, J. M. C.; Bergstrom, G. C., Influence of growth stage on Fusarium head blight and deoxynivalenol production in wheat. *Journal of Phytopathology* **2007,** *155*, 577-581.

51. Wagacha, J. M.; Muthomi, J. W., *Fusarium culmorum*: infection process, mechanisms of mycotoxin production and their role in pathogenesis in wheat. *Crop Protection* **2007,** *26*, 877-885.

52. Schroeder, H. W.; Christensen, J. J., Factors affecting resistance of wheat to scab caused by *Gibberella zeae*. *Phytopathology* **1963,** *53*, 831-838.

53. Andersen, A. L., The development of *Gibberella zeae* head blight of wheat. *Phytopathology* **1948,** *38*, 595-611.

54. McCallum, B. D.; Tekauz, A., Influence of inoculation method and growth stage on Fusarium head blight in barley. *Canadian Journal of Plant Pathology* **2002,** *24*, 77-80.

55. Argyris, J.; Sanford, D. V.; TeKrony, D., *Fusarium graminearum* infection during wheat seed development and its effect on seed quality. *Crop Science* **2003,** *43*, 1782-1788.

56. Schwarz, P. B.; Schwarz, J. G.; Zho, A.; Prom, L. K.; Steffenson, B. J., Effect of *Fusarium graminearum* and *F. poae* infection on barley and malt quality. *Monatsschrift Fur Brauwissenschaft* **2001,** *314*, 55-63.

57. Gilbert, J.; Tekauz, A., Effects of Fusarium head blight and seed treatment on germination, emergence, and seedling vigour of spring wheat. *Canadian Journal of Plant Pathology* **1995,** *17*, 252-259.

58. Jones, R. K.; Mirocha, C. J., Quality parameters in small grains from Minnesota affected by Fusarium head blight. *Plant Disease* **1999,** *83*, 506-511.

59. Bechtel, D. B.; Kaleikau, L. A.; Gaines, R. L.; Seitz, L. M., The effects of *Fusarium graminearum* infection on wheat kernels. *Cereal Chemistry* **1985,** *62*, 191-197.

60. Jones, R. K., Seedling blight development and control in spring wheat damaged by *Fusarium graminearum* group 2. *Plant Disease* **1999,** *83*, 1013-1018.

61. Hare, M. C.; Parry, D. W.; Baker, M. D., The relationship between wheat seed weight, infection by *Fusarium culmorum* or *Microdochium nivale*, germination and seedling disease. *European Journal of Plant Pathology* **1999,** *105*, 859-866.

62. Browne, R. A.; Cooke, B. M., Resistance of wheat to *Fusarium* spp. in an *in vitro* seed germination assay and preliminary investigations into the relationship with Fusarium head blight resistance. *Euphytica* **2005,** *141*, 23-32.

63. Imathiu, S. M.; Hare, M. C.; Ray, R. V.; Back, M.; Edwards, S. G., Evaluation of pathogenicity and aggressiveness of *F. langsethiae* on oat and wheat seedlings relative to known seedling blight pathogens. *European Journal of Plant Pathology* **2010,** *126*, 203-216.

64. Wang, H.; Hwang, S. F.; Eudes, F.; Chang, K. F.; Howard, R. J.; Turnbull, G. D., Trichothecenes and aggressiveness of *Fusarium graminearum* causing seedling blight and root rot in cereals. *Plant Pathology* **2006,** *55*, 224-230.

65. Hestbjerg, H.; Felding, G.; Elmholt, S., *Fusarium culmorum* infection of barley seedlings, correlation between aggressiveness and deoxynivalenol content. *Journal of Phytopathology* **2002,** *150*, 308-312.

66. Bruins, M. B. M.; Karsai, I.; Schepers, J.; Snijders, C. H. A., Phytotoxicity of deoxynivalenol to wheat tissue with regard to *in vitro* selection for Fusarium head blight resistance. *Plant Science* **1993,** *94*, 195-206.

67. McLean, M., The phytotoxicity of selected mycotoxins on mature, germinating *Zea mays* embryos. *Mycopathologia* **1996,** *132*, 173-183.

68. Lemmens, M.; Reisinger, A.; Burstmayr, H.; Ruckenbauer, P., Breeding for head blight (*Fusarium* spp.) resistance in wheat, development of a mycotoxin based selection method of seedlings. *Plant Breeding for Mankind* **1994,** *355*, 223-232.

69. Dexter, J. E.; Clear, R. M.; Preston, K. R., Fusarium head blight: effect on the milling and baking of some Canadian wheats. *Cereal Chemistry* **1996,** *73*, 695-701.

70. Nightingale, M. J.; Marchylo, B. A.; Clear, R. M.; Dexter, J. E.; Preston, K. R., Fusarium head blight: effect of fungal proteases on wheat storage proteins. *Cereal Chemistry* **1999,** *76*, 150-158.

71. Wang, J.; Pawelzik, E.; Weinert, J.; Wolf, G. A., Impact of *Fusarium culmorum* on the polysaccharides of wheat flour. *Journal of Agricultural and Food Chemistry* **2005,** *53*, 5818-5823.

72. Jackowiak, H.; Packa, D.; Wiwart, M.; Perkowski, J., Scanning electron microscopy of *Fusarium* damaged kernels of spring wheat. *International Journal of Food Microbiology* **2005,** *98*, 113- 123.

73. Prange, A.; Birzele, B.; Kramer, J.; Meier, A.; Modrow, H.; Kohler, P., *Fusarium*-inoculated wheat: deoxynivalenol contents and baking quality in relation to infection time. *Food Control* **2005,** *16*, 739-745.

74. Mesterhazy, A., Types and components of resistance to Fusarium head blight of wheat. *Plant Breeding* **1995,** *144*, 377-386.

75. vanEeuwijik, F. A.; Mesterahzy, A.; Kling, C. I.; Ruckenbauer, P.; Saur, L.; Burstamayr, H.; Lemmens, M.; Keizer, L. C. P.; Maurin, N.; Snijders, C. H. A., Assessing non- specificty of resistance in wheat to head blight caused by inoculation with European strains of *Fusarium culmorum*, *F. graminearum* and *F. nivale* using a multiplicative model for interaction. *Theoretical and Applied Genetics* **1995,** *90*, 221-228.

76. Mesterházy, A.; Bartok, T.; Mirocha, C. G.; Komoroczy, R., Nature of wheat resistance to Fusarium head blight and the role of deoxynivalenol for breeding. *Plant Breeding* **1999,** *118*, 97-110.

77. Dill-Macky, R., Inoculation methods and evaluation of Fusarium head blight resistance in wheat. In *Fusarium head blight of wheat and barley*, Leonard, K. J.; Bushnell, W. R., Eds. The American Phytopathological Society: Saint Paul, 2003; pp 184-210.

78. Miller, J. D.; Young, J. C.; Sampson, D. R., Deoxynivalenol and Fusarium head blight resistance in spring cereals. *Journal of Phytopathology* **1985,** *113*, 359-367.

79. Gilsinger, J.; Kong, L.; Shen, X.; Ohm, H., DNA markers associated with low Fusarium head blight incidence and narrow flower opening in wheat. *Theoretical and Applied Genetics* **2005,** *110*, 1218-1225.

80. Lu, Q.; Lillemo, M.; Skinnes, H.; He, X.; Shi, J.; Ji, F.; Dong, Y.; Bjørnstad, Å., Anther extrusion and plant height are associated with Type I resistance to Fusarium head blight in bread wheat line 'Shanghai-3/Catbird'. *Theoretical and Applied Genetics* **2013,** *126*, 317-334.

81. He, X.; Skinnes, H.; Oliver, R. E.; Jackson, E. W.; Bjørnstad, Å., Linkage mapping and identification of QTL affecting deoxynivalenol (DON) content (*Fusarium* resistance) in oats (*Avena sativa* L.). *Theoretical and Applied Genetics* **2013,** *126*, 2655-2670.

82. Ciegler, A., Fungi that produce mycotoxins: conditions and occurence. *Mycopathologia* **1978,** *65*, 5-11.

83. Bottalico, A.; Perrone, G., Toxigenic *Fusarium* species and mycotoxins associated with head blight in small-grain cereals in Europe. *European Journal of Plant Pathology* **2002,** *108*, 611-624.

84. McCormick, S., The role of DON in pathogenecity. In *Fusarium head blight of wheat and barley*, Leonard, K. J.; Bushnell, W. R., Eds. The American Phytopathological Society: Saint Paul, 2003; pp 165-183.

85. Langevin, F. o.; Eudes, F. o.; Comeau, A., Effect of trichothecenes produced by *Fusarium graminearum* during Fusarium head blight development in six cereal species. *European Journal of Plant Pathology* **2004,** *110*, 735-746.

86. Eriksen, G. S.; Pettersson, H., Toxicological evaluation of trichothecenes in animal feed. *Animal Feed Science and Technology* **2004,** *114*, 205-239.

87. Conkova, E.; Laciakova, A.; Kovac, G.; Seidel, H., Fusarial toxins and their role in animal diseases. *The Vetrinary Journal* **2003,** *165*, 214-220.

88. Ciegler, A., Trichothecenes: occurence and toxicosis. *Journal of Food Protection* **1978,** *41*, 399-403.

89. Bergsjø, B.; Langseth, W.; Nafstad, I.; Jansen, J. H.; Larsen, H. J. S., The effects of naturally deoxynivalenol contaminated oats on the clinical condition, blood parameter, performance and carcass composition of growing pigs. *Veterinary Research Communications* **1993,** *17*, 283-294.

90. Bergsjø, B.; Matre, T.; Nafstad, I., Effects of diets with graded levels of deoxynivalenol on performance in growing pigs. *Journal of Veterinary Medicine* **1992,** *39*, 752-758.

91. Rotter, B. A.; Thompson, B. K.; Lessard, M., Effects of deoxynivalenol-contaminated diet on performance and blood parameters in growing swine. *Canadian Journal of of Animal Science* **1995,** *75*, 297-302.

92. European; Commission, Commission regulation (EC) No 1881/2006: setting maximum levels for certain contaminants in foodstuffs. *Official Journal of the European Union* **2006,** *L 364*, 5-24.

93. Scudamore, K. A.; Baillie, H.; Patel, S.; Edwards, S. G., Occurrence and fate of *Fusarium* mycotoxins during commercial processing of oats in the UK. *Food Additives and Contaminants* **2007,** *24*, 1374-1385.

94. Trenholm, H. L.; Charmley, L. L.; Prelusky, D. B.; Warned, R. M., Two physical methods for the de-contamination of four cereals contaminated with deoxynivalenol and zearalenone. *Journal of Agriculatural and Food Chemistry* **1991,** *39*, 356-360.

95. Clear, R. M.; Patrick, S. K.; Nowicki, T.; Gaba, D.; Edney, M.; Babb, J. C., The effect of hull removal and pearling on *Fusarium* species and trichothecenes in hulless barley. *Canadian Journal of Plant Science* **1997,** *77*, 161-166.

96. Yan, W. K.; Fregeau-Reid, J.; Rioux, S.; Pageau, D.; Xue, A.; Martin, R.; Fedak, G.; de Haan, B.; Lajeunesse, J.; Savard, M., Response of oat genotypes to Fusarium head blight in Eastern Canada. *Crop Science* **2010,** *50*, 134-142.

97. Tekauz, A.; McCallum, B.; Ames, N.; Fetch, J. M., Fusarium head blight of oat — current status in western Canada. *Canadian Journal of Plant Pathology* **2004,** *26*, 473-479.

98. Dexter, J. E.; Nowicki, T. W., Safety assurance and quality assurance issues associated with Fusarium head blight in wheat. In *Fusarium head blight of wheat and barley*, Leonard, K. J.; Bushnell, W. R., Eds. The American Phytopathological Society: Saint Paul, 2003; pp 420-460.

99. Schaafsma, A. W.; Savard, M. E.; Clear, R.; Dexter, J., Methods and issues regarding detection of deoxynivalenol, *Fusarium*-damaged kernels, and *Fusarium* spp. in commercial grain in Canada. *Canadian Journal of Plant Pathology* **2004,** *26*, 443-452.

100. Cigić, I. K.; Prosen, H., An overview of conventional and emerging analytical methods for the determination of mycotoxins. *International Journal of Molecular Sciences* **2009,** *10*, 62-115.

101. Veronica M.T. Lattanzio; Pascale, M.; Visconti, A., Current analytical methods for trichothecene mycotoxins in cereals. *Trends in Analytical Chemistry* **2009,** *28*, 758-768.

102. Pascale, M.; Visconti, A., Overview of detection methods for mycotoxins. In *Mycotoxins: detection methods, management, public health and agricultural trade*, Leslie, J. F.; Bandyopadhyay, R.; Visconti, A., Eds. CABI: United Kingdom, 2008.

103. Schneider, E.; Curtui, V.; Seidler, C.; Dietrich, R.; Usleber, E.; Märtlbauer, E., Rapid methods for deoxynivalenol and other trichothecenes. *Toxicology Letters* **2004,** *153*, 113-121.

104. Aamot, H.; Hofgaard, I.; Brodal, G.; Elen, O.; Holen, B.; Klemsdal, S., Evaluation of rapid test kits for quantification of HT-2 and T-2 toxins in naturally contaminated oats. *World Mycotoxin Journal* **2013,** *6*, 31-41.

105. Aamot, H.; Hofgaard, I.; Brodal, G.; Elen, O.; Jestoi, M.; Klemsdal, S., Evaluation of rapid test kits for quantification of deoxynivalenol in naturally contaminated oats and wheat. *World Mycotoxin Journal* **2012,** *5*, 339-350.

106. Blanco, M.; Villarroya, I., NIR spectroscopy: a rapid-response analytical tool. *Trends in Analytical Chemistry* **2002,** *21*, 240-250.

107. Cen, H.; He, Y., Theory and application of near infrared reflectance spectroscopy in determination of food quality. *Trends in Food Science & Technology* **2007,** *18*

108. Gowen, A. A.; O'Donnell, C. P.; Cullen, P. J.; Downey, G.; Frias, J. M., Hyperspectral imaging- an emerging process analytical tool for food quality and safety control. *Trends in Food Science & Technology* **2007,** *18*, 590-598.

109. Pasquini, C., Near Infrared spectroscopy: Fundamentals, practical aspects and analytical applications. *J. Braz. Chem. Soc.* **2003,** *14*, 198-219.

110. Davies, T., The history of near infrared spectroscopic analysis: Past, present and future- "From sleeping technique to the morning star of spectroscopy". *Analusis Magazine* **1998,** *26*, 17-19.

111. Williams, P. C., Implementation of near-infrared technology. In *Near-Infrared Technology in the Agricultural and Food Industries*, 2 ed.; Williams, P.; Norris, K., Eds. American Association of Cereal Chemists: Saint Paul, MN, 2001; pp 145-169

112. Næs, T.; Isaksson, T.; Fearn, T.; Davies, T., *A user-friendly guide to multivariate calibration and classification*. NIR publications: Chichester, UK, 2002; Vol. 6.

113. Delwiche, S. R.; Hareland, G. A., Detection of scab-damaged hard red spring wheat kernels by near-infrared reflectance. *Cereal Chemistry* **2004,** *81*, 643-649.

114. Dowell, F. E.; Ram, M. S.; Seitz, L. M., Predicting scab, vomitoxin, and ergosterol in single wheat kernels using near-infrared spectroscopy. *Cereal Chemistry* **1999,** *76*, 573-576.

115. Peiris, K. H. S.; Pumphrey, M. O.; Dong, Y.; Maghirang, E. B.; Berzonsky, W.; Dowell, F. E., Near-infrared spectroscopic method for identification of Fusarium head blight damage and prediction of deoxynivalenol in single wheat kernels. *Cereal Chemistry* **2010,** *87*, 511-517.

116. Pettersson, H.; Åberg, L., Near infrared spectroscopy for determination of mycotoxins in cereals. *Food Control* **2003,** *14*, 229-232.

117. Ruan, R.; Li, Y.; Lin, X.; Chen, P., Non-destructive determination of deoxynivalenol levels in barley using near-infrared spectroscopy. *Applied Engineering in Agriculture* **2002,** *18*, 549-553.

118. Peiris, K. H. S.; Pumphrey, M. O.; Dowell, F. E., NIR absorbance characterstics of deoxynivalenol and of sound and *Fusarium*-damaged wheat kernels. *Journal of Near Infrared Spectroscopy* **2009,** *17*, 213-221.

119. Siuda, R.; Balcerowska, G.; Kupcewicz, B.; Lenc, L., A modified approach to evaluation of DON content in scab-damaged ground wheat by use of diffuse reflectance spectroscopy. *Food Analytical Methods* **2008,** *1*, 283-292.

120. Delwiche, S. R.; Pearson, T. C.; Brabec, D. L., High-speed optical sorting of soft wheat for reduction of deoxynivalenol. *Plant Disease* **2005,** *89*, 1214-1219.

121. Delwiche, S. R., Classification of scab- and other mold-damaged wheat kernels by near-infrared reflectance spectroscopy. *Transactions of the ASAE* **2003,** *46*, 731-738.

122. Feng, Y.-Z.; Sun, D.-W., Application of hyperspectral imaging in food safety inspection and control: a review. *Critical Reviews in Food Science and Nutrition* **2012,** *52*, 1039-1058

123. Williams, P.; Manley, M.; Fox, G.; Geladi, P., Indirect detection of *Fusarium verticillioides* in maize (*Zea mays* L.) kernels by near infrared hyperspectral imaging. *Journal of Near Infrared Spectroscopy* **2010,** *18*, 49-58.

124. Polder, G.; Heijden, G. W. A. M. V. D.; Waalwijk, C.; Young, I. T., Detection of *Fusarium* in single wheat kernels using spectral imaging. *Seed Science and Technology* **2005,** *33*, 655-668.

125. Delwiche, S. R.; Kim, M. S.; Dong, Y., *Fusarium* damage assessment in wheat kernels by VIS/NIR hyperspectral imaging. *Sensory and Instrumentation for Food Quality* **2011,** *5*, 63-71.

126. Mahesh, S.; Manickavasagan, A.; Jayas, D. S.; Paliwal, J.; White, N. D. G., Feasibility of near-infrared hyperspectral imaging to differentiate Canadian wheat classes. *Biosystems Egineering* **2008,** *101*, 50-57.

127. Shahin, M. A.; Symons, S. J., Detection of *Fusarium* damage in Canadian wheat using visible/near-infrared hyperspectral imaging. *Food Measure* **2012,** *6*, 3-11.

128. Yao, H.; Hruska, Z.; Kincaid, R.; Brown, R. L.; Cleveland, T. E., Differentiation of toxigenic fungi using hyperspectral imagery. *Sensory and Instrumentation for Food Quality* **2008,** *2*, 215-224.

129. Shahin, M. A.; Symons, S. J., Detection of *Fusarium* damaged kernels in Canada Western Red Spring wheat using visible/near-infrared hyperspectral imaging and principal component analysis. *Computers and Electronics in Agriculture* **2011,** *75*, 107-112.

130. Martens, H.; Næs, T., *Multivariate Calibration*. Wiley: Chichester, U.K., 1989.

131. Kiecana, I.; Mielniczuk, E.; Kaczmarek, Z.; Kostecki, M.; Golinski, P., Scab response and moniliformin accumulation in kernels of oat genotypes inoculated with *Fusarium avenaceum* in Poland. *European Journal of Plant Pathology* **2002,** *108*, 245-251.

132. Pathre, S. V.; Mirocha, C. J., Trichothecenes: natural occurence and potential hazard. *Journal of the American Oil Chemists' Society* **1979,** *56*, 820-823.

133. Tekle, S.; Dill-Macky, R.; Skinnes, H.; Tronsmo, A. M.; Bjørnstad, Å., Infection process of *Fusarium graminearum* in oats (*Avena sativa* L.). *European Journal of Plant Pathology* **2012,** *132*, 431-442.

134. Tekle, S.; Skinnes, H.; Bjørnstad, Å., The germination problem of oat seed lots affected by Fusarium head blight. *European Journal of Plant Pathology* **2013,** *135*, 147-158.

135. Tekle, S.; Bjørnstad, Å.; Skinnes, H.; Dong, Y.; Segtnan, V. H., Estimating deoxynivalenol content of ground oats using VIS-NIR spectroscopy. *Cereal Chemistry* **2013,** *90*, 181–185.

Paper I

Selamawit Tekle, Ruth Dill-Macky, Helge Skinnes, Anne Marte Tronsmo and Åsmund Bjørnstad

Eur J Plant Pathol (2012) 132:431–442
DOI 10.1007/s10658-011-9888-x

Infection process of *Fusarium graminearum* in oats (*Avena sativa* L.)

Selamawit Tekle · Ruth Dill-Macky · Helge Skinnes · Anne Marte Tronsmo · Åsmund Bjørnstad

Accepted: 20 October 2011 / Published online: 6 November 2011

Abstract Fusarium head blight in small grain cereals has emerged as a major problem in the Nordic countries. However, the impact of this disease in oats has been less investigated than in other cereals. For this reason we have studied the infection process (the optimal time of infection and infection pathways) of *Fusarium graminearum* in oats and its subsequent effects on kernel infection, deoxynivalenol (DON) content and germination capacity. In a field experiment the oat cultivar Morton was spray-inoculated at different developmental stages, and the highest kernel infection and DON content and lowest germination percentage were observed when inoculation took place at anthesis. Field grown oats affected by a natural Fusarium head blight epidemic and spray-inoculated field and greenhouse oats were used to study the infection pathway. Results showed that the fungus entered primarily through the floret apex into the floret cavity, where it could infect *via* the internal surfaces of the palea, lemma and caryopsis. Both visual symptoms and fungal infections started at the apical portions of the florets and progressed to the basal portions. Hyphae of *F. graminearum* grew more profusely on the anthers than on other floret parts during initial stages of infection. Disease development within the oat panicle was slow and is primarily by physical contact between adjoining florets, indicating that the long pedicels give Type II resistance in oats.

Keywords Fusarium head blight · Infection pathway · Time of infection

Abbreviations

FHB	Fusarium head blight
DON	Deoxynivalenol
DAI	Days after inoculation

Introduction

Fusarium spp. are common pathogens of cereals and cause a wide range of diseases at all stages of plant development including seedling blight, root and foot rot, snow mould, leaf spot and Fusarium Head Blight (FHB) (McMullen et al. 1997; Parry et al. 1995). FHB results in shrivelled and chalky kernels with low germination rate (Gilbert and Tekauz 1995; Gilbert et al. 1997). Contamination of food and feed stuff with several mycotoxins due to FHB presents a serious health risk to humans and animals (Parry et al. 1995).

Fusarium graminearum, *F. culmorum*, *F. avenaceum*, *F. poae*, and *Microdochium nivale* are the most

S. Tekle (✉) · H. Skinnes · A. M. Tronsmo · Å. Bjørnstad
Department of Plant and Environmental Sciences,
Norwegian University of Life Sciences,
P.O. Box 5003, 1432 Ås, Norway
e-mail: selag@umb.no

R. Dill-Macky
Department of Plant Pathology, University of Minnesota,
1991 Upper Buford Circle,
St. Paul, MN 55108, USA

common FHB pathogens, although up to 17 causal organisms are associated with the disease (Parry et al. 1995). *Fusarium graminearum* dominates in North America (McMullen et al. 1997; Schroeder and Christensen 1963) while in cooler northern Europe environments, the most common *Fusarium* species are *F. avenaceum, F. tricinctum, F. poae, F. culmorum* and *F. graminearum* (Yli-Mattila 2010). From 416 samples of wheat, barley and oats collected from Norway during the years 1980–1983 *F. culmorum* (29%), *F. avenaceum* (25%), *F. graminearum* (8%) and *F. nivale* (7%) were isolated (Haave 1985). *Fusarium poae, F. equiseti, F. oxysporium, F. tricinctum* and *F. sporotrichioides* were also isolated, but at a lower frequency (Haave 1985). Recent studies in Norway have shown a shift in relative prevalence of FHB pathogens and increase in the importance of *F. graminearum* (Hofgaard et al. 2010). The Norwegian oat cv. Gere and the German cv. Bessin were withdrawn from the Norwegian seed market because of high deoxynivalenol (DON) contamination and poor germination rate (Bjørnstad and Skinnes 2008).

Infection by *Fusarium* spp. is influenced by factors such as moisture and temperature, cultivar susceptibility and cultivation practice (Shaner 2003). Infection and disease development are favoured by warm and humid conditions during flowering and early stages of kernel development (Parry et al. 1995). *Fusarium* spp. infect wheat and barley heads mainly around anthesis (Schroeder and Christensen 1963; Wagacha and Muthomi 2007), with decreasing severity at later stages of development (Andersen 1948). Mycotoxin content and effects on floret fertility, thousand grain weight and germination capacity vary according to time of infection (Del Ponte et al. 2007; Lacey et al. 1999; Yoshida et al. 2007). However, significant kernel infection and mycotoxin accumulation can occur in kernels inoculated as late as the hard dough stage (Del Ponte et al. 2007).

Barley and wheat florets are covered by a lemma and a palea having lignified thick-walled epidermal and hypodermal cells (Bushnell et al. 2003; Lewandowski et al. 2006). This makes direct penetration and infection of the external floret surfaces by head blight pathogens difficult and unlikely (Bushnell et al. 2003). However, the developing caryopses and internal surfaces of the palea and the lemma are thin-walled and can be penetrated more easily (Bushnell et al. 2003). Further, hyphae of *F. graminearum* are susceptible to desiccation (Skadsen and Hohn 2004). Therefore, spores germinating on external surfaces of florets that can gain access to internal surfaces avoid desiccation and increase the chances of successful infection.

First symptoms of FHB appeared on non-extruded anthers of wheat (Pugh et al. 1933) and this led researchers to investigate the importance of anthers in floret colonization. Strange and Smith (1971) observed a prolific mycelial growth on anthers of wheat which were exposed to ascospores of *F. graminearum*. Later, Strange et al. (1974) isolated and characterized betaine and choline as the fungal growth stimulants resulting in prolific *F. graminearum* growth. These chemicals were found in greater concentrations in anthers than in other floret parts (Strange et al. 1974). Miller et al. (2004) showed likewise that *F. graminearum* had high affinity to anthers and pollen. Kang and Buchenauer (2000) also noted that retained anthers were colonized densely by *F. culmorum* hyphae, but that inoculated wheat heads were also invaded at other easily penetrable parts of the floret regardless of the presence or absence of anthers. In addition, wheat genotypes with high levels of anther extrusion tended to develop less FHB and had lower levels of DON contamination (Skinnes et al. 2010). However, there are reports that did not confirm this, and the role of anthers was regarded as equivocal (Engle et al. 2004).

The objectives of this study were: *(a)* to investigate the optimal time of *F. graminearum* infection in oats and its subsequent effects on kernel infection, DON contamination and germination capacity; *(b)* to determine the infection pathway of this pathogen into the oat floret cavity based on macro- and microscopic observations; and *(c)* to determine the importance of anthers at the initial stages of the infection process. *Fusarium graminearum* was chosen among other FHB causing pathogens due to the observed increase in prevalence and importance of the pathogen in Nordic countries (Hofgaard et al. 2010; Yli-Mattila 2010).

Materials and methods

A field inoculation experiment and supplemental greenhouse study on infection pathways were conducted in 2008 at University of Minnesota

(UMN) Agricultural Research Station, St. Paul. The experiments were further supplemented by samples obtained from a natural epidemic in an oat field at Vollebekk Experimental Farm in 2007 and a greenhouse inoculation experiment conducted in 2009 at the Norwegian University of Life Sciences, Ås, Norway.

Optimal time of infection

The Minnesota field experiment was planted on May 01, 2008. Sixteen plots with four 1.8 m rows spaced 30 cm apart were seeded with the oat cv. Morton. This cultivar is late maturing, resistant to lodging and smut, and susceptible to crown rust and FHB. Plots were harvested at maturity on August 01, 2008.

The inoculum consisted of 41 *F. graminearum* isolates previously collected from commercial wheat and barley fields in Minnesota. Of the 41 isolates, 40 were collected from 2005 to 2007 while one isolate was from 1986. Isolates were collected, stored, and increased using the procedures described by Dill-Macky (2003) . The inoculum was adjusted to a spore concentration of 1×10^5 spores/ml and 8 ml of Tween20® per litre of inoculum was added. Inoculum was applied using a CO_2-powered backpack sprayer fitted with a flat-fan spray tip (TeeJet SS8003; Spraying Systems Co., Wheaton, Illinois) pressurized at 276 KPa. Each row was sprayed for 6–8 s distributing ~32 ml of inoculum per metre of plot row.

Plots were inoculated at anthesis (when ~50% of the spikes had fully emerged) or 1 or 2 weeks after anthesis. Each plot was inoculated twice; at the indicated time and 3 days after initial inoculation. This was done to enhance disease development and to catch the later developing tillers. Uninoculated plots provided the control. Treatments were replicated four times in a completely randomized design.

Following each inoculation, the plants were mist irrigated for 30 min. Subsequently, plots were mist irrigated for 9 min at 1 h intervals during evenings (17:00 to 21:00 h) and mornings (04:00 to 06:00 h). Harvested grain was dried in a commercial seed drier set at 95°C for 7 days. Representative samples were taken from each treatment to determine kernel infection, DON content and germination capacity.

Data collection and analysis

Kernel infection was determined by the modified freezer blotter test (Brodal 1991; Limonard 1966) at the Kimen Seed Testing Laboratory, Ås, Norway. One hundred seeds from each sample were soaked in 1% NaOCl for 10 min for surface sterilization. Kernels were then placed on moist filter paper (300 g/m^2, Munktell Filter AB, Falun, Sweden) in transparent, 24.5×24.5×2 cm polystyrene Nunc bio-assay incubation dishes (Nunc A/S, Roskilde, Denmark), and incubated at 20°C for 24 h. Subsequently, the dishes were transferred to a freezer at -20°C for 24 h to kill the embryo. Finally, dishes were kept under alternating 12 h of a combination of cool white light and UVA light and 12 h darkness at 20°C. After 2 weeks kernels were examined visually for the presence of *Fusarium* spp. colonies.

Germination tests also were done at the Kimen Seed Testing Laboratory. One hundred kernels were placed on moist paper towels in a room maintained at 10°C for 7 days and then moved to 20°C for 3 days. Seedlings and kernels were then classified as 'normal' seedlings, 'abnormal' seedlings, 'healthy non-germinated' kernels and 'dead' kernels according to the International Seed Testing Association (ISTA) standards. Normal seedlings and non-infected un-germinated kernels were grouped as 'germinated' while abnormal seedlings and dead kernels were considered as 'un-germinated'.

DON content was determined at the Mycotoxin Laboratory of UMN. Twelve grams of each sample were ground for 2 min with a Stein Laboratories Mill (Model M-2, Stein Laboratories Inc., Atchison, Kansas) and a 4 g sub-sample was used for extraction and derivation of DON using Gas Chromatography-Mass Spectroscopy as described by Mirocha et al. (1998).

One way analysis of variance on kernel infection, DON content and germination capacity was conducted using the MINITAB14 statistical software (Minitab Ltd., Coventry, UK). Values for each parameter are presented in the results section as mean ± standard error of the mean (SEM).

Infection pathways

St. Paul, Minnesota. Spikelets were collected for a laboratory study from the field experiment within

1 week after the first inoculation. These were examined for presence and location of lesions on apical or basal floret parts and glumes. Spikelets were dissected into glumes and florets after observation. The florets were further bisected into apical and basal portions. Cassettes containing parts from a single spikelet were soaked in 70% ethyl alcohol for 30 s followed by 10% bleach (Clorox®, 6% NaOCl) for 30 s and rinsed three times in sterile distilled water. These parts were placed on Komada's medium agar-KMA (Komada 1975) Petri plates. The plates were incubated at 20°C for 7 days under alternating 12 h of a combination of UVA and cool white light and 12 h of darkness. A small hyphal plug from the edge of the resulting colonies was transferred to carnation leaf agar (CLA) Petri-plates. These plates were incubated under similar conditions as the KMA plates for 10–14 days. Colonies of *F. graminearum* were identified as such when they produced perithecia on the carnation leaf pieces by the end of the incubation period.

An oat cv. Winnona, a spring oat cultivar developed by UMN in 2005, was used for the greenhouse experiment. This is an early maturing, short cultivar with high resistance to loose smut and lodging and moderate resistance to crown rust. Kernels were seeded once a week for five consecutive weeks from June 6/2008 to July 4/2008. Six seeds were initially planted per pot (15 cm×15 cm×16 cm) and subsequently thinned to four seedlings. The soil mixture used was 50% field soil v/v and 50% growing medium (MetroMix® 200series, SunGro Horticulture Canada Ltd., Vancouver, British Columbia). At the 2–3 leaf stage, one teaspoonful of a slow release fertilizer Osmocote® (The Scotts Company, Marysville, Ohio) was applied per pot. Plants were treated with the fungicide Baylathon (Bayer Corporation Crop Protection Products, Kansas City, Missouri) and the systemic insecticide Marathon (Olympic Horticultural Products Inc. Mainland, Pennsylvania). Conserve® SC (Dow AgroSciences LLC, Indianapolis, Indiana) was specially applied to control thrips. Temperature in the greenhouse varied in the range 20–23°C.

Fully emerged panicles marked prior to inoculation were sprayed with *F. graminearum* inoculum (as used in the field experiment) until runoff using CO_2-powered backpack sprayer. Plants were then placed in an adult plant dew chamber (100% relative humidity; 16 h fluorescent light) for 72 h before being returned to the greenhouse.

Spikelets were sampled randomly from the marked panicles 1 to 7 days after inoculation (DAI). Excised spikelets were placed in plastic bags and transported to the laboratory in a cooler containing ice. Florets for the anther colonization study were collected two, three, four and seven DAI.

Samples from the greenhouse were stained and fixed in a lactophenol blue (Fluka 61335 Lactophenol Blue Solution®) and alcohol solution. The solution consisted of one part lactophenol blue mixed with two parts 96% ethyl alcohol. This was heated to boiling point in a fume hood and poured into screw-capped glass tubes containing spikelets from each sampling time. These were left in the fume hood overnight and then kept in a refrigerator at 4°C for 7 days. Spikelets were washed twice with 50% alcohol for 15 min and rinsed twice with sterile distilled MilliQ water for 10 min. These were then transferred to a 25% glycerol solution for preservation until they were examined under the microscope (Lewandowski et al. 2006). This procedure resulted in fungal hyphae stained deep blue whilst most of the host plant tissue remained unstained.

Sixty florets from each sampling time were examined to study the pattern of floret colonization. For this observation, florets and floret parts were dissected and paleas and lemmas were mounted between two glass slides. Paleas and lemmas were examined under a compound microscope while the surface of the caryopsis was studied under a dissecting microscope. Anthers from fresh florets were mounted in a drop of water on a glass slide and examined under a compound microscope for the presence or absence of fungal hyphae.

Ås, Norway. During an extended period of mist and rain in July 2007 at Ås, a natural *Fusarium* epidemic developed in a commercial field of 'Belinda' oats. Panicles from plants at this site were sampled 8–10 days after anthesis. Symptomatic florets were fixed for microscopy in 2% paraformaldehyde and 1.25% glutaraldehyde in 0.05 M PIPES buffer with pH 7.2. Other bulk samples of panicles were kept frozen at −15°C. From the frozen samples, 100 florets with FHB-like symptoms were soaked in 1% NaOCl solution for 10 min and then dried in a chamber at 35°C. The florets were placed on potato dextrose agar (PDA) plates and kept under alternating 12 h of a

combination of cool white light and UVA and 12 h darkness at 20°C for 10 days. At the end of the incubation period each culture was transferred to synthetic nutrient-poor agar (SNA) for subsequent identification of *Fusarium* species.

As a follow up to determine the role of anthers in floret infection, a limited greenhouse experiment was carried out in Norway in August—October 2009. The cv. Hurdal and four breeding lines: '38–8', '3–11', '1287' and '1286' from UMN were used. The first three are normal white-seeded oats displaying low anther extrusion while the latter two display strong anther extrusion likely because they carry the wild type allele for shattering. The plants were inoculated at anthesis with a macroconidial mixture of two *F. graminearum* isolates (Isolates 101177 and 101023, obtained from the Norwegian Veterinary Institute) with a concentration of 1×10^5 spores/ml. At 7 DAI, 25 florets were harvested from each genotype, stained and examined under the microscope as described in the infection pathway study carried out at UMN. The percentage of florets with hyphae (palea and/or lemma and/or caryopsis) was then calculated.

Results

Optimal time of infection

All three parameters: kernel infection, DON content, and germination capacity were significantly affected by the timing of *F. graminearum* inoculation (p value< 0.0001 for all parameters). Inoculation at anthesis resulted in a significantly higher percentage of infected kernels (89±3.1%) compared to inoculation one (52±3.9%) or two (30±5.5%) weeks after anthesis. The uninoculated control had the lowest level of infected kernels (21.5±2.63%), but it was not significantly different from inoculations 1 or 2 weeks after anthesis (Fig. 1).

Similar patterns were found for DON content and germination. DON level was highest for inoculation at anthesis (19±0.28 ppm) followed by inoculation 1 week later (3.5±0.57 ppm). Inoculation 2 weeks after anthesis (1.1±0.27 ppm) did not give significantly different DON levels from the uninoculated control (0.7±0.21 ppm). Germination was highly suppressed (73±1.75%) in grain inoculated at anthesis. However, the germination capacity of samples from the other inoculation times and the non-inoculated control were >90% and were not significantly different from each other (Fig. 1).

Infection pathways

St Paul, Minnesota. First visual symptoms appeared at the floret tip and later spread to basal floret parts in samples from the field experiment that were collected within 1 week after the first inoculation date. Basal floret parts usually developed putative FHB symptoms only after the disease had spread to the entire floret. This was evident from the disparity in the percentage of symptomatic apical vs. basal floret parts (Table 1). Isolation of *F. graminearum* from the apical

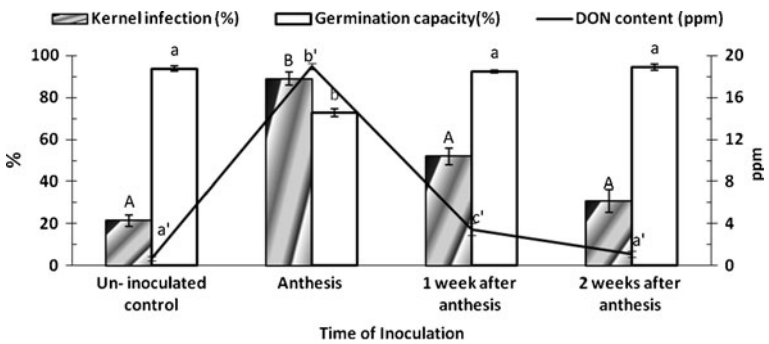

Fig. 1 Effect of time of inoculation with *Fusarium graminearum* on kernel infection, deoxynivalenol content, and germination capacity of oats (cv. Morton). Data is from a field inoculation experiment conducted in St. Paul, Minnesota in 2008. Kernel infection and germination capacity were measured in percentage while deoxynivalenol content was measured in ppm. One way analysis of variance was conducted and different letters belonging to each parameter represent significant difference (P<0.0001). Bars represent standard error of means of four replicates

Table 1 Location of lesions and infections with *Fusarium graminearum* on apical (A) and basal (B) floret portions and glumes of the oat cultivar Morton

	Glume 1		Glume 2		1° floret		2° floret		3° floret	
	A	B	A	B	A	B	A	B	A	B
Number examined	102	102	102	102	102	102	102	102	38	38
Symptomatic (%)	95	26	85	15	73	31	76	24	86	76
F. graminearum infected (%)	49	20	29	16	66	21	54	15	82	71

and the basal floret parts followed a similar pattern showing higher infection at the apical parts compared to the basal floret parts. The pathogen was observed to grow profusely from apical parts during the first stages of the infection process and spread to the basal portion of the floret (Table 1 and Fig. 2). However, both the apical and basal parts of the tertiary florets were usually found symptomatic and colonized in a few days after inoculation. The difference between symptomatic and colonized apical and basal floret parts of the tertiary floret was minimal compared to the primary and secondary florets (Table 1).

Florets collected from the greenhouse experiment allowed for a more detailed examination of the infection process. First visual symptoms started to appear at 3 DAI. However, hyphal growth was observed on the different floret parts as early as 1 DAI (Table 2). The floret mouth is the major entry pathway into the floret cavity.

The observations from this study showed a similar pattern to the study of the samples collected from the field inoculation experiment. Apical parts were found symptomatic and colonized with *F. graminearum* hyphae more often than basal floret parts. From 420 paleas studied 1–7 DAI, 157 had hyphae growing on the apical halves while only 22 had hyphae growing on the basal halves. The same numbers of lemmas and caryopses were examined and 168 and 65 respectively showed hyphae growing on the apical halves while only 61 and 4 respectively had hyphae growing on the basal halves (Table 3).

Hyphae on external surfaces of the palea and lemma tend to accumulate on the apical halves, but a few random hyphae were also found on the basal halves (Fig. 3). Hyphae were seen to grow from the apical parts of the lemma into the floret cavity and colonize the caryopsis and the external surfaces of the upper parts of the palea wings. Fungal hyphae on internal surfaces were observed either at the very tip or at the edges of the distal half of the palea and lemma. Hyphae on basal internal surfaces were exclusively found on the wings of the palea and lemma where the two overlap, possibly extending hyphal growth from external surfaces (Figs. 3 and 4). Hyphae on the caryopses were typically first found on the trichomes; hyphal growth extending from colonized anthers. Basal portions (both dorsal and ventral surfaces) of the caryopses were rarely found colonized and only in completely damaged and dead florets (Fig. 3).

Anthers appear to play an important role during the initial stages of the infection process (Fig. 5a and b).

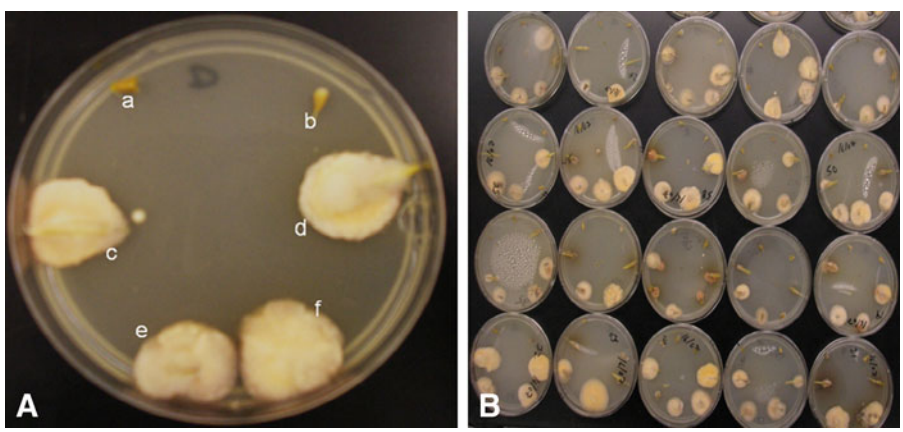

Fig. 2 Higher rate of colonization of apical floret portions than basal floret portions. **a** Glumes and florets dissected into apical and basal parts were placed on Komada's medium agar: *a* and *b* are basal parts while *e* and *f* are apical parts; *c* and *d* are glumes. **b** Additional Komada's medium agar plates with apical and basal floral parts with a similar arrangement as described in **a**

Table 2 Number of florets and floret parts of the oat cultivar Winnona colonized by hyphae of *Fusarium graminearum* based on 60 florets collected on 1 to 7 days after inoculation (DAI)

Days after inoculation	Entire Floret	Palea	Lemma	Caryopsis
1	2	2	0	0
2	7	4	6	1
3	40	34	30	13
4	42	34	35	9
5	41	30	34	18
6	44	28	42	8
7	40	29	33	16
Total	216	161	180	65

Hyphae of the fungus were observed to grow profusely out of anthers. Heavily colonized anthers appeared black to brownish in color (Fig. 5c and d). At 2 DAI and 3 DAI, more than 50% of the examined anthers were found colonized (Table 4) compared to lower numbers of the paleas, lemmas and caryopses (Table 2), suggesting that the anthers provide a more conducive environment for *F. graminearum* growth than any other floret part during the first few days after infection. The proportion of anthers colonized by *F. graminearum* at 4 DAI and 7 DAI was lower than that of 2 DAI and 3 DAI (Table 4). In addition, hyphae on anthers collected 4 DAI and 7 DAI appeared desiccated and thinner than those observed at 2 DAI and 3 DAI.

The importance of anthers in FHB in oats and the possible influence of anther extrusion were demonstrated in the greenhouse experiment conducted in Ås. The shattering genotypes with strong anther extrusion ('1286' and '1287') had 12–20% infected florets, whereas in the 'normal' oat genotypes (Hurdal, '3–11', '38–8'), this varied from 40% to 52% (Fig. 6).

ÅS, Norway. The symptoms on florets collected from the 2007 natural epidemic in Norway were similar to symptoms observed from field-inoculated samples from Minnesota in 2008, with brownish water-soaked lesions first appearing at floret apices and spreading towards basal portions (Fig. 7a and b). Bleached areas surrounded by a brownish discolouration were often observed on glumes. Fungal hyphae were often observed to spread from primary floret to secondary and tertiary florets, suggesting disease spread in a single spikelet is due to physical contact between the florets rather than through the rachilla (Fig. 7c). Pathogens isolated from florets collected from the 2007 natural epidemic in Norway included *F. avenaceum, F. poae, F. langsethiae* and *Microdochium nivale*. As only FHB causing fungi were isolated, the symptoms described above were interpreted as resulting from FHB.

Discussion

Results from kernel infection, DON contamination and germination capacity indicate that anthesis is the most susceptible stage for *F. graminearum* infection in oats. Conversely, susceptibility to successful infection decreased at later stages of development. Inoculation 2 weeks after anthesis was statistically equivalent to the uninoculated control in terms of kernel infection, DON contamination and germination capacity. In addition, inoculation 1 week after anthesis did not affect germination capacity showing that the

Table 3 Number of apical and basal portions of palea, lemma, and caryopsis colonized by hyphae of *Fusarium graminearum* based on 60 florets collected on 1 to 7 days after inoculation (DAI)

	Apical			Basal		
Days after inoculation	Palea	Lemma	Caryopsis	Palea	Lemma	Caryopsis
1	2	0	0	0	0	0
2	3	6	1	1	0	0
3	34	28	13	4	10	1
4	34	32	9	4	12	0
5	29	33	18	2	16	0
6	27	38	8	3	11	1
7	28	31	16	8	12	2
Total	157	168	65	22	61	4

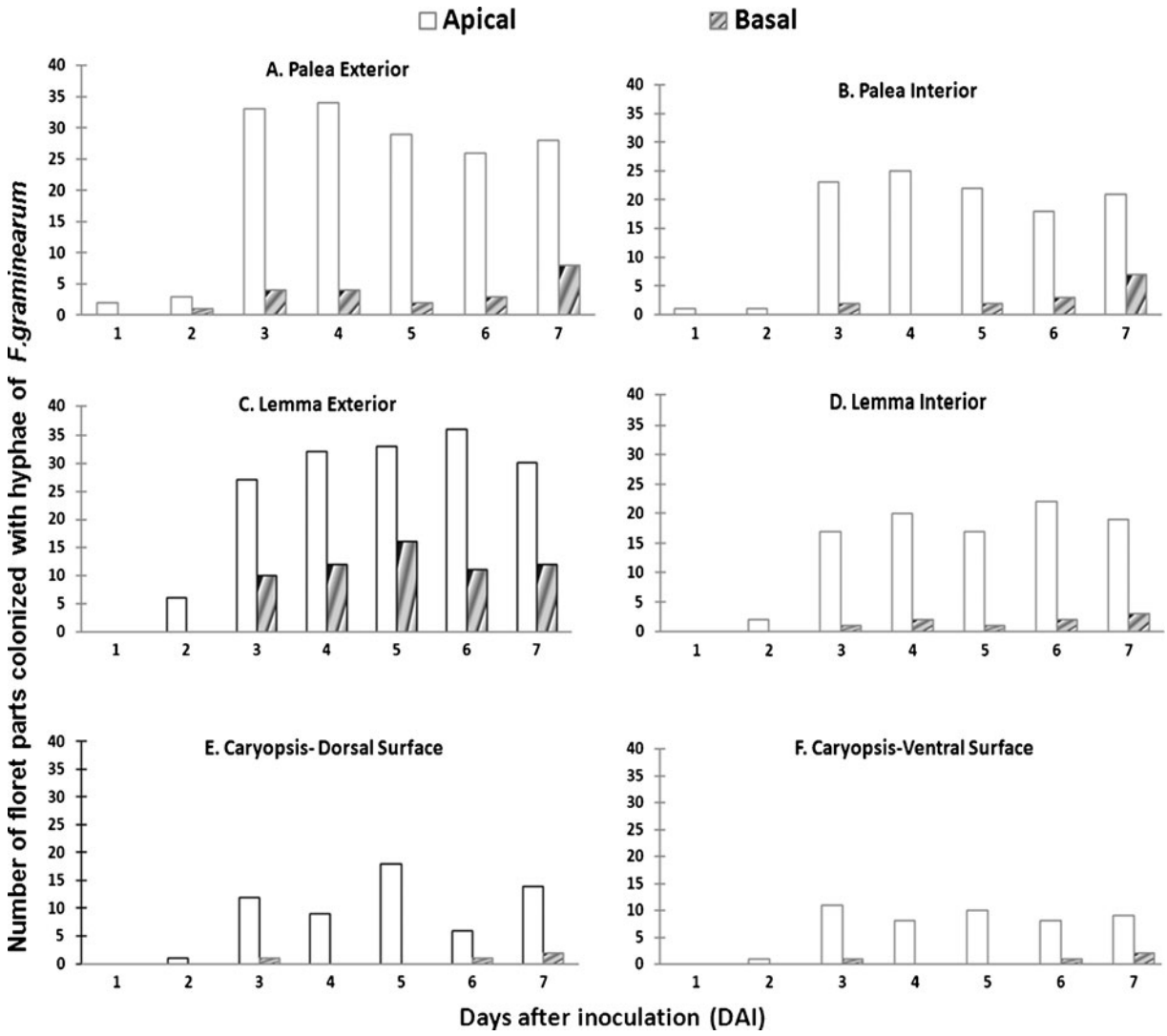

Fig. 3 Number of oat florets colonized by *Fusarium graminearum* on apical and basal halves of the external and internal surfaces of the palea (**a** and **b**), and the lemma (**c** and **d**), and the dorsal and ventral surfaces of the caryopsis (**e** and **f**). Floret parts were studied under the microscope after staining with lactophenol blue solution

effect of *F. graminearum* infection on germination capacity is restricted to just a few days after anthesis. *Fusarium graminearum* infections occurring at anthesis may cause complete decay of the caryopses or result in infected kernels with severely depressed germination and elevated mycotoxin contamination.

The trend in barley and wheat is more or less similar showing infections at and a few days after anthesis are more severe and devastating in terms of production of shriveled and scabby kernels and mycotoxin contamination as compared to infections ocurring later in kernel development (Del Ponte et al. 2007; Lacey et al. 1999; McCallum and Tekauz 2002) . Barley is susceptible to *F. graminearum* infection up to 14 days after heading with the highest seed colonization occurring at 7 days after heading (McCallum and Tekauz 2002). In another study, effect of time of infection with *F. graminearum* was found to be dependent on type of flowering where cleistogamous barley cultivars were susceptible 10 days after anthesis when spent anthers were exposed, whereas chasmogamous barley cultivars were susceptible at anthesis (Yoshida et al. 2007). On the other hand, wheat (cv. Norm) was found to be susceptible to *F. graminearum* infection

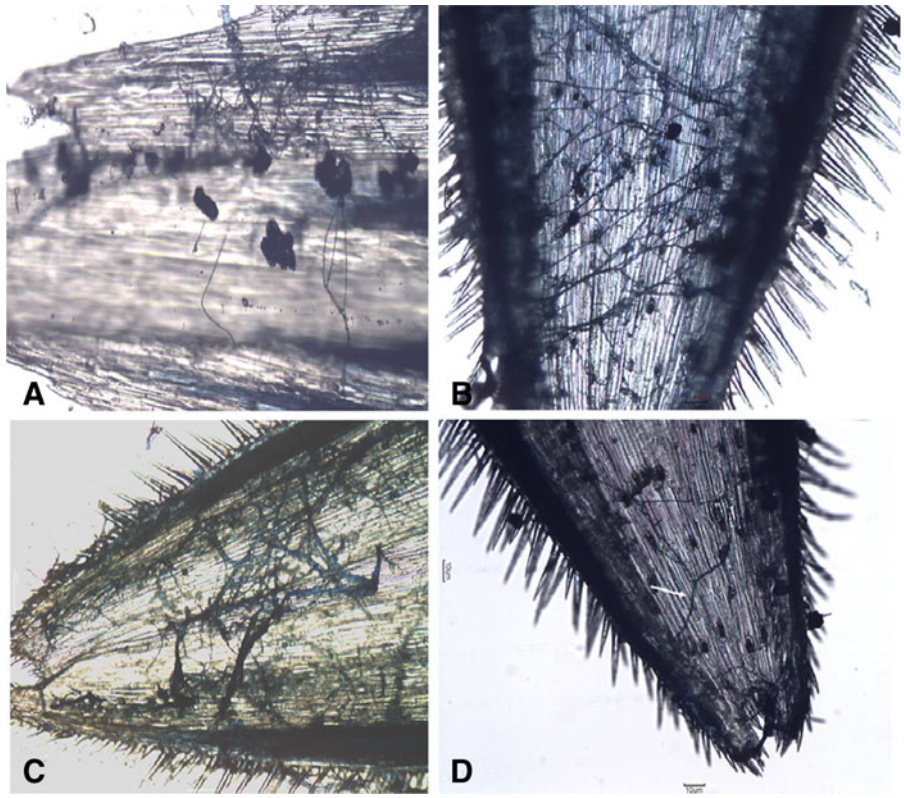

Fig. 4 Hyphae of *Fusarium graminearum* on lemma and palea of oat florets stained with lactophenol blue solution. **a** Hyphae growing at the edge of apical part of the lemma, 4 days after inoculation (DAI). **b**, **c** Apical part of the palea with hyphal network of *F. graminearum*, 4 DAI. **d** Hyphae (*indicated by the arrow*) growing on the surface of the palea at the initial stage of infection, 1 DAI

from flowering to the hard dough stage with highest incidence of scabby kernels and DON contamination recorded at early inoculations (Del Ponte et al. 2007). In another experiment in wheat, highest disease incidence and DON contamination occurred after inoculation at about mid-anthesis with decreasing effects of later inoculations (Lacey et al. 1999).

The field- and greenhouse-grown oats inoculated with *F. graminearum*, as well as the florets collected from the natural FHB epidemic in Norway, showed that the floret mouth is the principal pathway of the fungus into the floret cavity. In addition, the crevices between the palea wing and the lemma wing near the floret mouth served as an alternate avenue. Anthers also played an important role at the initial stages of the infection process. In barley (cv. Robust), Lewandowski et al. (2006) found the floret mouth and the crevices between the overlapping palea and lemma to be the principal entry pathways to *F. graminearum*. However, unlike our results, they found that anthers played a minimal role in floret colonization. Some of the differences in infection in oats and barley can be attributed to the difference between the floral structures of the two crops. Oat panicles have spikelets hanging down while barley has an erect spike type. Water from irrigation or rainfall accumulates at the tips of the individual oat florets while in barley it accumulates at the basal portion of florets between individual spikelets. This high moisture creates a more conducive environment for spore germination and infection than the relatively drier parts. This can be one reason why Lewandowski et al. (2006) found more lesions and mycelial colonies of *F. graminearum* colonizing external surfaces of basal portions of barley florets while we found on oats more on the apical portions.

The observations that anthers appear to play a significant role during the initial stages of infection in oats agrees with the observations in wheat by Pugh et al. (1933) and Strange and Smith (1971). Skinnes et al. (2010) found that a high degree of anther extrusion was strongly associated with reduced levels of FHB: unless they are extruded from the florets, anthers become an infection focal point, which has to be addressed by other mechanisms of active resistance. They suggested that *Fusarium* spp. have a high affinity to anthers because they are also successful

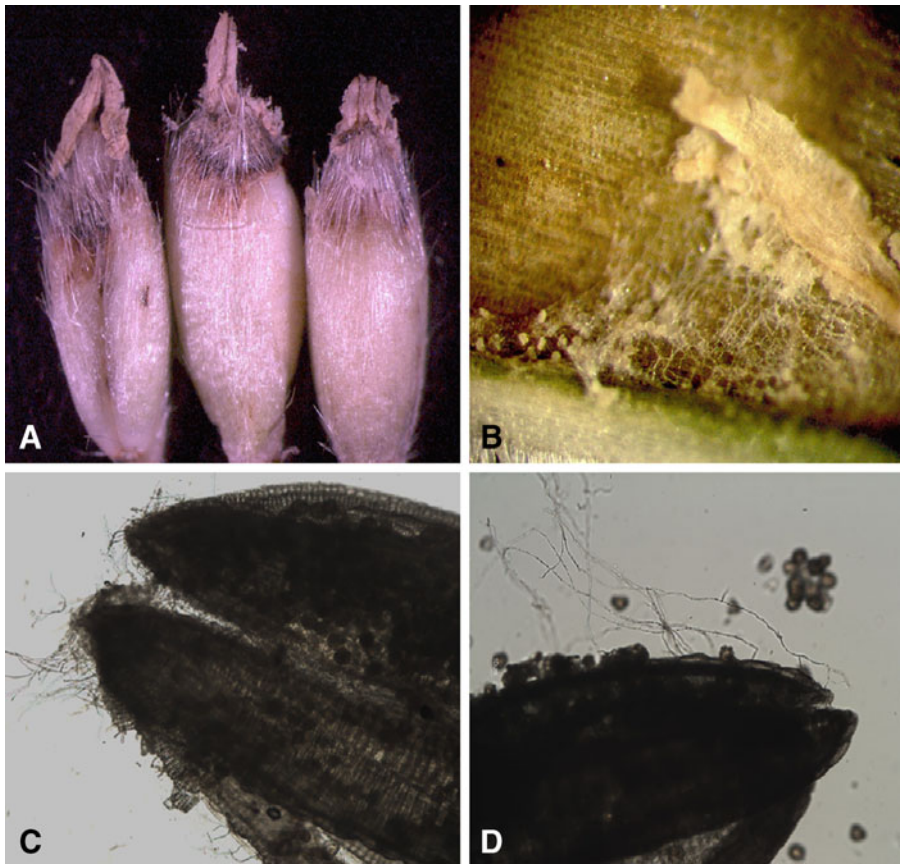

Fig. 5 Oat anthers colonized by *Fusarium* spp. **a** Kernels of oat cv. Belinda with anthers colonized with *Fusarium* spp., **b** anthers colonized with *Fusarium* spp. on the surface of the lemma, and (**c**, **d**) anthers of the oat cv. Winnona colonized with hyphae of *Fusarium graminearum*, 3 days after inoculation. **a** and **b** are from the 2007 natural epidemic in Norway while **c** and **d** are from the greenhouse experiment at the University of Minnesota

saprophytes and anthers constitute dead tissue subsequent to anthesis (Skinnes et al. 2010).

Alternatively, as shown in cleistogamous barley, enclosed anthers escape infection until they are forced out of the floret by the developing kernel. This makes these type of barley cultivars more susceptible to *Fusarium* infection 7–10 days after anthesis (Yoshida et al. 2007). Similar to our observations, FHB symptoms in such barleys appeared first on the tips where the extended anthers were retained and

Table 4 Number and percentage of anthers of the oat cultivar Winnona colonized by *Fusarium graminearum* based on fresh and unstained anthers examined under the microscope on 2, 3, 4, and 7 days after inoculation (DAI)

Days after inoculation	# of anthers examined	# of anthers colonized	% colonized anthers
2DAI	50	29	58
3DAI	66	39	59
4DAI	66	22	33
7DAI	66	31	47

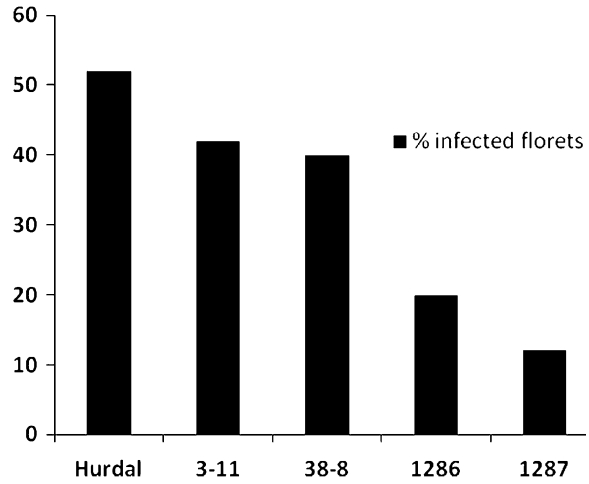

Fig. 6 Percentage of infected florets of five oat genotypes inoculated with *Fusarium graminearum* at flowering and examined under the microscope after staining with lactophenol blue solution. Three genotypes (Hurdal, 3–11, 38–8) exhibit low anther extrusion and the remaining two (1286 and 1287) exhibit strong anther extrusion. Percentages are based on 25 florets of each genotype sampled at 7 days after inoculation

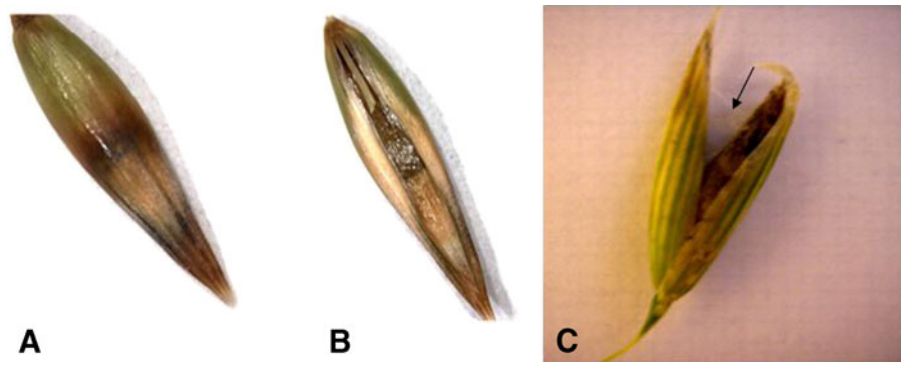

Fig. 7 a, **b** Initial symptoms of FHB starting from the apices and spreading to the basal portions of the floret. **c** *Fusarium* spp. mycelia extending from the primary floret and infecting the secondary floret. Pictures are of infected samples from the natural *Fusarium* epidemic in 2007, Norway

exposed, and then progressed towards the basal portions. In the same experiment, chasmogamous barley cultivars showed severe FHB and high DON and nivalenol contamination when inoculated at anthesis (Yoshida et al. 2007). The results from our study show that similar factors may apply in the initial stages of oat infection by *Fusarium* spp. Oats become less susceptible as the floret tissues develop and the anthers are lost. Therefore oat genotypes extruding their anthers appear to be at a lower risk of FHB than genotypes that retain them, but this needs further investigation.

The high rate of colonization of anthers can explain the typical symptomatic apical floret parts. The lag in time of infection in other floret parts compared to the anthers suggests that early infections on the anthers lead to later infections of the other floret parts during the first few days after inoculation. The thinner hyphae observed on anthers collected at 4 DAI and 7 DAI might simply be due to desiccation of hyphae after the plants were transferred from the dew chamber to the greenhouse after 3 DAI. In addition, as disease progresses, the fungus finds other nutrient sources as it grows into the floret cavity colonizing the internal surfaces of the palea, lemma and the caryopses.

Spread of infection within a single spikelet, mainly due to physical contact between florets but never between different spikelets, confirmed that oats have high type II resistance to FHB (Langevin et al. 2004). This observation also explained the relatively small difference between the percentage of symptomatic apical and basal parts of the tertiary florets in the field inoculated samples from the UMN trial. As the tertiary florets are located between the apical parts of the primary and secondary florets, spread from infected apical parts of primary and secondary florets is relatively easy. In addition, the tertiary floret is much smaller than the other florets, likely making it possible for the whole floret to be invaded in a relatively short time, reducing any difference between symptomatic apical and basal parts. An established infection in the primary and secondary florets may make the later flowering florets more vulnerable to infection from earlier flowering florets. A more detailed microscopic study of the infection biology of *F. graminearum* investigating the spread of infection from spikelet to spikelet as done in wheat by Brown et al. (2010) would give thorough results and complement our findings.

Acknowledgement The first author is indebted to the collaborative program between the University of Minnesota and the Norwegian University of Life Sciences for a travel grant, and to Prof. Ruth Dill-Macky for the supervision of her M.Sc. experiments in Saint Paul during the summer in 2008. The authors also acknowledge the financial support of the Norwegian Research Council and the breeding company Graminor to the project *Safe Grains: Mycotoxin prevention through resistant wheat and oats* (Project number 178273/I10). The authors would also like to thank the anonymous reviewers for their valuable comments and suggestions on the manuscript.

References

Andersen, A. L. (1948). The development of *Gibberella zeae* head blight of wheat. *Phytopathology, 38*, 595–611.

Bjørnstad, Å., & Skinnes, H. (2008). Resistance to *Fusarium* infection in oats (*Avena sativa* L.). *Cereal Research Communications, 36*, 57–62.

Brodal, G. (1991). *Occurrence, pathogenicity and transmission of seed-borne fungi on grasses in Norway*. Dissertation: Agricultural University of Norway.

Brown, N. A., Urban, M., Van De Meene, A. M. L., & Hammond-Kosack, K. E. (2010). The infection biology of *Fusarium graminearum*: defining the pathways of spikelet

to spikelet colonisation in wheat ears. *Fungal Biology, 114*, 555–571.

Bushnell, W. R., Hazen, B. E., & Pritsch, C. (2003). Histology and physiology of Fusarium head blight. In K. J. Leonard & W. R. Bushnell (Eds.), *Fusarium head blight of wheat and barley* (pp. 44–83). Saint Paul: The American Phytopathological Society.

Del Ponte, E. M., Fernandes, J. M. C., & Bergstrom, G. C. (2007). Influence of growth stage on Fusarium head blight and deoxynivalenol production in wheat. *Journal of Phytopathology, 155*, 577–581.

Dill-Macky, R. (2003). Inoculation methods and evaluation of Fusarium head blight resistance in wheat. In K. J. Leonard & W. R. Bushnell (Eds.), *Fusarium head blight of wheat and barley* (pp. 184–210). Saint Paul: The American Phytopathological Society.

Engle, J. S., Lipps, P. E., Graham, T. L., & Boehm, M. J. (2004). Effects of choline, betaine, and wheat floral extracts on growth of *Fusarium graminearum*. *Plant Disease, 88*, 175–180.

Gilbert, J., & Tekauz, A. (1995). Effects of fusarium head blight and seed treatment on germination, emergence, and seedling vigour of spring wheat. *Canadian Journal of Plant Pathology, 17*, 252–259.

Gilbert, J., Tekauz, A., & Woods, S. M. (1997). Effect of storage on viability of fusarium head blight-affected spring wheat seed. *Plant Disease, 81*, 159–162.

Haave, R. (1985). *Forekomst og patogenitet av Fusarium-arter på korn i Norge*. Dissertation, Agricultural University of Norway.

Hofgaard, I. S., Aamot, H. U., Klemsdal, S. S., Elen, O., Jestoy, M., & Brodal, G. (2010). Occurrence of *Fusarium* spp. and mycotoxins in Norwegian wheat and oats. In I. S. Hofgaard and E. Fløistad (Eds.), *Nordic Baltic fusarium seminar* (p. 37). Bioforsk, Ski.

Kang, Z. S., & Buchenauer, H. (2000). Cytology and ultrastructure of the infection of wheat spikes by *Fusarium culmorum*. *Mycological Research, 104*, 1083–1093.

Komada, H. (1975). Development of a selective medium for quantitative isolation of *Fusarium oxysporum* from natural soil. *Review of Plant Protection Research, 8*, 114–125.

Lacey, J., Bateman, G. L., & Mirocha, C. J. (1999). Effects of infection time and moisture on development of ear blight and deoxynivalenol production by *Fusarium* spp. in wheat. *Annals of Applied Biology, 134*, 277–283.

Langevin, F., Eudes, F., & Comeau, A. (2004). Effect of trichothecenes produced by *Fusarium graminearum* during Fusarium head blight development in six cereal species. *European Journal of Plant Pathology, 110*, 735–746.

Lewandowski, S. M., Bushnell, W. R., & Evans, C. K. (2006). Distribution of mycelial colonies and lesions in field-grown barley inoculated with *Fusarium graminearum*. *Phytopathology, 96*, 567–581.

Limonard, T. (1966). A modified blotter test for seed health. *Netherlands Journal of Plant Pathology, 72*, 319–321.

McCallum, B. D., & Tekauz, A. (2002). Influence of inoculation method and growth stage on fusarium head blight in barley. *Canadian Journal of Plant Pathology, 24*, 77–80.

McMullen, M., Jones, R., & Gallenberg, D. (1997). Scab of wheat and barley: a re-emerging disease of devastating impact. *Plant Disease, 81*, 1340–1348.

Miller, S. S., Chabot, D. M. P., Ouellet, T., Harris, L. J., & Fedak, G. (2004). Use of a *Fusarium graminearum* strain transformed with green fluorescent protein to study infection in wheat (*Triticum aestivum*). *Canadian Journal of Plant Pathology, 26*, 453–463.

Mirocha, C. J., Kolaczkowski, E., Xie, W. P., Yu, H., & Jelen, H. (1998). Analysis of deoxynivalenol and its derivatives (batch and single kernel) using gas chromatography mass spectrometry. *Journal of Agricultural and Food Chemistry, 46*, 1414–1418.

Parry, D. W., Jenkinson, P., & McLeod, L. (1995). Fusarium ear blight (scab) in small-grain cereals—a review. *Plant Pathology, 44*, 207–238.

Pugh, G. W., Johann, H., & Dickson, J. G. (1933). Factors affecting infection of wheat heads by *Gibberella saubinetti*. *Journal of Agriculatural Research, 46*, 771–797.

Schroeder, H. W., & Christensen, J. J. (1963). Factors affecting resistance of wheat to scab caused by *Gibberella zeae*. *Phytopathology, 53*, 831–838.

Shaner, G. E. (2003). Epidemiology of Fusarium head blight of small grain cereals in North America. In K. J. Leonard & W. R. Bushnell (Eds.), *Fusarium head blight of wheat and barley* (pp. 84–119). Saint Paul: The American Phytopathological Society.

Skadsen, R. W., & Hohn, T. A. (2004). Use of *Fusarium graminearum* transformed with gfp to follow infection patterns in barley and *Arabidopsis*. *Physiological and Molecular Plant Pathology, 64*, 45–53.

Skinnes, H., Semagn, K., Tarkegne, Y., Maroy, A. G., & Bjornstad, A. (2010). The inheritance of anther extrusion in hexaploid wheat and its relationship to Fusarium head blight resistance and deoxynivalenol content. *Plant Breeding, 129*, 149–155.

Strange, R. N., & Smith, H. (1971). A fungal growth stimulant in anthers which predisposes wheat to attack by *Fusarium graminearum*. *Physiological Plant Pathology, 1*, 141–150.

Strange, R. N., Majer, J. R., & Smith, H. (1974). The isolation and identification of choline and betaine as the two major components in anthers and wheat germ that stimulate *Fusarium graminearum in vitro*. *Physiological Plant Pathology, 4*, 277–290.

Wagacha, J. M., & Muthomi, J. W. (2007). *Fusarium culmorum*: infection process, mechanisms of mycotoxin production and their role in pathogenesis in wheat. *Crop Protection, 26*, 877–885.

Yli-Mattila, T. (2010). Ecology and evolution of toxigenic *Fusarium* species in cereals in northern Europe and Asia. *Journal of Plant Pathology, 92*, 7–18.

Yoshida, M., Kawada, N., & Nakajima, T. (2007). Effect of infection timing on Fusarium head blight and mycotoxin accumulation in open- and closed-flowering barley. *Phytopathology, 97*, 1054–1062.

Paper II

Selamawit Tekle, Helge Skinnes, Åsmund Bjørnstad

Eur J Plant Pathol (2013) 135:147–158
DOI 10.1007/s10658-012-0074-6

The germination problem of oat seed lots affected by Fusarium head blight

Selamawit Tekle · Helge Skinnes · Åsmund Bjørnstad

Accepted: 22 August 2012 / Published online: 14 September 2012

Abstract Mycotoxin contamination and reduced germination capacity (GC) of oats affected by Fusarium head blight (FHB) have become serious concerns in Norway. Spawn- and spray-inoculated field trials were conducted from 2007 to 2010 to screen for resistant genotypes and to study the relationship between GC and deoxynivalenol (DON) contamination. Correlation coefficients between GC and DON level varied from −0.412 to −0.711 ($P<0.001$). The strongest and the weakest correlations were recorded for the spray- and spawn-inoculated experiments of 2009, respectively. High DON levels were associated with low GCs but low DON levels did not guarantee higher GCs. DON did not inhibit initiation of germination, but did retard seedling growth in a germination assay conducted on DON-amended water agar. Most of the seedlings grown on the modified WA containing even as little as 2 ppm DON had abnormal morphology and would not be considered as 'germinated' in official tests. A greenhouse experiment studying the effect of time of inoculation on GC, DON level, and seed infection (SI) showed a rapid reduction in DON levels resulting from later inoculations. Increments in GC were observed although they were not as strong as the decrements in DON level. Seed infection remained consistently high (> 60 %) for all inoculations. Seed dressing and dehulling individually were not effective in improving GC, but when combined increased GC to the percentage of kernels having viable germ. We hypothesize that in addition to the level of DON, SI influences the GC of *Fusarium*-damaged oats, especially in wet years that may facilitate late-initiated infections.

Keywords Deoxynivalenol · Dehulling · Infection time · Seed dressing · Seedling blight

Abbreviations

DON	Deoxynivalenol
FHB	Fusarium head blight
GC	Germination capacity
SI	Seed infection

Introduction

Fusarium species cause interrelated diseases such as foot and root rot, Fusarium seedling blight (FSB), and Fusarium head blight (FHB) in small grain cereals in many parts of the world. FHB is economically more important than FSB and root rot diseases in wheat and barley production (Wang et al. 2006), due to the associated mycotoxins posing serious health risks to humans and animals (Parry et al. 1995; Placinta et al. 1999). Even though several species in the genus are associated with the *Fusarium* disease complex in

S. Tekle (✉) · H. Skinnes · Å. Bjørnstad
Department of Plant and Environmental Sciences,
Norwegian University of Life Sciences,
P.O. Box 5003, 1432 Ås, Norway
e-mail: selag@umb.no

cereals, *F. graminearum*, *F. culmorum,* and *F. avenaceum* are the most important and frequently isolated ones (Parry et al. 1995).

The epidemiological cycle of the *Fusarium* disease complex begins with the inoculum surviving in the soil and on plant debris as saprophytic mycelia or as thick-walled resting spores. Sowing in such soils could lead to development of foot rot and seedling blight. FHB will develop from splash dispersed conidia and/or windblown ascospores during flowering. Grain contaminated by *Fusarium*, if used as a seed source, will provide primary inoculum for development of FSB and foot rot, completing the disease cycle (Parry et al. 1995).

Environmental conditions play an important role in the epidemiology of *Fusarium* diseases. Warm and dry soil conditions are favourable to the development of foot rot and production of inoculum on stem bases, while intense rainfall during flowering will effectively disperse inoculum to aerial parts leading to successful infection of heads (Parry et al. 1995). Prolonged warm temperature with frequent rainfall and/or dew around flowering and early kernel fill can lead to heavy epidemics of FHB (McMullen et al. 1997; Parry et al. 1995). Dickson et al. (1923) found severity of seedling blight of wheat caused by *Gibberella saubinetii,* the sexual stage of *F. graminearum,* to increase with increasing soil temperature from 10 °C to about 20–24 °C.

Seed lots infested and/or infected by *Fusarium* spp. have reduced germination capacity (GC). This can be due to loss of germinability, reduced emergence, and/or post emergence seedling blight (Dickson et al. 1923; Jones 1999). Germination capacity of wheat was increased by 32 % following surface sterilization that killed viable propagules of *F. graminearum* (Jones 1999) which could have led to seedling blight during germination. Bechtel et al. (1985) found that *F. graminearum* was most prevalent in the aleurone and pericarp tissues of wheat kernels and that the germ was usually spared from infection except when heavily invaded. However, it is important to keep in mind that kernels with initially healthy and viable germ may fail to germinate, or will produce abnormal seedlings, due to infection during germination.

Species of *Fusarium* widely differ in aggressiveness. In wheat, *F. graminearum* caused the greatest reduction in GC followed by *F. avenaceum* and *F. culmorum,* with *F. poae* having the least effect (Browne and Cooke 2005). In another trial, *F. langsethiae* and *F. poae* failed to cause seedling blight in oat and wheat seedlings, while *F. culmorum*, *Microdochium nivale,* and *M. majus* did so (Imathiu et al. 2010).

Trichothecene production is a factor of aggressiveness in *Fusarium* infection (Wang et al. 2006). A significant correlation between disease index and deoxynivalenol (DON) content of blighted seedlings was found in barley infected with *F. culmorum* (Hestbjerg et al. 2002). Emergence and survival of barley, triticale, common wheat and durum wheat seedlings were significantly reduced by trichothecene producing strains compared to non-trichothecene producing strains of *F. graminearum* (Wang et al. 2006). DON inhibited growth of wheat seedlings, coleoptile segments, and anther derived callus and embryos (Bruins et al. 1993). DON and diacetoxyscirpenol preferentially inhibited root elongation, while T-2 treated *Arabidopsis* seedlings showed dwarfism and aberrant morphological changes, demonstrating that phytotoxic action is dependent on the type (Masuda et al. 2007) and the relative concentration of the trichothecenes (Lemmens et al. 1994; McLean 1996).

Seed dressing has been used to reduce germination problems arising from *Fusarium* infection. For example, seed treatments containing maneb or thiabendazole significantly improved GC in wheat (Jones 1999). However, when seed quality is very poor, with a high proportion of *Fusarium* damaged kernels, also known as tombstone or scabby kernels, the effect of seed dressing can be minimal (Gilbert and Tekauz 1995). Size sorting has also been shown to increase germination and emergence of *Fusarium* infected wheat seed lots by removing light-weight scabby kernels which result from heavy *Fusarium* infections (Hare et al. 1999). Combining cleaning with seed dressing resulted in a significant increase in GC of *Fusarium*-damaged spring wheat (Gilbert and Tekauz 1995).

In Norway, incidence and severity surveys of FHB have been carried out and models for disease forcasting and risk assessment are being developed (Elen et al. 2010; Hofgaard et al. 2010). Results from these studies show that FHB incidence has increased, *F. graminearum* has become more prevalent in recent years, and higher levels of mycotoxin contamination, especially in oats, have been detected (Elen et al. 2010; Hofgaard et al. 2010). Previous work by Langseth and Rundberget (1999) had also shown that samples of commercially produced oats during 1996–1998 had higher levels of HT- 2 and DON than wheat

and barley. Fusarium head blight greatly reduced GC of oat seed of the Norwegian cv. 'Gere' and the German cv. 'Bessin' and this led to the withdrawal of these cultivars from the Norwegian seed market (Bjørnstad and Skinnes 2008). Thus, the issues of mycotoxin contamination and reduced germination capacity of *Fusarium*-infected oats have become major concerns. Hence, our objectives were to: *i)* investigate the relationship between DON level and GC in oats; *ii)* evaluate the impact of time of infection and prevailing environmental conditions on the relationship between GC and DON level; and *iii)* evaluate the effect of seed dressing and dehulling on GC of *Fusarium*-infected oat seed lots.

Materials and methods

Field experiments

Several oat cultivars and breeding lines from the Norwegian breeding company, Graminor AS, were evaluated for their resistance to FHB from 2007 to 2010 at the Vollebekk Research Farm of Norwegian University of Life Sciences, Ås. The number of genotypes tested during the experimental years ranged from 32 to 99, with 8–12 genotypes being evaluated each year to serve as checks across the experimental years. Each genotype was replicated twice in an alpha lattice experimental design. Plots were 0.45 m x 2.0 m spaced 0.3 m apart, with a 1.0 m alley between blocks. Each plot was planted with 50 g seed as four rows spaced 0.15 m apart. A compound fertilizer (NPK 21-4-10) was applied just before planting at a rate of 400 kg/ha.

Inoculum and inoculation

In 2009, both spray and spawn inoculations were carried out while in the other experimental years only spawn inoculation was used. Four isolates of *F. graminearum,* 101118, 101018, 101177 and 101023, obtained from the Norwegian Veterinary Institute, were used to prepare the spawn and spray inocula. A protocol from Dr. Bernd Rodemann (Julius Kühn-Institut, Germany) was followed to produce the spawn inoculum. The isolates were grown on potato dextrose agar (PDA) for 7 days at ambient temperature and light. At the end of the incubation period, three to five pieces of PDA of each isolate were transferred to 100 ml of autoclaved and deionized water containing 1 g of oat flour. These preparations were kept on a horizontal shaker set at 90 rpm for 7 days at ambient temperature and light to produce liquid cultures of *F. graminearum*. Two kilograms of oat kernels in heat stable polyethylene bags (cv. Belinda, soaked in water overnight, autoclaved at 121 °C for 1 h) were re-autoclaved, cooled down to room temperature, and inoculated with 100 ml of the liquid culture. The bags were left in upright position for 3 weeks at ambient temperature and light to facilitate mycelial growth. Subsequently, the infested oat kernels were spread on trolleys and misted with water for 3 weeks to initiate perithecial development. The spawn inoculum was applied in the experimental plots at a rate of 10 g/m^2 at Zadoks growth stage 31/32 (Zadoks et al. 1974). Less inoculum (2–3 g/m^2) was applied in 2010 due to build up of inoculum in the experimental fields from previous applications. Three nine-minute-long cycles of mist irrigation were applied every hour from 19:00–22:00 h following spawn application until the first date of flowering, and increased to four cycles from 19:00–23:00 h until 10 days after the last flowering date.

For spray inoculations in 2009, the isolates were cultivated on mungbean agar (MBA) at 23 °C for 1 week under alternating 12 h of darkness and 12 h of a combination of fluorescent white light and UVA light. Macroconidia were harvested by spraying deionized water on the MBA. An isolate mixture containing equal proportion of each isolate, adjusted to a spore concentration of 10^5 spores/ml, was prepared and kept frozen at −18 °C until time of inoculation. Plots were inoculated on dates of flowering (when ~50 % of the panicles had fully emerged) after thawing the frozen inoculum at 25 °C and adding 0.5 ml of Tween20® per litre of inoculum. The two middle rows were sprayed with 70 ml of inoculum using a backpack sprayer (Solo 416, Sindelfingen, Germany). Each plot was inoculated twice; on the date of flowering and 3 days after the first inoculation to catch late emerging panicles. Inoculations were carried out during the evening (after 18:00 h) and plots were mist irrigated (four nine-minute-long cycles) from 19:00–23:00 h immediately following inoculation, and every evening until 10 days after all inoculations were completed.

Effect of time of inoculation

A greenhouse experiment to study the effect of time of inoculation on GC, DON level and seed infection (SI)

was conducted during spring 2010. Twenty four pots of the moderately resistant oat cultivar 'Hurdal' were planted every week for five consecutive weeks in order to obtain plants at different developmental stages. Eight pots from each planting date (four inoculated and four uninoculated controls) were placed in three separate greenhouse rooms to provide replicates. Each pot had 10 adult plants grown under a photoperiod of 18 h HPI/SON light at 18 °C and 6 h darkness at 15 °C. Plants were spray-inoculated using the same inoculum as described in the spray-inoculated field experiments using a handheld sprayer distributing 10 ml of inoculum per pot. Inoculations were carried out at 2 days before flowering, and 5, 12, and 19 days after flowering, and at yellow maturity (Zadoks growth stage 91/92). Following inoculation, plants were kept under a polyethylene tent for 48 h to maintain high relative humidity to facilitate infection. Seeds were hand-harvested 1 week following yellow maturity for analyses.

Germination test on DON-amended water agar

A controlled environment chamber trial was conducted in 2011 to study the effect of different levels of DON on germination and seedling vigour of the oat cv. 'Hurdal'. Kernels were dehulled prior to surface sterilization to expose any microflora present under the hulls that could potentially affect germination. Kernels were surface sterilized by soaking in 70 % ethanol for 20 s, then in 1 % NaOCl for 90 s. Kernels were then rinsed three times in sterile distilled water (SDW) and placed on wet filter paper to imbibe over night.

Water agar (WA) was prepared by dissolving 8 g of Difco agar in 1 l of SDW followed by autoclaving. Two millilitres of methanol were used to dissolve 5 mg of DON (Sigma Aldrich, product number D0156) to prepare a stock DON-WA solution. After serial dilution, WA containing 0, 2, 5, 10, 15, and 20 ppm of DON was prepared. Forty kernels were tested at each DON level with five kernels placed in each magenta box (7.5 cm×7.5 cm×10 cm) containing 25 ml of the DON-amended WA. The magenta boxes were placed in a controlled environment chamber in darkness for 3 days followed by a 16 h photoperiod for 11 days. Temperature was set at 10 °C during the first 10 days and raised to 16 °C during the final 4 days of incubation. Data on coleoptile length, radicle length, and germination percentage were recorded at the end of the 14-day long incubation period.

Effects of dehulling and seed dressing

The moderately resistant cultivar 'Hurdal', a susceptible cultivar 'Bessin', and two breeding lines ('Z595-7' and 'Z615-4', both moderately resistant) were used to evaluate the effect of dehulling and seed dressing on GC of *Fusarium*-infected seed. The seed lots originated from spawn-inoculated experiments conducted from 2009 to 2011. Seed from 2009 to 2011 was analyzed within 2 months after harvest while seed from 2010 was kept frozen at −18 °C for 1 year before analysis. In addition, seed from 2009 was re-analyzed after 2 years of storage in a non-heated storage room. Germination capacity was determined on the untreated seed and after seed dressing and/or dehulling. Kernels were dehulled manually to minimize physical damage. For seed dressing, the fungicide Celest Formula M (25 g/l Fludioxonil) was applied at a rate of 2 ml a.i. per kg of seed.

The reduction in GC of the untreated seed was assumed to be the combined result of dead germ resulting from previous *Fusarium* infection and seedling blight occurring during germination. The percentage of kernels with viable germ (referred to as 'viable seeds' or 'seed viability' from here on) was used to quantify the percentage of kernels with dead germ. Hence, reduction in GC which was not caused by dead germ was attributed to seedling blight. Individual effects of seed dressing and dehulling were estimated by subtracting GC of the untreated seed from the GC of the dressed and GC of the dehulled seed, respectively. Further, the difference between GC of the untreated seed and GC of the dehulled and seed dressed seed provided an estimate of the combined effect of seed dressing and dehulling.

Determination of GC, seed viability, SI, and DON level

Germination capacity and seed viability were determined at the Kimen Seed Testing Laboratory, Ås, Norway. Kernels were placed in sand in darkness at 10 °C for 7 days and then under 8 h of fluorescent light at 20 °C for 3 days. Germination tests on filter paper were avoided because preliminary tests

indicated that highly prolific fungal growths from diseased kernels were affecting neighbouring kernels. At the end of the 10-day long incubation period, seedlings/kernels were categorized as normal seedlings, abnormal seedlings, dormant (healthy, un-germinated) kernels, or dead kernels according to International Seed Testing Association (ISTA) standards (ISTA 2006). Normal seedlings and dormant kernels were summed and considered as the total GC of the seed lot. Seed viability was determined by the tetrazolium test in which a colourless solution, 2, 3, 5-triphenyl tetrazolium chloride, is reduced to a red, stable and non-diffusible formazan within living cells, indicating viability. Both GC and seed viability were determined by testing two lots of 100 kernels from each sample and taking the average of the two lots.

Seed infection was determined by the modified freezer blotter test (Brodal 1991; Limonard 1966), also at the Kimen Seed Testing Laboratory. One hundred seeds from each sample were soaked in 1 % chlorine for 10 min for surface sterilization and placed on a double moist filter paper (300 g/m^2, Munktell Filter AB, Falun, Sweden) in a transparent, 24.5 cm×24.5 cm×2 cm bio-assay polystyrene incubation dish (Nunc AS, Roskilde, Denmark). The dishes were kept under ambient light and temperature for 24 h to initiate germination and then at −20 °C for 24 h to kill the germ. Subsequently, the dishes were incubated at 20 °C under alternating 12 h of darkness and 12 h of a combination of cool white light and UVA light for 2 weeks. At the end of the incubation period, colonies from diseased kernels were examined and identified based on morphological features, and percentage of kernels with *Fusarium* infection was determined.

For DON analysis, 15 g of seed from the 2007–2009 experiments and 70 g from the 2010 experiment were sent to University of Minnesota, Department of Plant Pathology. DON level was determined from a 4 g flour subsample (ground for 2 min using a Stein Laboratories Mill, Model M-2, Stein Laboratories Inc., Atchison, Kansas) by Gas Chromatography and Mass Spectrometry (detection limit of 0.05 ppm) as described by Mirocha et al (1998).

Data analysis

Regression analyses and Pearson correlations between GC and DON level were conducted using Minitab 16 (Minitab Ltd., UK). Since each experiment evaluated different numbers of genotypes, we conducted a separate analysis for the 8–12 check genotypes to compare the experimental years. Two-way analysis of variance (ANOVA) for the dehulling/seed dressing experiment, and one way ANOVA on the coleoptile and radicle lengths for the controlled environment chamber experiment and the greenhouse time of infection experiment, were carried out using GenStat 14 (VSN International Ltd., UK).

Results

Field experiments

Mean, maximum, minimum and standard deviations for DON levels and GC for each field experiment are shown in Table 1. The highest mean DON level and

Table 1 Summary statistics and correlation coefficients for deoxynivalenol level (DON, ppm) and germination capacity (GC, %) of oat cultivars and breeding lines tested for Fusarium head blight resistance during 2007–2010 at the Vollebekk Research Farm, Ås, Norway

	2007 spawn		2008 spawn		2009 spawn		2009 spray		2010 spawn	
	DON	GC	DON	GC	DON	GC	DON	GC	DON	GC
# Genotypes	99	99	55	55	67	67	32	32	76	76
Mean	1.80	66.06	7.49	76.61	18.31	52.23	12.30	55.66	13.48	67.90
Maximum	3.27	79.33	19.60	88.25	29.80	74.00	25.70	77.00	20.20	84.33
Minimum	0.77	45.50	3.45	60.75	8.80	31.50	2.80	31.50	5.70	57.00
StDv[a]	0.57	5.76	2.95	5.65	4.54	9.03	5.91	12.59	3.42	5.74
Correlation	−0.498		−0.584		−0.412		−0.711		−0.414	
P	0.000		0.000		0.001		0.000		0.000	

[a] Standard deviation

lowest mean GC were recorded in the 2009 spawn inoculation experiment, while the lowest mean DON level and the highest mean GC were found in 2007 and 2008 experiments, respectively. In 2007, DON levels were exceptionally low, ranging from 0.77 ppm to 3.27 ppm. However, the mean GC in 2007 was not the highest among the experiments. In 2009, a comparable mean GC was recorded for both spawn- and spray-inoculated experiments, even though higher DON levels were recorded in the spawn-inoculated experiment (Table 1).

The relationship between DON level and GC for each experimental year is shown in Fig. 1. Negative and statistically significant correlations were found for all experiments. The strongest correlation was found for the spray-inoculated experiment in 2009 (−0.711, P=0.000), while the weakest occurred for the spawn-inoculated experiment of the same year (−0.412, P=0.000). Considering only the spawn-inoculated experiments, the strongest correlation was recorded in 2008 (−0.584, P=0.000) (Table 1 and Fig. 1).

DON level, GC, and correlation coefficients for the 8–12 check genotypes are shown in Table 2. The correlation between DON level and GC for the 2010 spawn-inoculated experiment was exceptionally weak with a P value of 0.9, possibly because of the fewer genotypes considered (n=8). Although, only the correlations for the 2008 spawn-inoculated and 2009 spray-inoculated experiments were statistically significant, the general trend of the relationship between DON level and GC was maintained in this small set of genotypes, except in 2010. The strongest and weakest correlation coefficients were recorded in the 2009 spray- and spawn-inoculated experiments (−0.826 and −0.368, respectively) and among the spawn inoculation experiments, that of 2008 had the strongest correlation coefficient of −0.645.

Flowering usually occurred from early- to mid-July. Environmental conditions in July and August 2007–2010 are shown in Table 3. While temperatures among years showed minimal variation, there was some variability in the levels and distribution of precipitation. 2007 was the driest among the experimental years both in terms of total precipitation and number of days with >2 mm of rain while 2009 was the wettest. Considering July precipitation only, 2008 was the driest in terms of number of days with >2 mm, while 2010 was the driest in terms of total precipitation (Hansen and Grimenes 2008, 2009, 2010, 2011). The effect on GC was most pronounced in the wet 2009 with mean GC of 52.2 % and 55.7 % for the spawn- and spray-inoculated experiments, respectively (Table 1).

Effect of time of inoculation

All measured parameters in this experiment were affected by date of inoculation (P=0.001, 0.039, and 0.025 for DON, GC, and SI, respectively). DON content was highest for inoculations done 5 days after flowering and decreased rapidly for later inoculations showing that a 1 week difference in infection time can significantly reduce the risk of DON contamination (Fig. 2). The corresponding increase in GC was not as rapid: and only the inoculation at yellow maturity gave a GC>70 %. Inoculations done 2 days before flowering resulted in a slightly lower DON and a higher GC than those done 5 days following flowering. SI was high for all inoculation dates (75–91 %), except at yellow maturity which was 61 %. The uninoculated control had 100 % GC, 0 % SI and a non-detectable DON level (Fig. 2).

Germination test on DON-amended water agar

The GC of the kernels tested on the control (0 ppm) was 100 %. Germination was also initiated in all kernels at the various DON concentrations, except for two kernels in the 15 ppm DON treatment group. However, seedling growth was retarded as displayed by the shorter coleoptile and radicle lengths in all seedlings exposed to DON (Fig. 3). Higher DON concentrations led to greater growth retardation. Most of the seedlings exposed to more than 2 ppm DON had abnormal morphology and would not be considered as ‘germinated’ by ISTA standards (Fig. 4).

Effects of dehulling and seed dressing

The GC of the untreated seed lots was usually lower than the percentage of viable seeds. The 2009 samples which were analyzed within 2 months after harvest had a mean GC of 54.5 %, and a statistically insignificant increase to 57.5 % and 60.3 % was achieved after dehulling or seed dressing. However, combining dehulling with seed dressing increased GC significantly (P <0.001) to the percentage of viable seeds (mean GC=74.5 % and seed viability=71.8 %). The stored

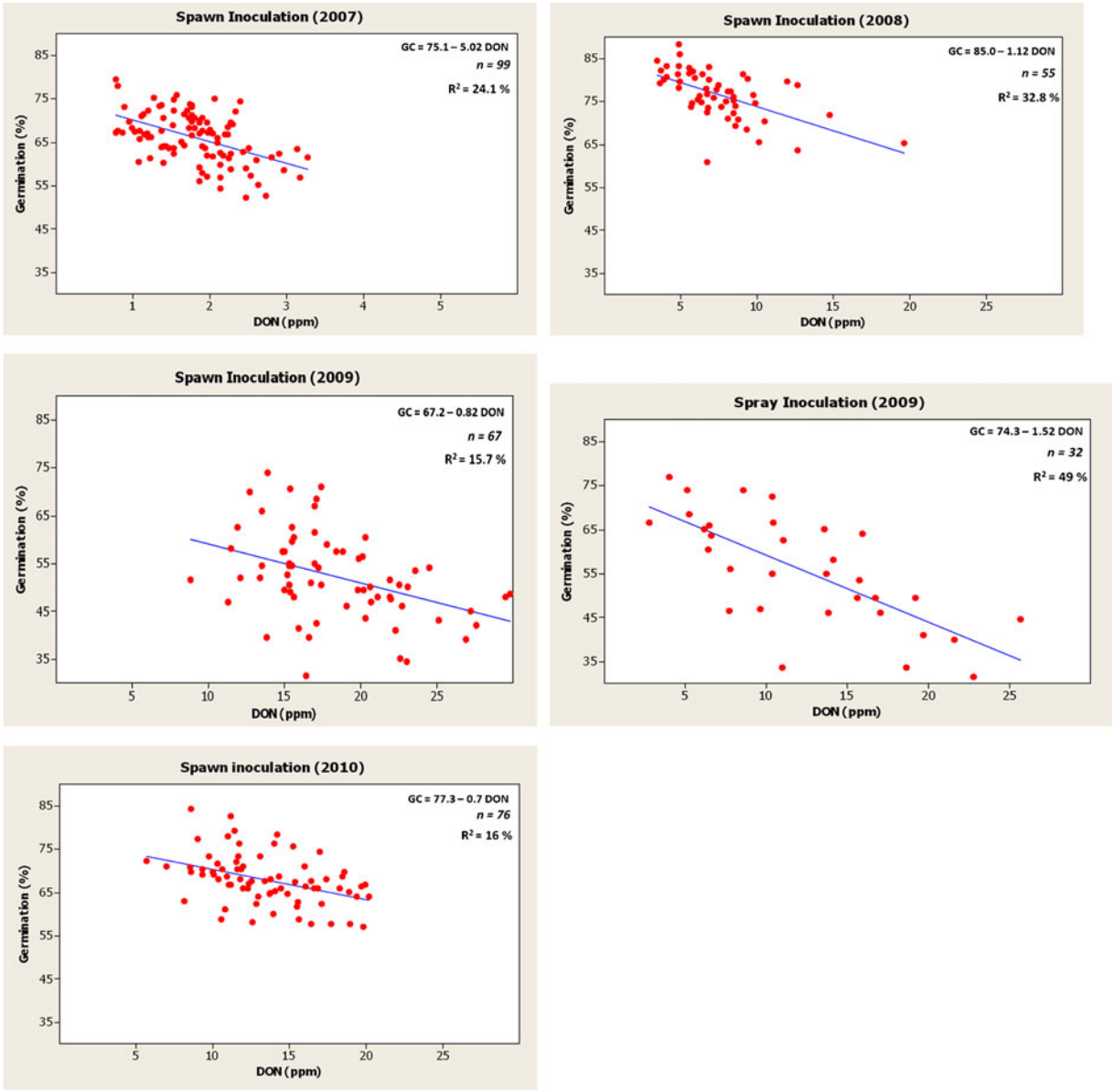

Fig. 1 Relationship between deoxynivalenol level (DON, ppm) and germination capacity (GC, %) in oat cultivars and breeding lines tested for Fusarium head blight resistance from 2007–2010 at the Vollebekk Research Farm, Ås, Norway. Note the different scale on the x-axis for the spawn-inoculated experiment of 2007

samples from 2009 germinated much better than the non-stored samples with a mean GC of 67.8 %. The results for treatments of the stored seed were not statistically different from each other (P=0.15) even though a slight increase in GC was observed following dehulling and/or seed dressing. In 2010 and 2011, the GC for dehulled or seed dressed lots was not statistically different from the untreated seed lots. However, dehulling and seed dressing combined, increased the GC significantly (P <0.001) in both years (Table 4).

A significant proportion of the germination problem in the infected seed lots was due to dead germ. However in wet years such as 2009, a considerable proportion could also be ascribed to seedling blight. Two years of storage reduced seedling blight from 17.3 % to 7.5 %. The reductions in GC following

Table 2 Deoxynivalenol levels (DON, ppm), germination capacities (GC, %) and correlation coefficients for check oat cultivars and breeding lines tested for Fusarium head blight resistance during 2007–2010 at the Vollebekk Research Farm, Ås, Norway

Genotype	2007 spawn		2008 spawn		2009 spawn		2009 spray		2010 spawn	
	DON	GC	DON	GC	DON	GC	DON	GC	DON	GC
Aveny	2.10	66.00	7.20	76.00	21.90	51.50	17.1	46.0	–	–
Belinda	1.70	71.00	9.10	81.00	19.40	57.50	10.5	66.5	14.14	74.50
Gere	1.90	58.00	9.80	77.00	24.50	54.00	13.6	65.0	12.27	66.00
GN04008	0.90	73.00	6.80	79.00	11.30	47.00	6.2	65.0	9.33	69.00
GN04070	1.20	67.00	5.00	80.00	15.30	55.00	5.3	68.5	–	–
GN04399	1.80	67.00	4.90	88.00	21.90	48.00	19.2	49.5	–	–
Hurdal	1.10	77.00	7.40	81.00	–	–	13.7	55.0	10.07	74.67
Nes	1.40	60.00	6.80	77.00	15.60	48.00	13.9	46.0	15.40	67.33
NK03112	1.10	68.00	5.80	81.00	17.20	54.00	16.7	49.5	–	–
Odal	1.10	67.00	3.50	84.50	12.70	70.00	6.5	66.0	11.87	70.33
Ringsaker	1.10	61.00	4.90	83.00	17.10	42.50	8.6	74.0	8.35	66.33
Steinar	2.00	62.00	8.60	69.00	27.60	42.00	15.8	53.5	13.73	64.67
Mean	1.45	66.42	6.65	79.71	18.59	51.77	12.23	58.71	11.90	69.10
Correlation	−0.43		−0.645		−0.368		−0.826		−0.053	
P	0.16		0.023		0.265		0.001		0.902	

dehulling or seed dressing in 2010 may be artifacts of sampling and physical damage during dehulling. The combined effect of dehulling and seed dressing was greatest in the non-stored samples of 2009 and was lowest in the stored samples of the same year. This effect seems to be closely related to the magnitude of seedling blight in the samples: the non-stored samples from 2009 had the highest level of seedling blight while the stored samples displayed the lowest (Table 4).

Discussion

This paper summarizes the results of field, greenhouse, and controlled environment chamber experiments conducted to study factors influencing the germination capacity of oats affected by FHB and evaluates measures to manage such germination problem in affected seed lots. Our hypothesis was that high moisture at and shortly after flowering facilitates early infection capable of killing the germ and significantly reducing the GC of the seed. Such infections can also result in high levels of DON and may reduce yield up to 30 % (Kiecana et al. 2002). Late infections facilitated by wet conditions later in the growing season can also contribute to low GC, most likely as a result of superficial infections that can lead to seedling blight during germination and emergence.

The greenhouse experiment demonstrated that infection can occur as late as yellow maturity. Significantly lower DON levels were recorded for late inoculations,

Table 3 Environmental data for July and August of 2007–2010 at Ås, Norway

	Mean Temperature (°C)			Total precipitation (mm)			# days >2 mm precipitation		
	July	August	Mean	July	August	Total	July	August	Total
2007	15.4	15.7	15.6	142.2	75.2	217.4	14	4	18
2008	17.2	14.5	15.8	118.7	184.6	303.3	7	14	21
2009	16.4	15.5	16	150.9	157.9	308.8	17	14	31
2010	16.9	15.3	16	100.7	149.5	250.2	11	14	25

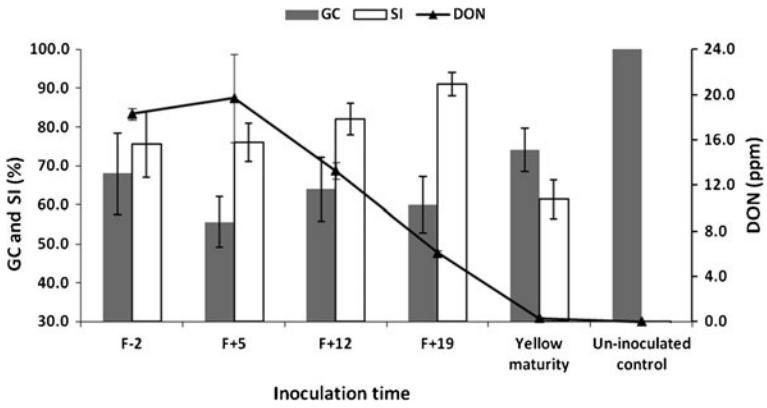

Fig. 2 Germination capacity (GC, %), seed infection (SI, %), and deoxynivalenol level (DON, ppm) in the oat cv. 'Hurdal' inoculated with *Fusarium graminearum* at different crop developmental stages (from two days before flowering until yellow maturity) in a greenhouse experiment conducted at the Norwegian University of Life Sciences. Error bars represent standard error of the mean of three replicates

but these were accompanied by higher levels of SI. With decreases in DON levels, we expected corresponding increases in GC. However, this relationship was not as evident as expected. Therefore, we propose that in addition to DON level, SI plays a role in the GC of *Fusarium* infected oat seed lots. In a previous study we investigated the infection process of *F. graminearum* in oats and found that GC was most affected when infection occurs at anthesis (Tekle et al. 2012). Germination capacity at 1 or 2 weeks after anthesis was not statistically different from the uninoculated control (GC>90 %). However, practical experience as well as regression of weather data (Elen et al. 2010) indicate that prolonged wet periods during the maritime Norwegian summer may affect DON level and GC of harvested seeds differently than under the drier continental conditions of a St. Paul, USA summer, where the above experiments were carried out.

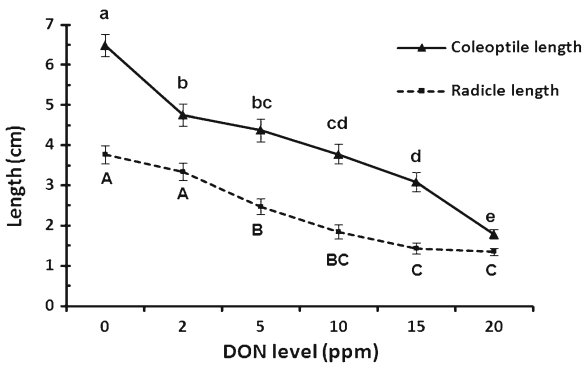

Fig. 3 Coleoptile and radicle lengths of 14 days-old seedlings of the oat cv. 'Hurdal' grown on water agar amended with different levels of deoxynivalenol. Error bars represent standard errors of the mean of measurements taken from 40 seedlings. Means followed by different letters are statistically different ($P<0.001$)

The importance of environmental factors such as temperature, precipitation, and relative humidity on *Fusarium* spore production and release, success of infection, and level of DON contamination has been pointed out in several previous studies (Francl et al. 1999; Hooker et al. 2002; Rossi et al. 2002; Tschanz et al. 1976; Turner and Jennings 1997). Perithecium production by *G. zeae* increased with increasing temperature between 15.3 °C and 28.5 °C (Tschanz et al. 1976). A sharp increase in the number of airborne macroconidia from wheat fields naturally affected by FHB was detected following rainfall episodes compared to none, or very few, in prior sampling (Rossi et al. 2002).

Spawn inoculation, unlike spray inoculation, can provide inoculum continuously if conditions are conducive for perithecium development and ascospore release. Prolonged wet and warm conditions later in the growing season in spawn-inoculated fields can, therefore, lead to late infections. In such cases, SI might be a better indicator of GC than the level of DON. The weak correlation between DON level and GC of the spawn-inoculated experiment of 2009 might be explained by this. In a spawn-inoculated experiment with wheat, Argyris et al. (2003) found a stronger correlation between SI and GC than between DON level and GC across developmental stages. By contrast, factors that reduce the possibility of late infection, such as spray inoculation, would lead to a stronger correlation between GC and DON level, as observed in our spray-inoculated experiment of 2009.

DON did not inhibit initiation of germination, but affected seedling growth in the controlled environment chamber trial. Inhibition of seedling growth, coleoptile, and root elongation due to DON toxicity has previously been reported in *Arabidopsis thaliana,* wheat, and maize

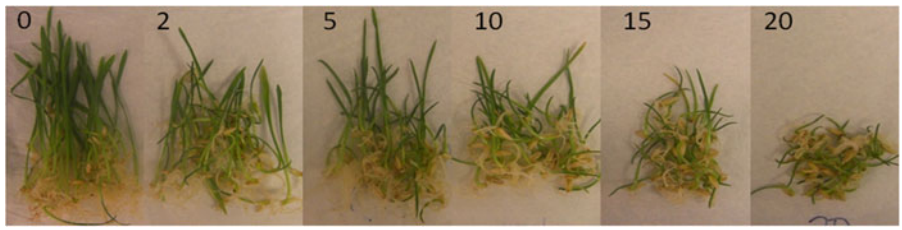

Fig. 4 Fourteen days-old seedlings of the oat cv. 'Hurdal' grown on water agar amended with different levels (shown above the seedlings) of deoxynivalenol

seedlings (Bruins et al. 1993; Masuda et al. 2007; McLean 1996). In our study, the seeds were imbibed overnight on wet filter paper before plating on DON-amended WA. The result might have been different if the seeds had been imbibed in water containing the toxin. As such, the DON levels in the WA may not correspond to the DON level accumulating in kernels affected by FHB. Additionally, kernels affected by FHB may be co-contaminated with toxins other than DON. Such toxin combinations could cause more harm to the developing caryopsis during early infection than what we observed in the mature kernels during this germination assay. Furthermore, FHB deteriorates different quality parameters of the affected kernels. We assume this deterioration may directly affect the GC as observed in the tetrazolium test. Despite any differences between the DON levels in *Fusarium*-damaged seeds and those in the modified WA, we were able to conclude that DON-contaminated kernels produce abnormal and less vigorous seedlings with shorter coleoptiles and roots, compared to healthy kernels.

Dehulling and pearling have been shown to decrease mycotoxin contamination in hulled and hulless barley and in oats (Clear et al. 1997; Trenholm et al. 1991; Yan et al. 2010). Several studies in barley have also shown that dehulling can decrease the number of viable *Fusarium* propagules (Clear et al. 1997; Schwarz et al. 2001). A high number of propagules have been detected in the husk of a hull-less barley, with the inoculum load decreasing after dehulling and pearling (Clear et al. 1997). Viable spores and mycelium of *F. graminearum* have been detected on the outer layer of the endosperm as well as under the husk in barley (Schwarz et al. 2001). In oats, dehulling can both decrease and expose *Fusarium* propagules, increasing the efficacy of seed dressing. In our study, dehulling or seed dressing alone did not increase the GC of the *Fusarium* infected seed lots significantly. Combining them, however, effectively eliminated seedling blight in all the samples tested. Therefore, it is likely that kernels having viable germ with superficial infections will have a better chance of germinating properly if dehulled and seed dressed.

The considerable difference between seed viability and actual GC of the non-stored 2009 samples confirms the afore-mentioned hypothesis that

Table 4 Mean seed viability (%), germination capacity (GC, %), and individual and combined effects of dehulling, seed dressing, and level of seedling blight of *Fusarium*-affected oat seed lots. The results presented are means of four oat genotypes which were tested in spawn-inoculated field experiments during 2009–2011at the Vollebekk Research Farm, ÅS, Norway

Samples	Seed viability	Mean GC				Effect of[a]			Seedling blight[b]
		Untreated	Seed dressed	Dehulled	Dehulled+ Seed dressed	Dehulling	Seed dressing	Dehulling+ Seed dressing	
2009	71.8	54.5	60.3	57.5	74.5	3.0	5.8	20.0	17.3
2009 stored	75.4	67.9	69.9	71.3	71.6	3.4	2.0	3.8	7.5
2010	83.6	73.5	70.4	73.3	83.0	−0.3	−3.1	9.5	10.1
2011	80.3	70.2	71.7	73.5	77.3	3.3	1.5	7.2	10.2

[a] Effect of:

Dehulling=(GC of dehulled-GC of untreated)

Seed dressing=(GC of seed dressed-GC of untreated)

Seed dressing and dehulling=(GC of dehulled and seed dressed-GC of untreated)

[b] Seedling Blight=(Seed viability-GC of untreated)

prolonged wet weather later in season may facilitate superficial infections which do not kill the germ but are capable of causing seedling blight during germination. The 2009 stored samples had minimal seedling blight and the effects of seed dressing and/or dehulling, therefore, were not significant. This can be attributed to reduction in viability of *F. graminearum* propagules during storage. An increase in GC and reduction in viability of *Fusarium* propagules following storage has previously been reported in wheat (Gilbert and Tekauz 1995; Gilbert et al. 1997; Homdork et al. 2000). Heat treatment has also been shown to reduce viability of *Fusarium* propagules and increase germination capacity of *Fusarium*-affected spring wheat (Gilbert et al. 2005). We also have observed an increase in GC and decrease in viability of *Fusarium* propagules following heat treatment in both *Fusarium*-affected oats and wheat (data not shown).

The gap observed between levels of seed viability and actual GC indicates there is a potential to increase the GC of *Fusarium*-infected oat seed lots. Increasing the GC of heavily infected seed from artificially inoculated experiments to a commercially acceptable level may not be achievable, but the results from our studies suggest that seedling blight arising from superficial infections during natural epidemics can successfully be managed by combining seed dressing with other treatments such as storage or heat treatment to lower the risk of seedling blight.

Acknowledgments The authors would like to acknowledge the financial support of the Norwegian Research Council and the Norwegian breeding company Graminor AS to the projects 'Safe Grains: Mycotoxin prevention through resistant wheat and oats (Project number 178273)' and 'Mycotoxin contamination in Norwegian food and feed: Modeling reductive approaches and risk assessment with regards to the whole food chain (Project number 19412)'. We also would like to thank our senior technician Yalew Tarkegne for his help during inoculum preparation and conducting the field experiments and Dr. Yanhong Dong (University of Minnesota) for toxin analyses. The comments and suggestions made by the anonymous reviewers are highly appreciated.

References

Argyris, J., Sanford, D. V., & TeKrony, D. (2003). *Fusarium graminearum* infection during wheat seed development and its effect on seed quality. *Crop Science, 43*, 1782–1788.

Bechtel, D. B., Kaleikau, L. A., Gaines, R. L., & Seitz, L. M. (1985). The effects of *Fusarium graminearum* infection on wheat kernels. *Cereal Chemistry, 62*, 191–197.

Bjørnstad, Å., & Skinnes, H. (2008). Resistance to *Fusarium* infection in oats (*Avena sativa* L.). *Cereal Research Communications, 36*, 57–62.

Brodal, G. (1991). Occurrence, pathogenicity and transmission of seed-borne fungi on grasses in Norway. Dissertation, Agricultural University of Norway.

Browne, R. A., & Cooke, B. M. (2005). Resistance of wheat to *Fusarium* spp. in an in vitro seed germination assay and preliminary investigations into the relationship with Fusarium head blight resistance. *Euphytica, 141*, 23–32.

Bruins, M. B. M., Karsai, I., Schepers, J., & Snijders, C. H. A. (1993). Phytotoxicity of deoxynivalenol to wheat tissue with regard to in vitro selection for Fusarium head blight resistance. *Plant Science, 94*, 195–206.

Clear, R. M., Patrick, S. K., Nowicki, T., Gaba, D., Edney, M., & Babb, J. C. (1997). The effect of hull removal and pearling on *Fusarium* species and trichothecenes in hulless barley. *Canadian Journal of Plant Science, 77*, 161–166.

Dickson, J. G., Eckerson, S. H., & Link, K. P. (1923). The nature of resistance to seedling blight of cereals. *Pathology, 9*, 434–439.

Elen, O., Hofgaard, I. S., Brodal, G., Aamot, H. U., & Klemsdal, S. S. (2010). Prediction models for deoxynivalenol content of Norwegian wheat and oats. In I. S. Hofgaard & E. Fløistad (Eds.), *Nordic Baltic Fusarium Seminar* (p. 22). Ski: Bioforsk.

Francl, L., Shaner, G., Bergstrom, G., Gilbert, J., Pedersen, W., Dill-Macky, R., Sweets, L., Corwin, B., Jin, Y., Gallenberg, D., & Wiersma, J. (1999). Daily inoculum levels of *Gibberella zeae* on wheat spikes. *Plant Disease, 83*, 662–666.

Gilbert, J., & Tekauz, A. (1995). Effects of Fusarium head blight and seed treatment on germination, emergence, and seedling vigour of spring wheat. *Canadian Journal of Plant Pathology, 17*, 252–259.

Gilbert, J., Tekauz, A., & Woods, S. M. (1997). Effect of storage on viability of Fusarium head blight-affected spring wheat seed. *Plant Disease, 81*, 159–162.

Gilbert, J., Woods, S. M., Turkington, T. K., & Tekauz, A. (2005). Effect of heat treatment to control *Fusarium graminearum* in wheat seed. *Canadian Journal of Plant Pathology, 27*, 448–452.

Hansen, V. T., & Grimenes, A. A. (2008). *Meterologiske data for Ås 2007*. Ås: Universitetet for miljø- og biovitenskap.

Hansen, V. T., & Grimenes, A. A. (2009). *Meterologiske data for Ås 2008*. Ås: Universitetet for miljø- og biovitenskap.

Hansen, V. T., & Grimenes, A. A. (2010). *Meterologiske data for Ås 2009*. Ås: Universitetet for Miljø- og Biovitenskap.

Hansen, V. T., & Grimenes, A. A. (2011). *Meterologiske data for Ås 2010*. Ås: Universitetet for Miljø- og Biovitenskap.

Hare, M. C., Parry, D. W., & Baker, M. D. (1999). The relationship between wheat seed weight, infection by *Fusarium culmorum* or *Microdochium nivale*, germination and seedling disease. *European Journal of Plant Pathology, 105*, 859–866.

Hestbjerg, H., Felding, G., & Elmholt, S. (2002). *Fusarium culmorum* infection of barley seedlings, correlation between aggressiveness and deoxynivalenol content. *Journal of Phytopathology, 150*, 308–312.

Hofgaard, I. S., Aamot, H. U., Klemsdal, S. S., Elen, O., Jestoy, M., & Brodal, G. (2010). Occurrence of *Fusarium* spp. and mycotoxins in Norwegian wheat and oats. In I. S. Hofgaard & E. Fløistad (Eds.), *Nordic Baltic Fusarium Seminar* (p. 37). Ski: Bioforsk.

Homdork, S., Fehrmann, H., & Beck, R. (2000). Influence of different storage conditions on the mycotoxin production and quality of *Fusarium*-infected wheat grain. *Journal of Phytopathology, 148*, 7–15.

Hooker, D. C., Schaafsma, A. W., & Tamburic-Ilincic, L. (2002). Using weather variables pre- and post-heading to predict deoxynivalenol content in winter wheat. *Plant Disease, 86*, 611–619.

Imathiu, S. M., Hare, M. C., Ray, R. V., Back, M., & Edwards, S. G. (2010). Evaluation of pathogenicity and aggressiveness of *F. langsethiae* on oat and wheat seedlings relative to known seedling blight pathogens. *European Journal of Plant Pathology, 126*, 203–216.

ISTA. (2006). *ISTA handbook on seedling evaluation* (3rd ed.). Bassersdorf: The International Seed Testing Association (ISTA).

Jones, R. K. (1999). Seedling blight development and control in spring wheat damaged by *Fusarium graminearum* group 2. *Plant Disease, 83*, 1013–1018.

Kiecana, I., Mielniczuk, E., Kaczmarek, Z., Kostecki, M., & Golinski, P. (2002). Scab response and moniliformin accumulation in kernels of oat genotypes inoculated with *Fusarium avenaceum* in Poland. *European Journal of Plant Pathology, 108*, 245–251.

Langseth, W., & Rundberget, T. (1999). The occurrence of HT-2 toxin and other trichothecenes in Norwegian cereals. *Mycopathologia, 147*, 157–165.

Lemmens, M., Reisinger, A., Burstmayr, H., & Ruckenbauer, P. (1994). Breeding for head blight (*Fusarium* spp.) resistance in wheat, development of a mycotoxin based selection method of seedlings. *Plant Breeding for Mankind, 355*, 223–232.

Limonard, T. (1966). A modified blotter test for seed health. *Netherlands Journal of Plant Pathology, 72*, 319–321.

Masuda, D., Ishida, M., Yamaguchi, K., Yamaguchi, I., Kimura, M., & Nishiuchi, T. (2007). Phytotoxic effects of trichothecenes on the growth and morphology of *Arabidopsis thaliana*. *Journal of Experimental Botany, 58*, 1617–1626.

McLean, M. (1996). The phytotoxicity of selected mycotoxins on mature, germinating *Zea mays* embryos. *Mycopathologia, 132*, 173–183.

McMullen, M., Jones, R., & Gallenberg, D. (1997). Scab of wheat and barley, A re-emerging disease of devastating impact. *Plant Disease, 81*, 1340–1348.

Mirocha, C. J., Kolaczkowski, E., Xie, W. P., Yu, H., & Jelen, H. (1998). Analysis of deoxynivalenol and its derivatives (batch and single kernel) using gas chromatography mass spectrometry. *Journal of Agricultural and Food Chemistry, 46*, 1414–1418.

Parry, D. W., Jenkinson, P., & McLeod, L. (1995). Fusarium ear blight (scab) in small-grain cereals—a review. *Plant Pathology, 44*, 207–238.

Placinta, C. M., D'Mello, J. P. F., & Macdonald, A. M. C. (1999). A review of worldwide contamination of cereal grains and animal feed with *Fusarium* mycotoxins. *Animal Feed Science and Technology, 78*, 21–37.

Rossi, V., Languasco, L., Pattori, E., & Giosue, S. (2002). Dynamics of airborne *Fusarium* macroconidia in wheat fields naturally affected by head blight. *Journal of Plant Pathology, 84*, 53–64.

Schwarz, P. B., Schwarz, J. G., Zhou, A., Prom, L. K., & Steffenson, B. J. (2001). Effect of *Fusarium graminearum* and *F. poae* infection on barley and malt quality. *Monatsschrift Fur Brauwissenschaft, 54*, 55–63.

Tekle, S., Dill-Macky, R., Skinnes, H., Tronsmo, A. M., & Bjørnstad, Å. (2012). Infection process of *Fusarium graminearum* in oats (*Avena sativa* L.). *European Journal of Plant Pathology, 132*, 431–442.

Trenholm, H. L., Charmley, L. L., Prelusky, D. B., & Warned, R. M. (1991). Two physical methods for the decontamination of four cereals contaminated with deoxynivalenol and zearalenone. *Journal of Agriculatural and Food Chemistry, 39*, 356–360.

Tschanz, A. T., Horst, R. K., & Nelson, P. E. (1976). Effect of environment on sexual reproduction of *Gibberella zeae*. *Mycologia, 68*, 327–340.

Turner, J. A., & Jennings, P. (1997). The effect of increasing humidity on Fusarium ear blight and grain quality. *Cereal Research Communications, 25*, 825–826.

Wang, H., Hwang, S. F., Eudes, F., Chang, K. F., Howard, R. J., & Turnbull, G. D. (2006). Trichothecenes and aggressiveness of *Fusarium graminearum* causing seedling blight and root rot in cereals. *Plant Pathology, 55*, 224–230.

Yan, W. K., Fregeau-Reid, J., Rioux, S., Pageau, D., Xue, A., Martin, R., Fedak, G., de Haan, B., Lajeunesse, J., & Savard, M. (2010). Response of oat genotypes to Fusarium head blight in Eastern Canada. *Crop Science, 50*, 134–142.

Zadoks, J. C., Chang, T. T., & Konzak, C. F. (1974). A decimal code for the growth stages of cereals. *Weed Research, 14*, 415–421.

Paper III

Selamawit Tekle, Åsmund Bjørnstad, Helge Skinnes, Yanhong Dong, Vegard H. Segtnan

Estimating Deoxynivalenol Content of Ground Oats Using VIS-NIR Spectroscopy

Selamawit Tekle,[1,2] Åsmund Bjørnstad,[1] Helge Skinnes,[1] Yanhong Dong,[3] and Vegard H. Segtnan[4]

Cereal Chem. 90(3):181–185

ABSTRACT

The potential of VIS-NIR spectroscopy as a rapid screening method for resistance of *Fusarium*-inoculated oats to replace the costly chemical measurements of deoxynivalenol (DON) was investigated. Partial least squares (PLS) regression was conducted on second-derivative spectra (400–2,350 nm) of 166 DON-contaminated samples (0.05–28.1 ppm, mean = 13.06 ppm) with separate calibration and test set samples. The calibration set had 111 samples, and the test set had 55 samples. The best model developed had three PLS components and a root mean square error of prediction (RMSEP) of 3.16 ppm. The residual predictive deviation (RPD) value of the prediction model was 2.63, an acceptable value for the purpose of rough screening. Visual inspection and the VIS spectra of the samples revealed that high-DON samples tended to be darker in color and coarser in texture compared with low-DON samples. The second-derivative spectra showed that low-DON samples tended to have more water and fat content than high-DON samples. With an RMSEP value of 3.16 and RPD of value of 2.63, it seems possible to use VIS-NIR spectroscopy to semiquantitatively estimate DON content of oats and discard the worst genotypes during the early stages of screening.

Fusarium head blight (FHB) is an important disease of small grain cereals such as wheat, barley, and oats. It is caused by several *Fusarium* species, but the most important and frequently isolated ones in northern and central Europe are *F. graminearum, F. culmorum,* and *F. avenaceum* (Parry et al 1995; Bottalico and Perrone 2002). The disease is favored by warm weather accompanied by prolonged moist conditions at and around flowering (Parry et al 1995; McMullen et al 1997).

FHB leads to floret sterility and lightweight scabby kernels, causing overall yield reduction (Parry et al 1995; Dexter et al 1996; Goswami and Kistler 2004). In addition to yield reduction, FHB is also associated with reductions in malting quality of barley (Schwarz et al 2001) and milling and baking quality of wheat (Dexter et al 1996; Wang et al 2005). *Fusarium*-infected kernels show weaker gluten strength, reduced loaf volume, and deterioration in pasta color (Dexter et al 1996, 1997). Increases in reducing sugars and nonstarch lipids and decreases in cellulose, hemicellulose, glutenin, and water-extractable protein were reported in *Fusarium*-damaged kernels (FDK) (Boyacioglu and Hettiarachchy 1995).

Mycotoxins produced by *Fusarium* spp. are of major concern because of the associated health risks to humans and animals (Ciegler 1978; Bergsjø et al 1993; Parry et al 1995). Symptoms can be manifested as severe vomiting, bloody diarrhea, extensive hemorrhaging, decreased weight gain, feed refusal, dermatitis, reproductive disorders, and death (Ciegler 1978; Bergsjø et al 1993; D'Mello et al 1999). Therefore, the European Commission (EC) has set maximum permissible limits for *Fusarium* mycotoxins in processed and unprocessed food and feed to ensure consumer safety (Scudamore et al 2007). The EC limit of deoxynivalenol (DON) in unprocessed wheat and oats is set at 1,750 ppb; in finished cereal-based food items it is 500 ppb (Scudamore et al 2007).

Spectroscopic methods have gained attention as rapid tools for semiquantification of DON contamination and detection of scab damage in wheat and barley (Dowell et al 1999; Ruan et al 2002; Delwiche 2003; Delwiche and Hareland 2004; Beyer et al 2010; Peiris et al 2010). Most of these studies focused on classification of kernels as scabby or sound with the aim of reducing DON contamination by removing the scab-damaged kernels. For example, single-kernel near-infrared spectroscopy (SKNIRS) successfully classified single wheat kernels as scabby or sound. More DON-contaminated kernels were identified by this method than by visual inspection of the samples (Dowell et al 1999). The SKNIRS method also semiquantitatively classified wheat kernels as low-DON (<60 ppm) or high-DON (>60 ppm) with 96% accuracy (Peiris et al 2010). Sorting *Fusarium*-infected wheat samples by a commercial high-speed bichromatic sorter using 675 and 1,480 nm reduced FDK level significantly (Delwiche et al 2005). The DON concentrations of the "accepts" and the "rejects" compared with that of the unsorted wheat were 51 and 650%, respectively. Successive passes through the sorter were successful at further reducing DON contamination (Delwiche et al 2005).

Overall shape of NIR spectra of sound and scab-damaged wheat kernels was found to be similar, but scab-damaged kernels had lower spectral absorption compared with sound kernels. This difference was suggested to be the result of the higher optical density and moisture content of the sound kernels (Delwiche 2003). Further investigation showed that the slope of the short wavelength side of a broad carbohydrate absorption band centered at 1,200 nm was effective in discriminating sound and scab-damaged kernels with test set accuracies of 95%. The accuracy was further improved by including kernel mass in the model (Delwiche and Hareland 2004), as scab-damaged kernels have lower kernel mass compared with sound ones.

The most economical and environmentally friendly option of managing FHB is the use of resistant cultivars. Identifying and selecting resistant cultivars involves testing and evaluating thousands of genotypes every year. This process is highly labor intensive and economically demanding (Mesterhazy 2003; Steffenson 2003). Therefore, rapid methods such as NIR spectroscopy that have previously been reported to successfully identify FDK and semiquantitatively determine DON contamination in wheat and barley could facilitate resistance breeding programs by reducing the cost of chemical analysis. Therefore, the objectives of this study were 1) to identify and characterize wavelength regions that are important in estimating DON content of *Fusarium*-infected oats and 2) to test the feasibility of NIR spectroscopy as a rapid method in quantifying DON contamination of oats originating from *Fusarium*-inoculated nurseries.

*The ***e*-Xtra** logo stands for "electronic extra" and indicates that Figure 4 appears in color online.

[1] Department of Plant and Environmental Sciences, Norwegian University of Life Sciences, Ås, Norway.
[2] Corresponding author. Phone: +47 45521244. Fax: +47 64965001. E-mail: selag@umb.no
[3] Department of Plant Pathology, University of Minnesota, Saint Paul, MN, U.S.A.
[4] Nofima AS, Osloveien 1, NO-1430 Ås, Norway.

http://dx.doi.org/10.1094/CCHEM-07-12-0084-R

MATERIALS AND METHODS

Samples

DON-contaminated oat samples (n = 166, minimum = 0.05 ppm, maximum = 28.1 ppm, mean = 13.06 ppm, and SD = 8.40 ppm) were assembled from a large sample collection to cover a range of DON contamination relevant for evaluating FHB resistance of oat genotypes. Most of the samples (n = 135) originated from FHB resistance trials conducted from 2007 to 2010 at the Vollebekk Research Farm, Norwegian University of Life Sciences. These samples consisted of more than 60 genotypes from Nordic breeding companies. The FHB nurseries were inoculated with *F. graminearum*-infected oat kernels (Skinnes et al 2010) at Zadoks 31/32 stage (Zadoks et al 1974). Experimental plots were 0.45 × 2.0 m spaced 0.3 m apart. Plants were mist irrigated every evening following inoculation until 10 days after the last flowering date to facilitate *Fusarium* infection. A few samples (n = 31) collected from farmers' fields were included to increase the frequency of low-DON samples. These samples were of the cultivar Belinda, which was grown in 2010. The DON distribution of the samples is shown in Figure 1.

Grinding, Scanning, and Mycotoxin Analyses

The samples from the FHB nurseries were ground for 2 min with a Stein Laboratories mill (model M-2, Stein Laboratories, Atchison, KS, U.S.A.), and the samples from farmers' fields were milled into 2 mm particle size by a Perten laboratory mill (model 3303, Perten Instruments AB, Segeltorp, Sweden). Although grinding is considered a labor- and time-consuming step, scanning whole kernels was avoided to minimize noise that may arise from nonuniformity in scab damage and DON contamination among the kernels. Kernels from *Fusarium*-affected fields are neither uniformly DON-contaminated nor infected but rather are mixtures of kernels with a spectrum of infection and DON levels (Liu et al 1997).

All samples were scanned with an XDS Rapid Content analyzer (FOSS Analytical, Hillerød, Denmark) measuring in the 400–2,500 nm wavelength region at 0.5 nm intervals. The sample (≈5 g) was placed in a sample holder (4 cm i.d.), covered with a disposable cup-back, and placed in the spectrophotometer. Spectra were recorded as log(1/R) with FOSS NIRSystems Vision software. Three parallels from each sample were scanned, and the spectra were averaged for each sample prior to analyses.

DON contents of the samples from the FHB nurseries were analyzed at the University of Minnesota with GC-MS (detection limit of 0.05 ppm) following the protocol described by Mirocha et al (1998) and Fuentes et al (2005), whereas the samples from the farmers' fields were analyzed with LC-MS/MS (detection limit of 0.04 ppm) at the Finnish Food Safety Authority, Evira following the protocol described by Kokkonen and Jestoi (2009).

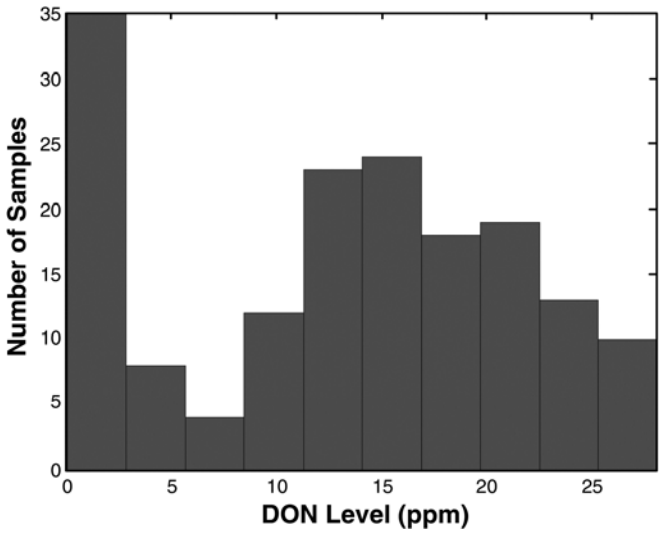

Fig. 1. Frequency plot for deoxynivalenol (DON) levels of the 166 samples used to develop and test the VIS-NIR prediction model.

Data Analysis

Prior to analysis, the samples were split into two classes; every third sample (according to DON level) was picked out to be in the test set. The splitting gave a calibration set of 111 samples and a test set of 55 samples. Data were analyzed with The Unscrambler X, version 10.1 (CAMO Software AS, Oslo, Norway). Spectra were pretreated with the second-derivative and second-polynomial order option of the Savitzky–Golay derivatives (Savitzky and Golay 1964) with 51 smoothing points. The smoothing was done in two separate windows (400–1,098 nm and 1,101–2,350 nm) because of the detector shift at 1,100 nm in the spectrophotometer. Partial least squares (PLS) regression (Martens and Næs 1989) was performed on the calibration set, with full cross-validation (Efron 1983), and the developed model was used to predict the test set samples.

RESULTS AND DISCUSSION

General Properties of the Spectra

The overall shape and general features of the spectra of the low-DON and high-DON samples were similar. However, differences in texture, density, and color in the samples influenced the light-scattering properties, and these differences were seen as varying apparent absorption levels in the spectra. Low-DON samples tended to have lower absorption at the VIS region and higher absorption at the NIR region than the high-DON samples (Fig. 2). Visual inspection of our samples showed that low-DON samples tended to be lighter in color and finer in texture, whereas high-DON samples tended to be darker in color and coarser in texture. Brownish discoloration of the hulls and the caryopses is a common symptom in *Fusarium*-infected oat kernels (Tekle et al 2012), and removal of such kernels has been shown to decrease the level of mycotoxin contamination (Scudamore et al 2007).

Calculating the second derivatives of the original spectra resolved the broad peaks in the original spectra and removed most of the light-scattering effects that seemed to be relevant in classifying the samples. However, the resolved peaks in the second-derivative spectra were able to segregate the samples into two-to-three classes (Fig. 3), revealing differences in chemical composition of the high- and low-DON samples. The peaks centered at ≈492 and ≈638 nm classified the samples into three classes, whereas the peaks centered at ≈1,210, ≈1,432, and ≈1,924 nm classified the samples into two classes (Fig. 3). The peaks at ≈1,432 and ≈1,924 nm were most likely water O-H bands (Segtnan et al 2001; Williams 2001; Segtnan and Isaksson 2004), indicating that low-DON samples tended to have more water than high-DON samples. The fat doublets at ≈1,701 and ≈1,725 nm also seemed to be important for calibration, with low-DON samples displaying more fat content than high-DON samples (Fig. 3).

Previous studies have shown that *Fusarium*-damaged and sound wheat kernels differ in their major food reserves and water contents (Boyacioglu and Hettiarachchy 1995; Delwiche 2003; Jackowiak et al 2005; Wang et al 2005). Therefore, spectral differences between sound and scabby kernels were attributed to differences in major seed constituents rather than DON content per se, due to the extremely low concentration of the toxin and because of overlap of bands in the NIR region from major seed constituents (Siuda et al 2008; Girolamo et al 2009; Liu et al 2009). Even though it was difficult to attribute specific spectral features to DON, the overall effects of *Fusarium* infection on the physical, chemical, and structural attributes

of kernels were correlated to DON contamination and were used to estimate DON level of samples (Siuda et al 2008; Girolamo et al 2009; Liu et al 2009).

Models

The models developed with the VIS, NIR, and whole wavelength regions are shown in Table I. In addition, the models for the 400–1,098 and 1,101–2,350 nm regions were also calculated by dividing the spectra at the detector shift. The best model was calculated by using the whole wavelength region. This model had only three PLS components, with root mean square error of cross-validation (RMSECV) and root mean square error of prediction (RMSEP) values of 4.06 and 3.16 ppm, respectively (Table I). The residual predictive deviation (RPD) value of 2.63 was considered poor but was acceptable for rough screening of resistance at the early stages of breeding programs (Williams 2001). A slight nonlinearity was observed in the measured versus predicted DON level plot. The error distribution was uniform along the different DON levels. The low-DON samples tended to be overestimated, whereas the high-DON samples tended to be underestimated (Fig. 4). The residual validation variance remained low after the recommended three PLS components, demonstrating the stability of the calibration model. The other calibration models that used only portions of the whole wavelength region were poorer than the

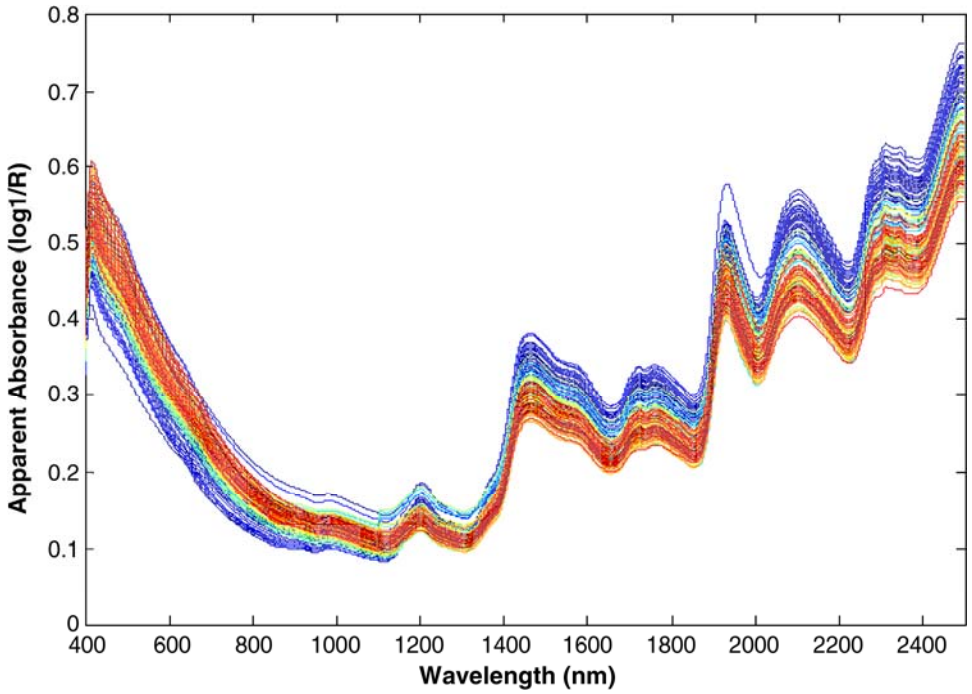

Fig. 2. Original spectra of ground oat samples (n = 166) contaminated with different levels of deoxynivalenol (DON). Spectra are colored according to DON levels (blue = low, green = medium, and red = high).

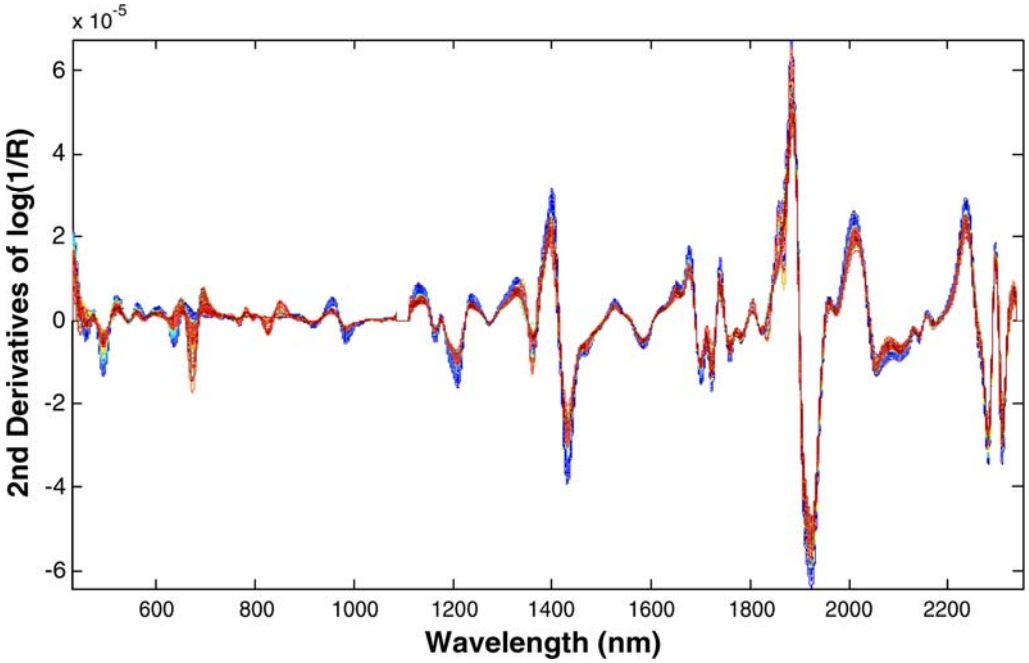

Fig. 3. Second-derivative spectra of ground oat samples (n = 166) contaminated with different levels of deoxynivalenol (DON). Spectra are colored according to DON levels (blue = low, green = medium, and red = high).

TABLE I
Prediction Performance Data for the Calibration Set and the Test Set[a]

Wavelength Regions	PLS-C	R^2_{xv}	R^2_{ts}	RMSECV	RMSEP	RPD_{xv}	RPD_{ts}
400–780	5	0.72	0.79	4.47	3.80	1.90	2.19
400–1,098	6	0.74	0.82	4.28	3.49	1.98	2.38
1,101–2,350	4	0.76	0.82	4.18	3.58	2.03	2.33
780.5–2,350	4	0.75	0.82	4.22	3.52	2.00	2.36
400–1,098 and 1,101–2,350	3	0.77	0.86	4.06	3.16	2.09	2.63

[a] Data for the calibration set (cross-validated results; R^2_{xv}, RMSECV, and RPD_{xv}) and the test set (R^2_{ts}, RMSEP, and RPD_{ts}). The calibration set consisted of 111 samples, and the test set consisted of 55 samples. PLS-C = the number of partial least squares components used in the different models; RMSECV = root mean square error of cross-validation; RMSEP = root mean square error of prediction; RPD_{xv} = ratio of standard error of calibration to standard deviation of measured values of the calibration set; and RPD_{ts} = ratio of standard error of prediction to standard deviation of measured values of the test set.

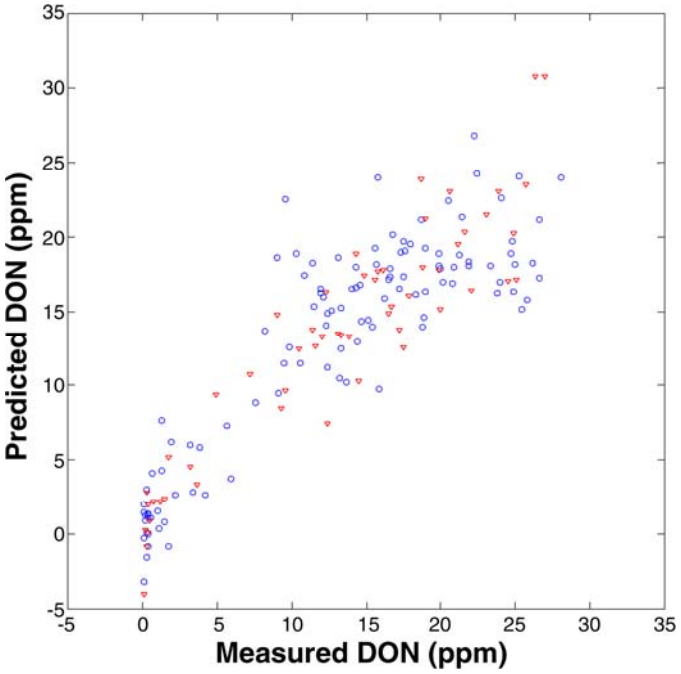

Fig. 4. Reference deoxynivalenol (DON) values plotted against the predicted values using a three-component PLS model based on the spectral region 400–2,350 nm. Blue circles are cross-validated results for the calibration set (111 samples). Red triangles are test set results (55 samples).

model developed using the whole wavelength region, as displayed by their higher RMSEP and lower RPD values (Table I).

The accuracy of spectroscopic methods in estimating DON contamination is highly dependent on the relationship between degree of scab damage and the actual DON level of the investigated samples (Siuda et al 2008). Apparently healthy-looking kernels can be contaminated with considerable levels of DON, and kernels with visible scab damage are not necessarily contaminated with corresponding high levels of DON (Dexter and Nowicki 2003). In addition, varietal differences and impact of growing season and location on the bulk chemistry of samples can weigh over the effect of scab damage. These factors can explain the relatively high RMSEP and poor RPD values of our models. Therefore, it is not possible to use our model in the milling industry, for which much lower DON levels than the RMSEP value are relevant and much higher RPD values than what we found are required.

CONCLUSIONS

The objective of this study was to test the feasibility of VIS-NIR spectroscopy in estimating DON contents of ground oat genotypes to evaluate their resistance to FHB. It was possible to develop stable calibration models by using the VIS, NIR, or whole wavelength regions, and the best model was developed by using the whole wavelength region (400–2,350 nm). The model had three PLS components and RMSECV and RMSEP values of 4.06 and 3.16 ppm, respectively. The RMSEP was not low enough to implement the model in the milling industry. However, the model was good enough for screening purposes, as the prediction error was low enough to discard the worst genotypes during successive selections, as high DON levels are common in artificially inoculated nurseries. It is important to update the calibration model with new samples from different growing seasons, locations, and genotypes to maintain its stability and be able to predict new samples with an acceptable level of prediction error.

ACKNOWLEDGMENTS

We acknowledge the financial support of the Norwegian Research Council and Graminor AS to the projects "Safe grains: Mycotoxin prevention through resistant wheat and oats" (Project number 178273) and "Mycotoxin contamination in Norwegian food and feed: Modelling reductive approaches and risk assessment with regards to the whole food chain" (Project number 19412). We thank Inger Skow Hofgaard (Bioforsk Planthelse) for providing the naturally contaminated samples and Yalew Tarekegn for inoculum preparation and for his help while conducting the field experiments.

LITERATURE CITED

Bergsjø, B., Langseth, W., Nafstad, I., Høgset Jansen, J., and Larsen, H. J. S. 1993. The effects of naturally deoxynivalenol-contaminated oats on the clinical condition, blood parameters, performance and carcass composition of growing pigs. Vet. Res. Commun. 17:283-294.

Beyer, M., Pogoda, F., Ronellenfitsch, F. K., Hoffmann, L., and Udelhoven, T. 2010. Estimating deoxynivalenol contents of wheat samples containing different levels of *Fusarium*-damaged kernels by diffuse reflectance spectrometry and partial least square regression. Int. J. Food Microbiol. 142:370-374.

Bottalico, A., and Perrone, G. 2002. Toxigenic *Fusarium* species and mycotoxins associated with head blight in small-grain cereals in Europe. Eur. J. Plant Pathol. 108:611-624.

Boyacioglu, D., and Hettiarachchy, N. S. 1995. Changes in some biochemical components of wheat grain that was infected with *Fusarium graminearum*. J. Cereal Sci. 21:57-62.

Ciegler, A. 1978. Trichothecenes: Occurence and toxicosis. J. Food Prot. 41:399-403.

Delwiche, S. R. 2003. Classification of scab- and other mold-damaged wheat kernels by near-infrared reflectance spectroscopy. Trans. ASAE 46:731-738.

Delwiche, S. R., and Hareland, G. A. 2004. Detection of scab-damaged hard red spring wheat kernels by near-infrared reflectance. Cereal Chem. 81:643-649.

Delwiche, S. R., Pearson, T. C., and Brabec, D. L. 2005. High-speed optical sorting of soft wheat for reduction of deoxynivalenol. Plant Dis. 89:1214-1219.

Dexter, J. E., and Nowicki, T. W. 2003. Safety assurance and quality assurance issues associated with Fusarium head blight in wheat. Pages 420-460 in: Fusarium Head Blight of Wheat and Barley. K. J. Leonard and W. R. Bushnell, eds. The American Phytopathological Society: Saint Paul, MN.

Dexter, J. E., Clear, R. M., and Preston, K. R. 1996. Fusarium head blight: Effect on the milling and baking of some Canadian wheats. Ce-

real Chem. 73:695-701.
Dexter, J. E., Marchylo, B. A., Clear, R. M., and Clarke, J. M. 1997. Effect of Fusarium head blight on semolina milling and pasta-making quality of durum wheat. Cereal Chem. 74:519-525.
D'Mello, J. P. F., Placinta, C. M., and Macdonald, A. M. C. 1999. *Fusarium* mycotoxins: A review of global implications for animal health, welfare and productivity. Anim. Feed Sci. Technol. 80:183-205.
Dowell, F. E., Ram, M. S., and Seitz, L. M. 1999. Predicting scab, vomitoxin, and ergosterol in single wheat kernels using near-infrared spectroscopy. Cereal Chem. 76:573-576.
Efron, B. 1983. Estimating the error rate of a prediction rule: Improvement on cross-validation. J. Am. Stat. Assoc. 78(382):316-331.
Fuentes, R. G, Mickelson, H. R., Busch, R. H., Dill-Macky, R., Evans, C. K., Thompson, W. G., Wiersma, J. V., Xie, W., Dong, Y., Anderson, J. A. 2005. Resource allocation and cultivar stability in breeding for Fusarium head blight resistance in spring wheat. Crop Sci. 45:1965-1972.
Girolamo, A. D., Lippolis, V., Nordkvist, E., and Visconti, A. 2009. Rapid and non-invasive analysis of deoxynivalenol in durum and common wheat by Fourier-transform near infrared (FT-NIR) spectroscopy. Food Addit. Contam. 26:907-917.
Goswami, R. S., and Kistler, H. C. 2004. Heading for disaster: *Fusarium graminearum* on cereal crops. Mol. Plant Pathol. 5:515-525.
Jackowiak, H., Packa, D., Wiwart, M., and Perkowski, J. 2005. Scanning electron microscopy of *Fusarium* damaged kernels of spring wheat. Int. J. Food Microbiol. 98:113-123.
Kokkonen, M. K., and Jestoi, M. N. 2009. A multi-compound LC-MS/MS method for the screening of mycotoxins in grains. Food Anal. Methods 2:128-140.
Liu, W., Langseth, W., Skinnes, H., Elen, O. N., and Sundheim, L. 1997. Comparison of visual head blight ratings, seed infection levels, and deoxynivalenol production for assessment of resistance in cereals inoculated with *Fusarium culmorum*. Eur. J. Plant Pathol. 103:589-595.
Liu, Y., Delwiche, S. R., and Dong, Y. 2009. Feasibility of FT–Raman spectroscopy for rapid screening for DON toxin in ground wheat and barley. Food Addit. Contam. 26:1396-1401.
Martens, H., and Næs, T. 1989. Multivariate Calibration. Wiley: Chichester, U.K.
McMullen, M., Jones, R., and Gallenberg, D. 1997. Scab of wheat and barley: A re-emerging disease of devastating impact. Plant Dis. 81: 1340-1348.
Mesterhazy, A. 2003. Breeding wheat for Fusarium head blight resistance in Europe. Pages 211-240 in: Fusarium Head Blight of Wheat and Barley. K. J. B. Leonard and W. R. Bushnell, ed. The American Phytopathological Society: Saint Paul, MN.
Mirocha, C. J., Kolaczkowski, E., Xie, W. P., Yu, H., and Jelen, H. 1998. Analysis of deoxynivalenol and its derivatives (batch and single kernel) using gas chromatography mass spectrometry. J. Agric. Food Chem. 46:1414-1418.
Parry, D. W., Jenkinson, P., and McLeod, L. 1995. Fusarium ear blight (scab) in small grain cereals—A review. Plant Pathol. 44:207-238.
Peiris, K. H. S., Pumphrey, M. O., Dong, Y., Maghirang, E. B., Berzonsky, W., and Dowell, F. E. 2010. Near-infrared spectroscopic method for identification of Fusarium head blight damage and prediction of deoxynivalenol in single wheat kernels. Cereal Chem. 87:511-517.
Ruan, R., Li, Y., Lin, X., and Chen, P. 2002. Non-destructive determination of deoxynivalenol levels in barley using near-infrared spectroscopy. Appl. Eng. Agric. 18:549-553.
Savitzky, A., and Golay, M. 1964. Smoothing and differentiation of data by simplified least squares procedures. Anal. Chem. 36:1627-1639.
Schwarz, P. B., Schwarz, J. G., Zhou, A., Prom, L. K., and Steffenson, B. J. 2001. Effect of *Fusarium graminearum* and *F. poae* infection on barley and malt quality. Monatsschr. Brauwiss. 54:55-63.
Scudamore, K. A., Baillie, H., Patel, S., and Edwards, S. G. 2007. Occurrence and fate of *Fusarium* mycotoxins during commercial processing of oats in the UK. Food Addit. Contam. 24:1374-1385.
Segtnan, V. H., and Isaksson, T. 2004. Temperature, sample and time dependent structural characteristics of gelatine gels studied by near infrared spectroscopy. Food Hydrocolloids 18:1-11.
Segtnan, V. H., Sasik, S., Isaksson, T., and Ozaki, Y. 2001. Studies on the structure of water using two-dimensional near-infrared correlation spectroscopy and principal component analysis. Anal. Chem. 73:3153-3161.
Siuda, R., Balcerowska, G., Kupcewicz, B., and Lenc, L. 2008. A modified approach to evaluation of DON content in scab-damaged ground wheat by use of diffuse reflectance spectroscopy. Food Anal. Methods 1:283-292.
Skinnes, H., Semagn, K., Tarkegne, Y., Marøy, A. G., and Bjørnstad, Å. 2010. The inheritance of anther extrusion in hexaploid wheat and its relationship to Fusarium head blight resistance and deoxynivalenol content. Plant Breed. 129:149-155.
Steffenson, B. J. 2003. Fusarium head blight of barley: Impact, epidemics, management, and strategies for identifying and utilizing genetic resistance. Pages 241-295 in: Fusarium Head Blight of Wheat and Barley. K. J. Leonard and W. R. Bushnell, eds. The American Phytopathological Society: Saint Paul, MN.
Tekle, S., Dill-Macky, R., Skinnes, H., Tronsmo, A. M., and Bjørnstad, Å. 2012. Infection process of *Fusarium graminearum* in oats (*Avena sativa* L.). Eur. J. Plant Pathol. 132:431-442.
Wang, J., Pawelzik, E., Weinert, J., and Wolf, G. A. 2005. Impact of *Fusarium culmorum* on the polysaccharides of wheat flour. J. Agric. Food Chem. 53:5818-5823.
Williams P. C. 2001. Implementation of near-infrared technology. Pages 145-169 in: Near-Infrared Technology in the Agricultural and Food Industries, 2nd Ed. P. Williams and K. Norris, eds. American Association of Cereal Chemists: Saint Paul, MN.
Zadoks, J. C., Chang, T. T., and Konzak, C. F. 1974. A decimal code for the growth stages of cereals. Weed Res. 14:415-421.

[Received July 16, 2012. Accepted February 8, 2013.]

Paper IV

Selamawit Tekle, Ingrid Måge, Vegard H. Segtnan, Åsmund Bjørnstad

Near Infrared Hyperspectral Imaging of *Fusarium*- Damaged Oats (*Avena sativa* L.)

Selamawit Tekle[1,2], Ingrid Måge[3], Vegard H. Segtnan[3], Åsmund Bjørnstad[1]

ABSTRACT

The feasibility of hyperspectral imaging (HSI) to detect deoxynivalenol (DON) content and *Fusarium* damage in single oat kernels was investigated. Hyperspectral images of oat kernels from a *Fusarium*-inoculated nursery were used after visual classification as asymptomatic, mildly damaged, and severely damaged. Uninoculated kernels were included as controls. The average spectrum from each kernel was paired with the reference DON value for the same kernel and a calibration model was fitted by partial least squares regression (PLSR). To correct for the skewed distribution of DON values and avoid nonlinearities in the model, the DON values were transformed as DON*= [log(DON)]^3. The model was optimized by cross-validation, and its prediction performance was validated by predicting DON* values for a separate set of validation kernels. The PLSR model and linear discriminant analysis (LDA) classification were further used on single-pixel spectra to investigate the spatial distribution of infection in the kernels. There were clear differences between the kernel classes. The first component separated the uninoculated/asymptomatic from the severely damaged kernels. Infected kernels showed higher intensities at 1920, 2070 and 2140 nm, while non-infected kernels were dominated by signals at 1420, 1620 and 1850 nm. The DON* value of the validation kernels were estimated using their average spectrum, and the correlation (R) between predicted and measured DON* was 0.8. Our

[1] Department of Plant Sciences, Norwegian University of Life Sciences, P. O. Box 5003, 1432 Ås, Norway
[2] Corresponding email: selag@nmbu.no
[3] Nofima AS, Osloveien 1, NO-1430 Ås, Norway

results show that HSI has great potential in detecting *Fusarium* damage and predicting DON in oats but it needs more work to develop a model for routine application.

Abbreviations

DON: Deoxynivalenol, FHB: Fusarium Head Blight, HSI: Hyperspectral Imaging, LDA: Linear Discriminant Analysis, NIR: Near Infrared, PCA: Principal Component Analysis, PLSR: Partial Least Squares Regression, VIS: Visible.

INTRODUCTION

Fusarium head blight (FHB) is one of the important diseases of cereals worldwide. The disease causes substantial yield and quality losses every year (Parry et al., 1995, McMullen et al., 1997). It results in light-weighted shriveled kernels with pink to brownish discoloration (McMullen et al., 1997). *Fusarium* spp. produce a wide array of toxins (Bottalico & Perrone, 2002) which are involved in isolate aggressiveness and species pathogenicity (Langevin et al., 2004). These toxins raise food and feed safety issues and impair animal production as they cause feed refusal, vomiting, and reduced weight gain in farm animals. They are also associated with various acute and chronic ailments in animals and humans (Bergsjø et al., 1993, D'Mello et al., 1999). Deoxynivalenol (DON) and its derivatives, mainly produced by *F. graminearum* and *F. culmorum,* are the most commonly encountered *Fusarium*-toxins in Europe (Bottalico & Perrone, 2002) and in Norwegian small grain cereals (Bernhoft et al., 2013). Among the small grain cereals produced in Norway, oats (*Avena sativa* L.) are the most frequently and highly DON-contaminated cereal species (Bernhoft et al., 2013).

Fusarium infection has a significant impact on grain quality. *Fusarium graminearum* infection in barley (*Hordeum vulgare* L.) results in significant reduction in germination and kernel plumpness (Schwarz et al., 2001). In wheat (*Triticum aestivum* L.), infection results in poor baking performance and flour color, reduced loaf volume, and weak dough properties (Dexter et al., 1996, Nightingale et al., 1999, Wang et al., 2005). Infection destroys starch granules, storage proteins, and cell walls (Bechtel et al., 1985, Wang et al., 2005). Wheat kernels infected with *F. culmorum* display damaged starch granules, complete or partial lack of the protein matrix and complete disappearance of the starchy endosperm under severe infection (Jackowiak et al., 2005). Significant degradation of the endosperm protein and lower content of

storage proteins in *F. avenaceum* and *F. graminearum*- infected wheat are also reported (Nightingale et al., 1999).

The level of fungal secondary metabolites in grains (such as DON) is very low compared to the major seed constituents. Conventional NIR spectroscopy is not very sensitive to such minor constituents (Gowen et al., 2007). Therefore, efforts to calibrate DON contamination in bulk samples using NIR spectroscopy must rely on major effects of the disease on grain constituents that are correlated with DON (Siuda et al., 2008, Tekle et al., 2013). Hyperspectral imaging (HSI) is a powerful non-destructive tool to detect contaminants in food and feed(Gowen et al., 2007, Feng & Sun, 2012). It has higher sensitivity to minor seed constituents than conventional NIR spectroscopy (Gowen et al., 2007) due to the local enhancement of constituent signals. It combines conventional imaging and spectroscopy to provide a three-way data matrix known as a hypercube made of two spatial (x, y) and one wavelength (z) dimensions. It is made of hundreds of single channel, grayscale images, each representing a single band of spectral wavelength (Gowen et al., 2007). This combination of spatial and spectral information enables building 'chemical maps' that show distribution of grain components in individual kernels (Feng & Sun, 2012, Williams et al., 2010). Powerful and efficient data processing methods, however, are required to extract useful information from such hyperspectral data (Feng & Sun, 2012).

Hyperspectral imaging has previously been used to classify kernels and kernel regions based on fungal damage and/ or DON contamination (Gowen et al., 2007, Polder et al., 2005, Williams et al., 2010). The technique has been adapted for detection of maize kernels and regions within each kernel that were infected by *F. verticillioides* (Williams et al., 2010). Others have used HSI to detect *Fusarium* damage in wheat (Delwiche et al., 2011, Shahin & Symons, 2011, Shahin & Symons, 2012). Visible-NIR HSI classified wheat kernels into sound and

Fusarium-damaged with an accuracy of 92% (Shahin & Symons, 2011). It was possible to further classify the *Fusarium*-damaged kernels as severely and mildly damaged with an accuracy of 86 %. Similar levels of accuracies were achieved by using only six selected wavelengths (484 nm, 567 nm, 684 nm, 817 nm, and 900 nm), (Shahin & Symons, 2011). An extended VIS-NIR (400-1000 /1000-1700) HSI was shown to discriminate between *Fusarium*-damaged and sound wheat kernels with an average accuracy of 95%. The spectral absorption near 1200 nm, which was tentatively attributed to ergosterol was found to be useful for classification (Delwiche et al., 2011).

The level of *Fusarium* damage and DON contamination varies widely within and among kernels in a given *Fusarium*-affected seed lot (Liu et al., 1997). We hypothesized that hyperspectral imaging could utilize this variation to develop a robust NIR calibration model and map the variation in individual kernels. The objectives of this experiment were i) to test the feasibility of hyperspectral imaging in classifying oat kernels based on *Fusarium* damage and DON level ii) to map DON contamination in single oat kernels, and iii) to develop a calibration model that integrates both *Fusarium* damage and DON contamination.

MATERIALS AND METHODS

Samples

A half kilogram sample of the oat cultivar 'Bessin' was obtained from a *Fusarium* inoculation trial conducted in 2012 at the Vollebekk Research Farm of the Norwegian University of Life Sciences. The bulk sample had a DON value of 6.8 ppm. Kernels were visually categorized as severely damaged (highly shriveled, light weighted kernels with brownish discoloration and pinkish-white mycelium on most of the kernel surface), mildly damaged

(kernels with modest kernel fill and localized brownish discoloration and pinkish-white mycelium), and asymptomatic (well filled kernels with no visible discoloration or mycelium). Clean seeds of the same cultivar from an uninoculated nursery were used as control. The kernels were assigned randomly to the calibration set (*n*= 4 categories x 31 kernels) or the validation set (*n*= 4 categories x 14 kernels) and for scanning microscopy (*n*= 4 categories x 10 kernels).

Hyperspectral imaging

Hyperspectral images were acquired using SWIR hyperspectral camera (Specim, Spectral Imaging Inc, Oulu, Finland) with a Mercury Cadmium Telluride (HgCdTe) detector. SpectralDAQ (Specim, Spectral Imaging Inc, Oulu, Finland) was used for image acquisition software. The images were obtained in the 1000-2500 nm wavelength range distributed in 256 channels. The images had a spatial resolution of 200µm. Image acquisition was set at 5 mm/s scanning speed, 5ms exposure time and a frame rate of 25HZ. The ventral and dorsal surfaces of 31 kernels representing the calibration set of each kernel category were scanned following the sample presentation shown in Figure 1A. The same was done on 14 kernels from each kernel category representing the validation set following the sample presentation shown in Figure 1B. Hyperspectral images of kernels comprising seven uninoculated, seven asymptomatic, seven mildly damaged and ten severely damaged kernels were taken following the sample presentation shown in Figure 5A. Kernels were directly placed on the black sample holder and a 99% reflecting white reference bar was included in each image.

Figure 1 comes here.

Analysis of hyperspectral images

All data analysis was done in MATLAB (Release 2013b, The MathWorks, Inc., Natick, Massachusetts), using the Image Processing Toolbox, Statistics toolbox and in-house routines for Principal Component Analysis (PCA) and Partial Least Squares Regression (PLSR). The analysis of the images followed these steps:

1. Transformation of raw signal into percent reflectance

Every image contains a white and black reference, as shown in Figure 1. The reflectance spectrum R_{rc} in row r and column c was calculated as

$$R_{rc} = \frac{I_{raw,rc} - I_{black,c}}{I_{white,c} - I_{black,c}},$$

where $I_{raw,rc}$ is the raw signal of row r and column c, and $I_{black,c}$ and $I_{white,c}$ were the average black and white references of column c. By doing the calculations column wise, variations due to line scanning were accounted for.

2. Remove background

In order to separate kernels from background, a threshold rule based on differences in reflectance spectra was used. The threshold was set by visual inspection of the spectra.

3. Preprocess spectra

Reflectance spectra were transformed to absorbance, and normalized by standard normal variate (SNV) to remove scattering effects.

4. Multivariate data analysis based on average spectra for each kernel

The average spectrum from each kernel was paired with the reference DON value, and a calibration model based on 248 images ((4 ventral + 4 dorsal images) x 31 kernels representing each kernel category) was fitted by PLS regression. The DON values were transformed as DON*= [log(DON)]^3 prior to analysis in order to obtain a more even distribution and avoid curvature in the prediction model. The model was optimized by full cross-validation, and the prediction performance was validated by predicting DON* values of 112 separate validation kernels ((4 ventral + 4 dorsal images) x 14 kernels representing each kernel category).

A linear discriminant analysis (LDA) classification model was built using the latent variables from the PLS model. Only uninoculated and severely damaged kernels were used to define the classification rule, in order to get a clear separation between infected and non-infected samples.

5. Application of pixel-level multivariate models

The PLSR model and LDA classification were used on single-pixel spectra to investigate the spatial distribution of *Fusarium* infection within the kernels.

Microscopy and DON analysis

Cross-sections and surfaces of hulled and dehulled kernels representing each kernel category were further studied under the scanning electron microscope, SEM (ZEISS EVO 50-EP Environmental Scanning Electron Microscope, Carl Zeiss AG, Germany) at the Imaging Centre of the Norwegian University of Life Sciences. Ten kernels representing each kernel category were used. Samples were dissected in the middle and near the embryo to study the effect of infection on the grain ultra structure. The samples were mounted on aluminum stubs with conductive carbon adhesive tabs and double coated with gold-palladium (SC7640 Auto/ manual

high resolution sputter coater) before examination under the SEM operating at an accelerating voltage of 25 kV.

Kernels used in the hyperspectral imaging were sent to the University of Minnesota, Department of Plant Pathology for single-kernel DON analyses. Deoxynivalenol content was determined by gas chromatography coupled with mass spectrometry following the protocol described in Jiang et al. (2006). The weight of each kernel was documented prior to grinding and DON analysis.

RESULTS AND DISCUSSIONS

Microscopy, DON content and kernel weight

Fusarium infection results in shriveled and light weighted kernels contaminated with DON (Snijders & Perkowski, 1990, Parry et al., 1995). Visual symptoms generally correlate with the level of DON contamination, but asymptomatic kernels can also be contaminated with significant levels of toxins. Therefore, accuracy of visual assessment of *Fusarium* damage is limited, and integrating DON analysis with visual assessment is a more robust way of evaluating the disease. Our results show that deoxynivalenol content and kernel weight of the visually categorized kernels followed the expected general trend. The asymptomatic kernels had the highest mean kernel weight and the lowest mean DON content while the severely damaged kernels had the lowest mean kernel weight and the highest DON content. The mildly damaged kernels had DON content and kernel weight values between the asymptomatic and the severely damaged ones (Table 1). However, there were a few exceptions to this general trend. There were kernels with very low DON (0.48 ppm, for example) in the severely damaged kernels category while there were kernels in the asymptomatic kernels category with substantial DON (21.91

ppm, for example). These kernels were detected with a better accuracy using HSI than our visual inspection.

Table 1 comes here

The microscopic study showed that the uninoculated and the asymptomatic kernels to be plump and free of any fungal mycelia. The severely damaged kernels were shriveled and heavily colonized with *F. graminearum*. Dense mycelial growth on the hulls and on the caryopsis of the severely damaged kernels was frequently observed. Denser mycelia were observed near the crease of the severely damaged kernels (Figures. 2 and 3). The cross-sections of the uninoculated kernels revealed a well-formed aleurone layer and intact endosperm, while the severely damaged kernels had collapsed and highly colonized aleurone layer with partially digested endosperm structure (Figures 3 and 4). Damage to the seed coat and the aleurone layers were also observed in the mildly damaged kernels, but the inner endosperm structure was intact. Similar effects of infection were observed in wheat (Bechtel et al., 1985, Jackowiak et al., 2005). Hyphae of *F. culmorum* were most prevalent in the layers of the seed coat tissues but were much less prevalent in the endosperm tissues of damaged wheat kernels (Jackowiak et al., 2005). Another study reported the pericarp and the aleurone layer to be the most affected tissues in *F. graminearum* infected wheat (Bechtel et al., 1985).

Figure 2, 3 and 4 come here

Hyperspectral image analysis

The level and the range of DON contamination in ground bulk samples do not correspond to that of individual kernels. In this study, the bulk DON content of the sample used was 6.8 ppm while the DON level of the individual kernels ranged from non-detectable levels to 386.5 ppm

(Table 1). In a previous study, we investigated the potential of conventional VIS-NIR spectroscopy to estimate DON content of *Fusarium*-inoculated oat genotypes. Spectra were taken and DON level was analyzed from bulk ground samples. One hundred sixty six samples with DON value ranging from 0.05 ppm to 28.1 ppm were used. It was possible to develop a calibration model which can be used for rough screening of the genotypes (Tekle et al., 2013). However, we hypothesized that a better calibration model for DON and *Fusarium* damage could be developed if the wider variation in DON among individual kernels and the higher sensitivity of HSI were utilized.

The average kernel size across all images was 554 pixels, ranging from 345 to 567 pixels. The correlation between the number of pixels and the measured kernel weight was 0.72, showing that the pixel size is fairly representative for the actual size of the kernels. The PLSR model, using the average spectra and the DON* values as x and y variables, respectively, was optimized by full cross-validation, and a 5-component model was selected. The model had a R^2 of 0.75 and 0.71 for calibration and cross-validation, respectively. The model was able to describe the majority of the DON* variation, although the prediction was not very good. The first PLS component was the most dominant, describing 32.9% of the DON* variation and 70.5% of the spectral variation. The second PLS component described additional 8.2% of the DON* variation and 14.2% of the spectral variation. The PLS score plot of component 1 versus component 2 in Figure 5A shows that there is a systematic pattern due to kernel category. These first two components separate uninoculated and asymptomatic kernels from severely damaged kernels. The mildly damaged kernels are overlapping with the severely damaged and the asymptomatic kernels. This can be explained by the large variation in DON value of the mildly damaged kernels (Table 1).

The line in Figure 5A is the LDA discrimination line that separates uninoculated kernels from severely damaged kernels. This line is used to discriminate between non-infected and infected pixels in the validation images. The loadings for the first component are shown in Figure 5B. The main peaks representing positive changes associated with increased infection are seen at 1925 nm, 2070 nm and 2140 nm, while negative changes at 1400 nm, 1626 nm and 1850 nm corresponded to non-infection. In a previous study, peaks centered at 1432 and 1924 nm classified DON-contaminated samples into high-DON and low-DON classes. These peaks were attributed to O-H bands of water (Tekle et al., 2013). In comparison, absorbance peaks for *F. verticillioides*-infected maize kernels were observed at 1960 nm and 2100 nm and at 1450 nm 2300 nm and 2350 nm for non-infected kernels (Williams et al., 2010).

Figure 5 comes here

Figure 6 shows the image analysis performed on the mixed calibration set kernels. The mixed calibration set kernels were comprised of seven uninoculated, seven asymptomatic, seven mildly damaged and ten severely damaged kernels arranged randomly as shown in Figure 6A. The reflectance image of a selected channel of these kernels is shown in Figure 6B. The background noise was removed by using the mask shown in Figure 6C. *Fusarium*-damaged/ DON contaminated regions (depicted by red pixels) and healthy/ DON free regions (depicted by green pixels) of each kernel were predicted using PLSR and LDA (Figure 6D). The severely damaged kernels were dominated by red pixels while the uninoculated and asymptomatic kernels were dominated by green pixels showing that HSI can successfully detect level of *Fusarium*-damage. This observation is clearly shown by the differences in the mean percentage of damaged pixels in the calibration images of each kernel category (Table 2).

Figure 6 comes here.

Figure 7 shows the PLS-LDA classification model used for classification of individual pixels in the eight validation images. There was a clear difference between classes, as indicated by the extent of red and green pixels and by the differences among the mean percentage of damaged pixels in the validation images of each kernel category. (Figure 7 and Table 2). Hyperspectral imaging detected *Fusarium* damage and DON level more precisely than visual examination. Kernels with very high DON but categorized as mildly damaged were dominated by infected regions. On the other hand, kernels with very low DON but categorized as severely damaged were dominated by healthy regions after image analysis (Figure 7).

Figure 7 comes here.

Table 2 comes here.

The DON* value for the 112 validation set kernels ((4 dorsal + 4 ventral images) x 14 kernels representing each kernel category) were predicted in two alternative ways: 1) using the average spectrum of the kernels as x-variables and the PLSR model, and 2) classifying every pixel using the PLS-LDA model, and calculating the ratio of damaged pixels in each grain. . The correlation (R) between predicted and measured DON* values were 0.81 and 0.79 respectively (Figure 8). The difference between the two prediction methods is not statistically significant, showing that they are equivalent. Both methods indicate a valid model showing a good potential of HSI in detecting *Fusarium* damage and predicting DON in oats.

Figure 8 comes here.

CONCLUSIONS

Hyperspectral images of individual oat kernels with different levels of *Fusarium* damage and DON content were analysed. Hyperspectral imaging successfully detected *Fusarium* damage of kernels with better accuracy than visual inspection. Detection of *Fusarium* damage with HSI gave a better indication of DON content of kernels than visual assessment of damage. Regions within single kernels were further classified as *Fusarium*-damaged and healthy regions. A PLSR model was developed using the transformed DON* values as y-variables and the average spectra of each kernel as x-variables. The model was proved to be valid and stable by detecting DON* values of a set of separate validation kernels. The results reported in this paper indicate that HSI can successfully be implemented to detect *Fusarium* damage and DON contamination in single oat kernels. Thus, highly damaged and contaminated kernels can be detected and removed to significantly lower toxin contamination and improve grain quality of seed lots. Kernels used in this paper are of a single oat genotype originating from a single experimental year. Testing the feasibility of HSI to detect *Fusarium* damage and DON contamination in several genotypes across experimental years would be an important step towards the routine application of the method for screening purposes.

ACKNOWLEDGEMENTS

We acknowledge the financial support of the Norwegian Research Council and Graminor AS to the project 'Mycotoxin contamination in Norwegian food and feed: Modelling reductive approaches and risk assessment with regards to the whole food chain (Project number 19412)'. We thank Dr. Yanhong Dong (Department of Plant Pathology, University of Minnesota) for DON analysis, Elin Ørmen (Imaging Center, Norwegian University of Life Sciences) for her help in microscopy and Andreas Flø (Institute of Mathematics and Technology, Norwegian University of Life Sciences) for his help in hyperspectral imaging.

LITERATURE CITED

Bechtel, D. B., Kaleikau, L. A., Gaines, R. L., Seitz, L. M. 1985. The effects of *Fusarium graminearum* infection on wheat kernels. Cereal Chem. 62: 191-7.

Bergsjø, B., Langseth, W., Nafstad, I., Jansen, J. H., Larsen, H. J. S. 1993. The effects of naturally deoxynivalenol contaminated oats on the clinical condition, blood parameter, performance and carcass composition of growing pigs. Vet. Res. Commun. 17: 283-94.

Bernhoft, A., Eriksen, G. S., Sundheim, L., et al., 2013. Risk assessment of mycotoxins in cereal grain in Norway: Opinion of the Scientific Steering Committee of the Norwegian Scientific Committee for Food Safety. In.: Norwegian Scientific Committee for Food Safety (VKM).

Bottalico, A., Perrone, G. 2002. Toxigenic *Fusarium* species and mycotoxins associated with head blight in small-grain cereals in Europe. Eur. J. Plant Pathol. 108: 611-24.

D'mello, J. P. F., Placinta, C. M., Macdonald, A. M. C. 1999. *Fusarium* mycotoxins: a review of global implications for animal health, welfare and productivity. Anim. Feed Sci.Technol. 80: 183-205.

Delwiche, S. R., Kim, M. S., Dong, Y. 2011. *Fusarium* damage assessment in wheat kernels by Vis/NIR hyperspectral imaging. Sensory and Instrumentation for Food Quality 5: 63-71.

Dexter, J. E., Clear, R. M., Preston, K. R. 1996. Fusarium head blight: effect on the milling and baking of some Canadian wheats. Cereal Chem. 73: 695-701.

Feng, Y. Z., Sun, D. W. 2012. Application of hyperspectral imaging in food safety inspection and control: a review. Critical Reviews in Food Science and Nutrition 52: 1039-58

283 Gowen, A. A., O'donnell, C. P., Cullen, P. J., Downey, G., Frias, J. M. 2007. Hyperspectral
284 imaging- an emerging process analytical tool for food quality and safety control. Trends
285 Food Sci. Tech. 18: 590-8.
286 Jackowiak, H., Packa, D., Wiwart, M., Perkowski, J. 2005. Scanning electron microscopy of
287 *Fusarium* damaged kernels of spring wheat. Int. J. Food Microbiol. 98: 113- 23.
288 Jiang, G., Dong, Y., Lewis, J. M., Siler, L., Ward, R. R., 2006. Characterization of resistance to
289 *Fusarium graminearum* in a recombinant inbred line population of wheat: resistance to
290 fungal spread, mycotoxin accumulation, and grain yield loss, and trait relationship. Crop
291 Sci. 46: 2590 - 7.
292 Langevin, F., Eudes, F., Comeau, A. 2004. Effect of trichothecenes produced by *Fusarium*
293 *graminearum* during Fusarium head blight development in six cereal species. Eur. J.
294 Plant Pathol. 110: 735-46.
295 Liu, W., Langseth, W., Skinnes, H., Elen, O. N., Sundheim, L. 1997. Comparison of visual head
296 blight ratings, seed infection levels, and deoxynivalenol production for assessment of
297 resistance in cereals inoculated with *Fusarium culmorum*. Eur. J. Plant Pathol. 103: 589-
298 95.
299 Mcmullen, M., Jones, R., Gallenberg, D. 1997. Scab of wheat and Barley: a re-emerging disease
300 of devastating impact. Plant Dis. 81: 1340-8.
301 Nightingale, M. J., Marchylo, B. A., Clear, R. M., Dexter, J. E., Preston, K. R. 1999. Fusarium
302 head blight: effect of fungal proteases on wheat storage proteins. Cereal Chem. 76: 150-8.
303 Parry, D. W., Jenkinson, P., Mcleod, L. 1995. Fusarium ear blight (scab) in small grain cereals—
304 a review. Plant Pathology 44: 207-38.

Polder, G., Heijden, G.W. M. V. D, Waalwijk, C., Young, I. T. 2005. Detection of *Fusarium* in single wheat kernels using spectral imaging. Seed Science and Technology 33: 655-68.

Schwarz, P. B., Schwarz, J. G., Zho, A., Prom, L. K., Steffenson, B. J. 2001. Effect of *Fusarium graminearum* and *F. poae* infection on barley and malt quality. Monatsschrift Fur Brauwissenschaft 314: 55-63.

Shahin, M. A., Symons, S. J. 2011. Detection of *Fusarium* damaged kernels in Canada Western Red Spring wheat using visible/near-infrared hyperspectral imaging and principal component analysis. Computers and Electronics in Agriculture 75: 107-12.

Shahin, M. A., Symons, S. J. 2012. Detection of *Fusarium* damage in Canadian wheat using visible/near-infrared hyperspectral imaging. Food Measure 6: 3-11.

Siuda, R., Balcerowska, G., Kupcewicz, B., Lenc, L. 2008. A modified approach to evaluation of DON content in scab-damaged ground wheat by use of diffuse reflectance spectroscopy. Food Anal. Methods 1: 283-92.

Snijders, C. H. A., Perkowski, J. 1990. Effects of head blight caused by *Fusarium culmorum* on toxin content and weight of wheat kernels. Phytopathology 80: 566-70.

Tekle, S., Bjørnstad, Å., Skinnes, H., Dong, Y., Segtnan, V. H. 2013. Estimating deoxynivalenol content of ground oats using VIS-NIR spectroscopy. Cereal Chem. 90: 181–185

Wang, J., Pawelzik, E., Weinert, J., Wolf, G. A., 2005. Impact of *Fusarium culmorum* on the polysaccharides of wheat flour. J. Agric. Food Chem. 53: 5818-23.

Williams, P., Manley, M., Fox, G., Geladi, P. 2010. Indirect detection of *Fusarium verticillioides* in maize (*Zea mays* L.) kernels by near infrared hyperspectral imaging. J. Near Infrared Spectrosc. 18: 49-58.

Table 1: Mean (± standard deviation), minimum and maximum kernel weight (g) and deoxynivalenol content (ppm) of calibration (*n*=31) and validation (*n*=14) set samples of asymptomatic (A), mildly damaged (MD), severely damaged (SD) and uninoculated (U) kernels. 'nd' stands for non-detectable level of DON (< 5 ng/ sample).

		Calibration set		Validation set	
		Kernel weight (g)	DON (ppm)	Kernel weight (g)	DON (ppm)
	A	0.054 ± 0.005	1.93 ± 4.49	0.056 ± 0.005	4.99 ± 7.83
	MD	0.048 ± 0.008	25.31 ± 53.94	0.046 ± 0.010	56.82 ± 107.43
	SD	0.036 ± 0.009	136.34 ± 123.04	0.032 ± 0.008	117.61 ± 107.25
Mean	U	0.050 ± 0.013	0.09 ± 0.05	0.045 ± 0.008	0.01 ± 0.05
	A	0.045	nd	0.051	0.18
	MD	0.034	nd	0.029	nd
	SD	0.019	0.48	0.018	0.52
Minimum	U	0.033	nd	0.034	nd
	A	0.062	20.50	0.064	21.91
	MD	0.061	267.37	0.061	355.32
	SD	0.056	386.51	0.048	340.10
Maximum	U	0.062	0.66	0.058	0.18

Table 2 Mean (± standard deviation) percentage of damaged pixels in uninoculated, asymptomatic, mildly damaged and severely damaged kernels of the calibration (*n*= 248) and validation (*n*=112) images. Ventral and dorsal images were pooled for each kernel category.

	Uninoculated	Asymptomatic	Mildly Damaged	Severely Damaged
Calibration set	21.5 ± 5.4	28.1 ± 8.0	39.8 ± 12.9	62.8 ± 16.4
Validation set	26.5 ± 7.4	29.3 ± 7.1	46.9 ± 18.4	73.3 ± 16.3

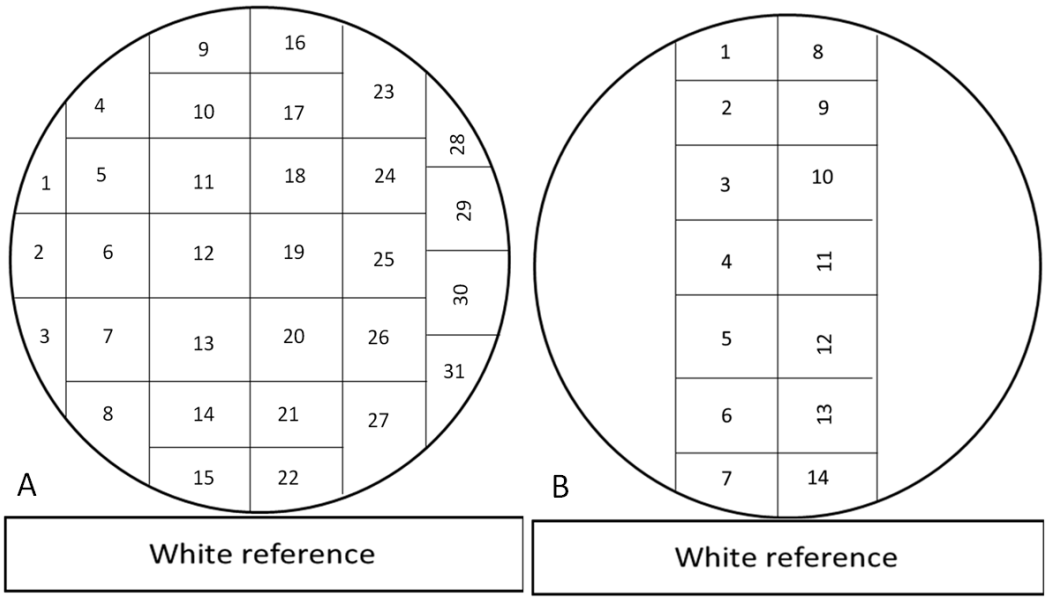

Figure 1: Presentation of kernels for hyperspectral imaging. Ventral and dorsal surfaces of 31 test set kernels (A) and the 14 validation set kernels (B) from each kernel category were scanned. Numbers in the cells represent kernel numbers. Kernels were scanned with their basal portions towards the white reference. Kernels 28, 29, and 30 in the calibration set and kernels 11, 12 and 13 in the validation set were rotated 90^{o} to serve as signposts.

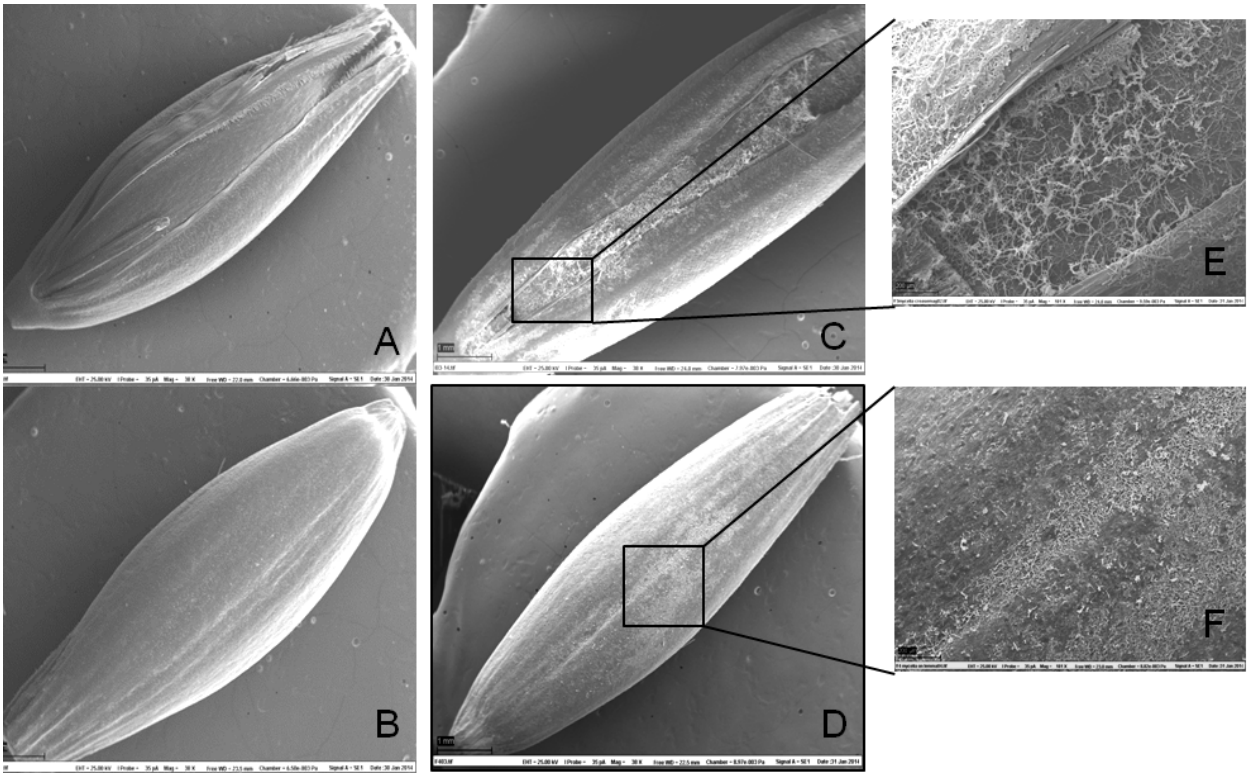

Figure 2: Scanning electron micrographs of ventral and dorsal surfaces of hulled kernels of healthy (A and B, magnification = 38 x) and *Fusarium*-damaged (C and D, magnification= 38x) kernels of the oat cv. Bessin. Higher magnification reveals profuse growth of *F. graminearum* mycelia in the crease on the palea (E, magnification= 181x) and on the lemma (F, magnification= 181x).

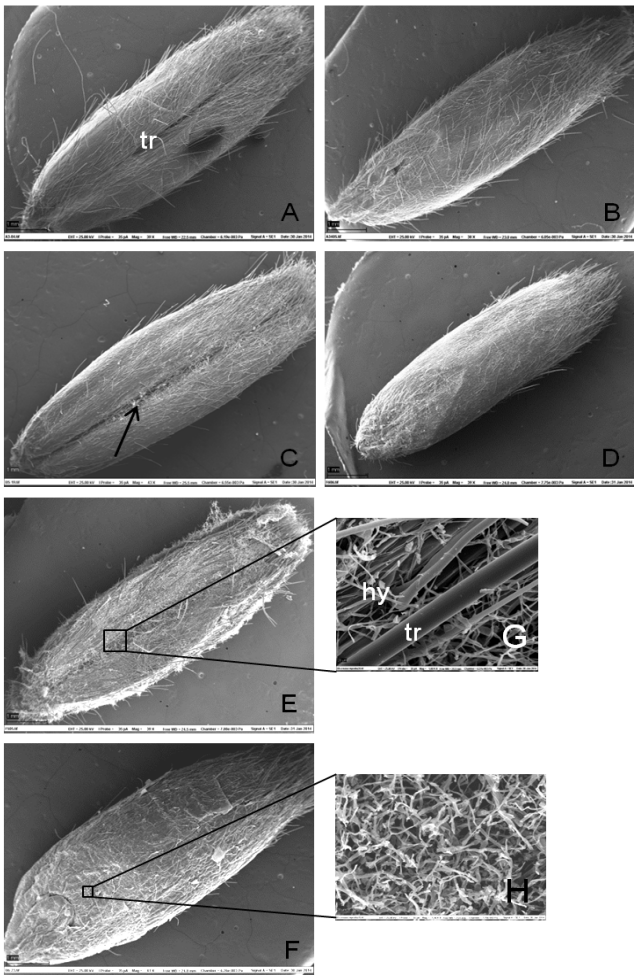

Figure 3: Scanning electron micrographs of ventral and dorsal surfaces of dehulled kernels of the oat cv. Bessin. A and B show well-formed mycelium on ventral (A, magnification= 39x) and dorsal (B, magnification= 38x) surfaces of healthy kernels, with the trichomes (tr). C and D show ventral (C, magnification= 43x) and dorsal (D, magnification= 39x) surfaces of mildly damaged kernels, arrow indicates mycelia of *Fusarium graminearum*. E and F are micrographs of ventral (E, magnification= 39x) and dorsal (F, magnification= 41x) surfaces of severely damaged kernels. G and H are higher magnifications of fungal growth on the ventral (G, magnification= 1.6kx, hy= hyphae, and tr= trichome) and dorsal surfaces (H, magnification= 1.46kx).

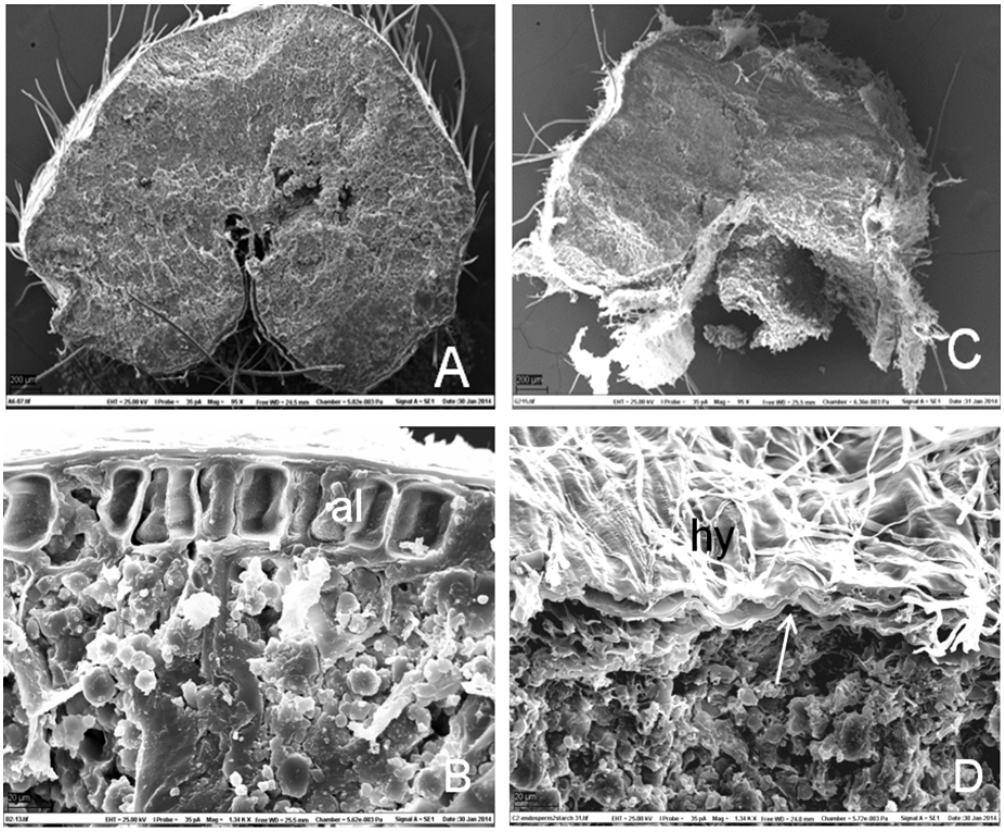

Figure 4: Scanning electron micrographs of cross sections of healthy (A, magnification= 95x; and B, magnification= 1.34 kx) and *Fusarium*-damaged (C, magnification= 95x; and D, magnification= 1,34 kx) kernels of the oat cv. Bessin. A well formed aleurone layer (al) and endosperm with small and large starch granules in the protein matrix of the healthy kernel is displayed in B. Hyphae (hy) of *Fusarium graminearum* and collapsed aleurone layer and damaged endosperm are shown in D.

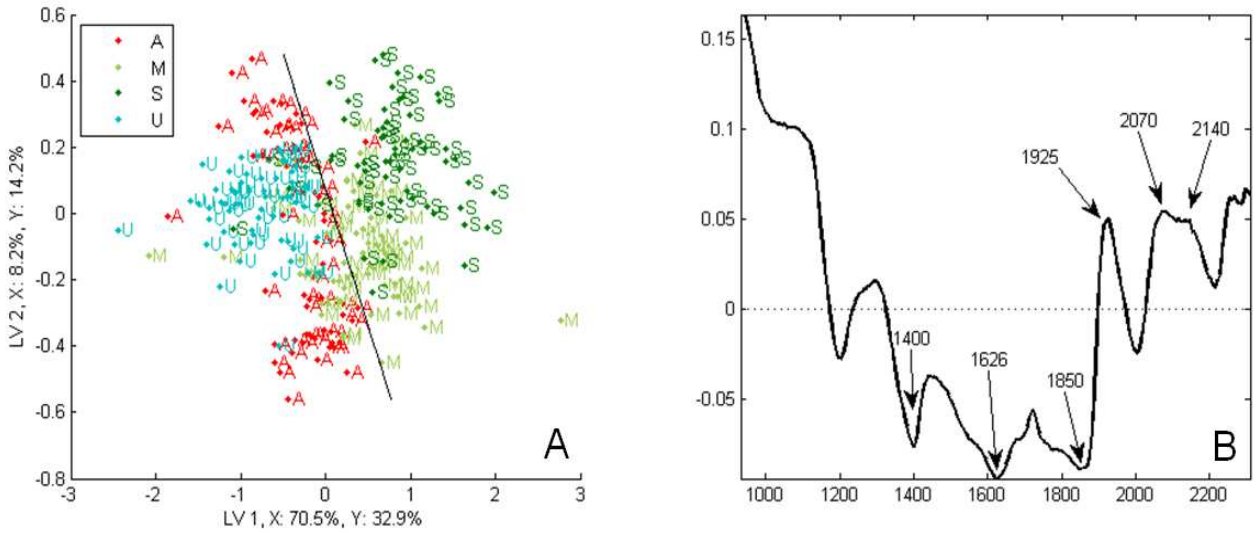

Figure 5: Partial least squares (PLS) regression on the calibration set kernels with the average spectra of kernels as X variables and DON*= [log(DON)]^3 values as Y variables. (A) PLS scores of calibration set kernels on component 1 versus component 2, with separation line from linear discriminant analysis. A- asymptomatic, M- mildly damaged, S- severely damaged and U- uninoculated kernels. (B) PLS loading weights from the first component. Wavelengths of interest are marked by arrows.

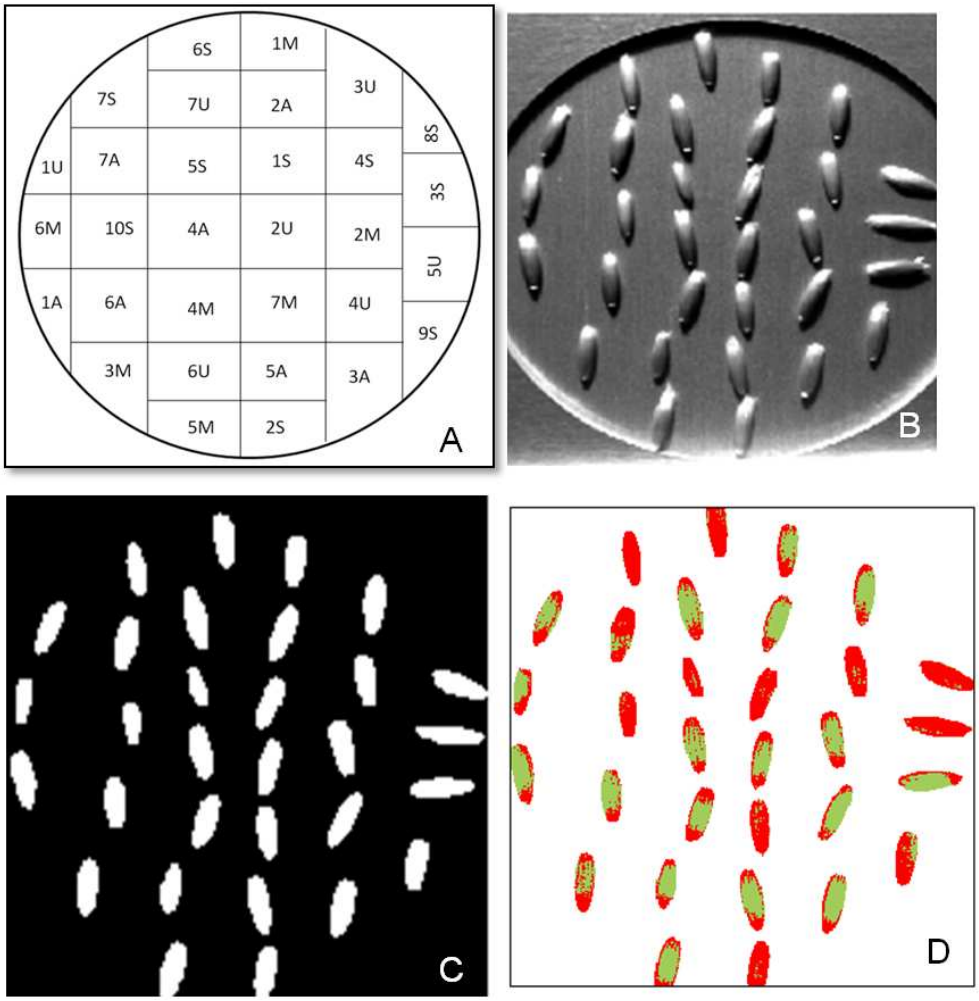

Figure 6: Image analysis of calibration set kernels comprising seven uninoculated, seven asymptomatic, seven mildly damaged and ten severely damaged kernels. (A) Sample presentation for scanning. Numbers represent the kernel number in the original calibration set and letters represent kernel category. A- asymptomatic, M- mildly damaged, S- severely damaged and U- uninoculated kernels. (B) Reflectance spectra of one selected channel. (C) Mask used to remove background from images. D) Image showing infection in grains. Red pixels represent DON-contaminated/ *Fusarium*-damaged areas and green pixels represent DON-free/ healthy areas.

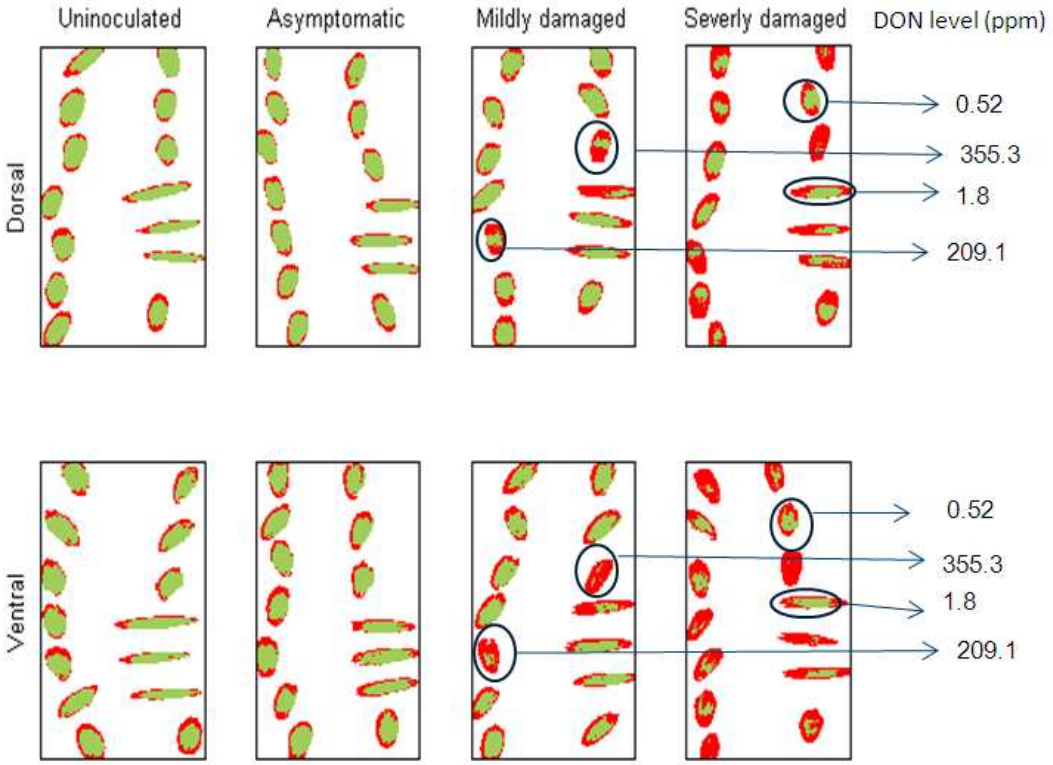

Figure 7: Classification of pixels in validation images. *Fusarium*-damaged/ DON-contaminated areas are depicted in red while healthy/ DON-free areas are depicted in green. DON values of kernels of interest (kernels with relatively high DON level in the mildly damaged category and kernels with low DON level in the severely damaged category) are shown.

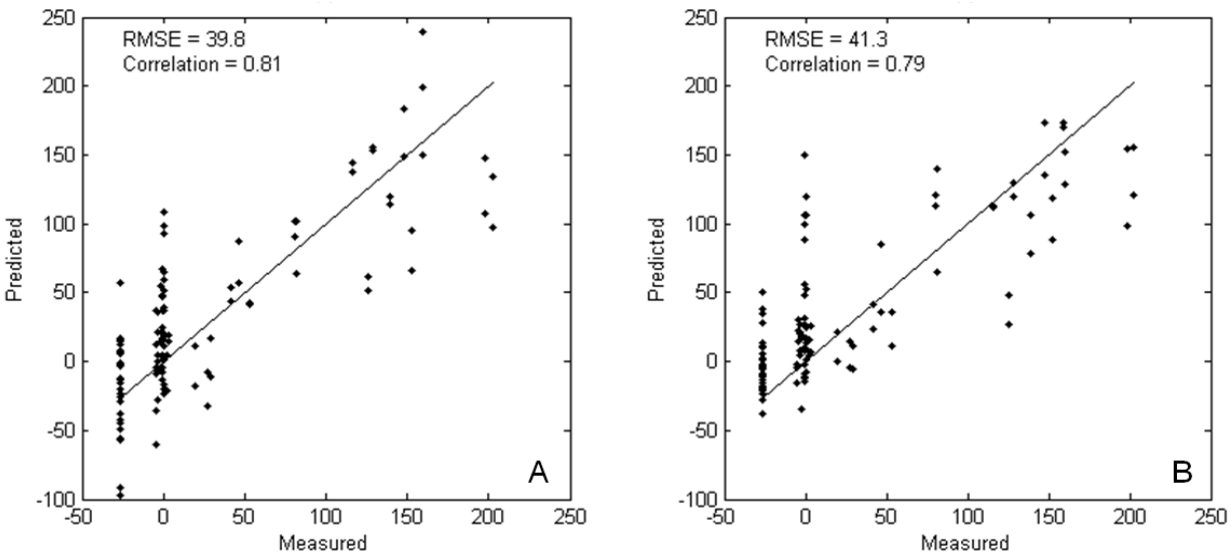

Figure 8: Measured versus predicted DON*= [log(DON)]^3 values of validation kernels using the partial least squares (PLS) regression model developed (A) and the PLS- linear discriminant analysis model (B).